universität
wien

MASTERARBEIT

Titel der Masterarbeit

„Developing a novel method for detecting transient protein-protein interactions in mammalian cells“

verfasst von

Wolfgang Hintringer, BSc

angestrebter akademischer Grad

Master of Science (MSc)

Wien, 2013

Studienkennzahl	A 066 834
Studienrichtung	Masterstudium Molekulare Biologie
Betreuerin / Betreuer:	ao. Univ. Prof. Dr. Egon Ogris

Abstract

Short-lived protein-protein interactions are of major significance in many essential regulatory processes in cells and therefore are of main interest for research. Unfortunately, currently available methods fall short in their ability to detect and identify transiently interacting proteins. Therefore the primary aim of this thesis was to develop a novel method that is able to detect transient interactions in mammalian cells. This method, named the preScission™ assay, relies on proteolysis of a substrate peptide fused to a "prey" by a human rhinovirus type 14 3C protease (preScission™™ protease) fused to a "bait" in order to confirm the interaction between the two proteins of interest. According to our model, ideal kinetic parameters of this proteolytic reaction consist of a high turnover number (k_{cat}) as well as a high Michaelis constant (K_m). As a first aim, I therefore compared kinetic parameters of preScission™ reactions *in vitro* to find an ideal substrate for the preScission™ assay, using two techniques: A Förster resonance energy transfer-based approach and a discontinuous enzyme assay coupled with in-gel western blotting. For the proof of principle, the most promising substrate, C3S6, was subsequently used to test whether the stable interaction between two subunits of mammalian protein phosphatase 2A, named PP2A-B55α and PP2A-Cα, could be detected in mammalian cells, aiming at identifying transient interactions in further studies. The results suggested that the preScission™ assay is unsuited for detecting mammalian protein-protein interactions such as the ones between PP2A-B55α and PP2A-Cα. The preScission™ fused to the bait cleaved the substrate fused to the prey to an equal or lesser extent compared to the tested negative controls suggesting that the detection enzyme itself cleaves the substrate independently of an interaction between the PP2A subunits. Subsequent experiments showed that endogenous PP2A subunits were present in the cells in high amounts. These could have interfered with the assay by binding to the ectopically expressed PP2A-B55α and Cα subunits, preventing interactions between the bait and prey fusion proteins. Further experiments should focus on knocking down endogenous PP2A subunit gene expression or on finding an enzyme-substrate pair with optimal kinetic parameters for PPI detection.

Abstract in German

Kurzlebige Protein-Protein-Interaktionen spielen eine zentrale Rolle in den meisten zellulären Signalkaskaden. Es besteht daher ein großes Interesse, die beteiligten Proteine einer solchen Interaktion zu identifizieren um ein besseres Verständnis der Regulierungsmechanismen der Zelle zu ermöglichen. Unglücklicherweise können derartige Interaktionen mit den momentan verfügbaren Methoden nur unzureichend nachgewiesen werden. Hauptziel dieser Arbeit war daher die Entwicklung einer neuen Methode, welche zum Nachweis von kurzlebigen Protein-Protein-Interaktionen in Säugetierzellen geeignet ist. Diese Methode, genannt der "preScission™ assay", verwendet die Proteolyse eines Substratpeptids, fusioniert an ein "Prey"-Protein, durch eine "Human rhinovirus typ 14 3C" protease (preScission™ protease), welche an ein "Bait"-Protein fusioniert wurde, um die Interaktion zwischen den "Bait"- und "Prey"-Proteinen nachzuweisen. Laut unserem Modell sollten die kinetischen Parameter dieser proteolytischen Reaktion idealerweise eine hohe turnover number (kcat) sowie eine hohe Michaeliskonstante (K_m) aufweisen Daher verglichen wir zuerst kinetische Parameter von preScission™-Reaktionen *in vitro*, um ein ideales Substrat für den preScission™ Assay zu finden. Hierfür wurden zwei Methoden angewandt: Ein auf Förster Resonanzenergietransfer basierender Ansatz sowie ein diskontinuierlicher Enzym-Assay kombiniert mit in-gel western blotting. Das aussichtsreichste Substrat, C3S6, wurde daraufhin benutzt um zu testen, ob Interaktionen zwischen zwei stabil interagierenden Untereinheiten der Protein Phosphatase 2A, genannt PP2A-B55α und PP2A-Cα, nachgewiesen werden können, mit dem Ziel, kurzlebige Interaktionen in weiteren Studien nachzuweisen. Die Ergebnisse zeigten, dass der preScission™ Assay, unter Verwendung von C3S6 als Substrat, nicht dafür geeignet ist, Protein-Protein-Interaktionen zwischen PP2A-B55α und PP2A-Cα zu erkennen. Weiterführende Experimente zeigten, dass hohe Mengen an endogenen PP2A-Untereinheiten in den Zellen vorhanden waren. Diese könnten durch Bindung an die ektopisch exprimierten PP2A-Untereinheiten die Interaktionen zwischen den "Bait"- und "Prey"-Fusionsproteinen verhindert haben. In Weiterführende Experimente sollten darauf abzielen, die Expression der endogenen PP2A-Untereinheiten zu verringern oder darauf, Enzym-Substratpaare mit optimalen kinetischen Parametern zu identifizieren.

ABSTRACT .... **II**

ABSTRACT IN GERMAN .... **III**

1. INTRODUCTION **1**

1.1. PROTEIN PHOSPHATASE 2A 1

1.1.1. Structure and subunits of Protein Phosphatase 2A *1*

1.1.2. Functions of Protein Phosphatase 2A *4*

1.2. USING THE PRESCISSION™ ASSAY TO DETECT PROTEIN-PROTEIN INTERACTIONS 5

1.2.1. Detecting mammalian protein-protein interactions (PPIs) *5*

1.2.2. Model of the preScission™ assay *7*

1.2.3. Structure and function of Human rhinovirus type 14 3Cpro/ PreScission™ protease *9*

1.2.4. In vitro substrate binding to Human rhinovirus type 14 3Cpro *10*

1.3. KINETIC CONSIDERATIONS FOR THE PRESCISSION™ ASSAY 13

1.3.1. Principles of Michaelis-Menten Kinetics *13*

1.3.2. Determining kinetic parameters of Michaelis-Menten enzymatic reactions *16*

1.3.3. Enzyme Assays - Types and Uses *17*

1.4. USING A FÖRSTER RESONANCE ENERGY TRANSFER (FRET) ENZYME ASSAY TO DETERMINE KINETIC PARAMETERS OF PRESCISSON REACTIONS 18

1.4.1. Mechanism of FRET *18*

1.4.2. Using fluorescent proteins to study FRET *19*

1.5. USING A DISCONTINUOUS ENZYME ASSAY COUPLED WITH IN- GEL WESTERN DETECTION TO DETERMINE ENZYMATIC ACTIVITY 22

1.6. AIM OF THE THESIS 24

2. MATERIALS AND METHODS **25**

2.1. WORKING WITH BACTERIA 25

2.1.1. Solutions and Media *25*

2.1.2. Growth of bacteria: *25*

2.1.3. Transformation of XL1-blue competent Escherichia coli *26*

2.1.4. Freezing/thawing of bacteria: *26*

2.1.5. Bacterial expression of fusion proteins *26*

2.2. WORKING WITH DNA 27

2.2.1. Solutions *27*

2.2.2. Minipreparation: QIAprep™ Spin Miniprep Kit (Qiagen #27106) *27*

2.2.3. Plasmid DNA isolation using alkaline lysis *28*

2.2.4. Plasmid Midi preparation using PureYield™ Plasmid Midiprep System *28*

2.2.5. Restriction Digest *28*

2.2.6. Gel Elution: Promega SV Gel and PCR-clean-up System *29*

2.2.7. Agarose Gel-electrophoresis for Gel Elution *29*

2.2.8. Plasmids *29*

2.2.9. PCR (Polymerase Chain Reaction) *30*

2.2.10. Annealing of Oligonucleotides and 5´-end Phosphorylation *30*

2.2.11. Ligation *31*

2.2.12. DNA sequencing *32*

2.3. WORKING IN TISSUE CULTURE 33
  2.3.1. *Solutions and Media* *33*
  2.3.2. *Tissue Culture: Cultivation and Propagation of HEK293Trex cells* *34*
  2.3.3. *Tissue Culture: Freezing/thawing of HEK293Trex cells* *34*
  2.3.4. *Transfection of mammalian cells using Lipofectamine 200* *35*
  2.3.5. *CASY Cell Concentration Determination* *35*
2.4. WORKING WITH PROTEINS 36
  2.4.1. *Solutions and Media* *36*
  2.4.2. *: Protein Expression and Extraction from HEK293Trex cells* *39*
  2.4.3. *BioRad Assay / Protein Concentration Measurement* *39*
  2.4.4. *Purification of bacterially expressed proteins* *39*
  2.4.5. *TCA precipitation of proteins* *40*
  2.4.6. *Sodium dodecyl sulfate polyacrylamide gel electrophoresis (SDS-PAGE)* *40*
  2.4.7. *Coomassie staining of gels* *41*
  2.4.8. *Silver staining of SDS-PAGE gels* *41*
  2.4.9. *Western Blot* *42*
  2.4.10. *In vitro enzyme kinetic assay* *43*
  2.4.11. *LI-COR™ in gel western* *44*
  2.4.12. *Co-Immunoprecipitation* *44*
  2.4.13. *Determination of kinetic parameters using FRET* *45*
3. RESULTS 46
3.1. DETERMINING KINETIC PARAMETERS OF THE PRESCISSION™ REACTION 46
  3.1.1. *Using a Förster Resonance energy transfer (FRET) enzyme assay to determine kinetic parameters of preScisson reactions* *49*
  3.1.2. *Using a discontinuous enzyme assay coupled with in-gel western detection to determine kinetic parameters of preScission™ reactions* *57*
3.2. USING THE PRESCISSION™ ASSAY TO DETECT PROTEIN-PROTEIN INTERACTIONS 62
3.3. EVALUATING THE PRESCISSION™ ASSAY 71
  3.3.1. *Co-Immunoprecipitations of recombinant fusion proteins* *71*
  3.3.2. *Evaluating the preScission™ assay by inhibiting bait and prey interaction* *75*
4. DISCUSSION 78
4.1. DETERMINING KINETIC PARAMETERS OF THE PRESCISSION™ REACTION 78
4.2. USING THE PRESCISSION™ ASSAY TO DETECT PROTEIN-PROTEIN INTERACTIONS 81
5. REFERENCES 83
6. APPENDIX 93
7. CURRICULUM VITAE 110

1. Introduction

1.1. Protein Phosphatase 2A

1.1.1. Structure and subunits of Protein Phosphatase 2A

Protein phosphorylation and dephosphorylation, by protein kinases and phosphatases respectively, are among the major regulatory mechanisms used in cells to control processes such as metabolism, cell-cycle progression, apoptosis, transcription and translation. Protein phosphatases are commonly grouped into families based on their specific catalytic signatures/domain sequences and substrate preference. They consist of the protein-serine/threonine phosphatases (PSTPases), protein-tyrosine phosphatases (PTPases) and dual specificity phosphatases (DSPases) (*Cohen et al*, *1990*). The serine/threonine family includes the essential phosphatase PP2A, which catalyzes the removal of phosphates from serine or threonine residues of target proteins via hydrolyzation (as reviewed by *Wera and Hemmings, 1995*). Mammalian PSTPs such as PP2A achieve their substrate specificity by combinatorial and regulatory complexity. The heterodynamic core consists of a catalytic subunit ($PP2A_C$) and a structural subunit ($PP2A_A$), which links the C subunit to a variety of regulatory subunits ($PP2A_B$) (Figure 1, *Jannsens and Goris, 2009*). Binding of the regulatory subunits to the core enzyme, consisting of a C and an A subunit, determines substrate specificity and localization of the holoenzyme.

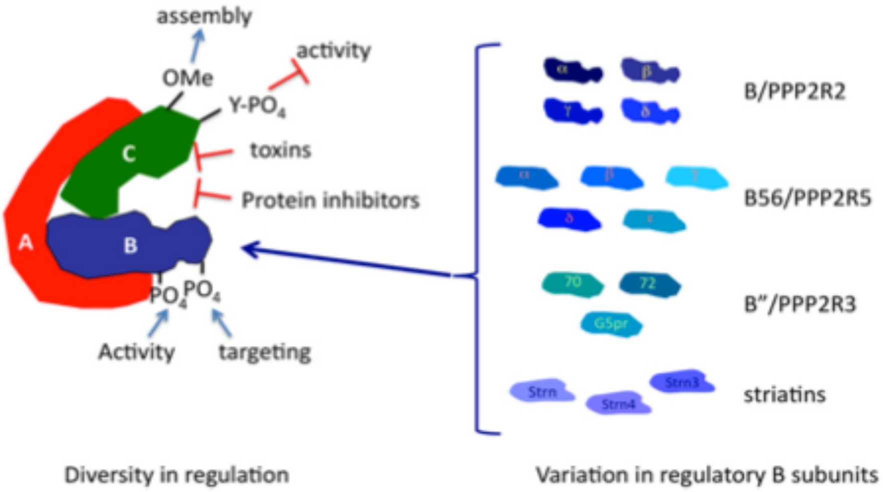
assembly
activity
OMe
Y-PO4
C
toxins
Protein inhibitors
A
B
PO4
PO4
Activity
targeting
B/PPP2R2
B56/PPP2R5
70
72
G5pr
B''/PPP2R3
Strn
Strn4
Strn3
striatins
Diversity in regulation
Variation in regulatory B subunits

Figure 1: **Diversity and complexity of PP2A**: PP2A functions as a heterotrimer consisting of a structural (A), regulatory (B) and a catalytic (C) subunit. The ability of the phosphatase to alter substrate specificity is largely due to the variety of regulatory B-subunits, which enables numerous combinatorial possibilities during holoenzyme assembly. (*Janssens and Goris, 2009*)

While there are over 400 different serine/threonine kinases encoded in the human genome (*Manning et al, 2002*), only 5 genes code for catalytic subunits of the two most abundant serine/threonine phosphatases, PP1 and PP2A, in mammals (*Virshup and Shenolikar, 2009*). The catalytic subunit of PP2A has two ubiquitously expressed isoforms, α and β, which are 97 % identical in their primary sequence (*Khew-Goodall and Hemmings, 1988*). The structure of this subunit is highly conserved and knockdown of the catalytic or several regulatory subunit genes leads to apoptosis (reviewed by *Virshup and Shenolikar, 2009*). In the catalytic center, three histidines, two aspartic acids and one asparagine coordinate the binding of two metal ions. Together, these residues and ions are essential for the catalytic activity and structural integrity of the enzyme (*Ogris, Mudrak et al 1999, Ogris, Du et al, 1999, Cho et al., 2007*).

PP2A achieves its complexity by combining the A-C-heterodynamic core with one of its many regulatory B subunits. To date, about 20 different isoforms of B subunits have been described. These have been grouped into four different families, termed PR55/B, PR61/B', and PR72/B'' (as reviewed by *Janssens et al, 2008*). The focus of this study lies on the B55α regulatory subunit, a 55 kDa protein also termed PR55α and PPP2R2A, which is part of the B family. In mammals, it is expressed in the majority of tissues throughout the body (*Hendrix et al, 1993; Mayer et al 1991*) and is primarily localized in the cytosol (*Strack et al, 1988*).

The C subunit is linked to the regulatory B subunit in two ways. On the one hand, B and C subunits are connected via the structural A subunit (*Kamibayashi and Mumby, 1995*). On the other hand, via direct binding of the B-subunit to the C-terminus of the catalytic subunit (*Xu et al, 2006, Cho et al, 2007, Xu et al, 2008).* This interaction may, in some cases, be facilitated by methylation of the C-terminus of $PP2A_C$, depending on the regulatory subunit involved (*Ogris et al, 1997; Bryant et al, 1999; Wei et al, 2001, Longin et al, 2007; Nunbakhdi-Craig et al, 2007*). Okadaic acid inhibits phosphatase activity of PP2A by binding close to the PP2A active site (*Li and Damuni, 1994; Floer and Stock, 1994, et al, 2006, Xing et al, 2006, Stanevich et al, 2011*).

Crystal structures of the PP2A holoenzyme (*Xu et al, 2006; Cho et al, 2007; Xu et al, 2008*) also revealed that the B56γ subunit makes considerably more interactions with the Cα subunit than the B55α subunit, suggesting a relatively loose holoenzyme when B55α is included (*reviewed by Martin et al, 2010*). Two isoforms of this horseshoe-shaped protein, α and β, are present in mammals (*Hemmings et al, 1990*). Each isoform presumbaly binds differentially to the various B- and C-subunits (*Zhou et al, 2003*).

1.1.2. Functions of Protein Phosphatase 2A

PP2A is involved in controlling numerous cellular processes, including but not limited to roles in cellular signaling, translation, apoptosis, stress response and cell cycle control (reviewed for example by *Janssens and Goris, 2001, Virshup and Shenolikar, 2009, Martin, 2010*).

Interestingly, PP2A is also a target of DNA tumorvirus antigens. Polyomavirus small t and middle T, as well as simian virus 40 (SV40) small t, form complexes with PP2A. PP2A has been shown to dephosphorylate proteins involved in the MAP-kinase pathway, including the mitogen activated protein kinase kinase MEK and the extracellular signal-regulated kinase ERK, thus inhibiting cellular proliferation (*Alessi et al, 1995).*

Most recent data suggest that PP2A also plays an important role in protecting melanoma cells upon endoplasmic reticulum stress (*Tay et al, 2012*) or in fine-tuning signals at the photoreceptor synapse in the retina (*Haeseleer et al, 2013*). The regulatory B55α subunit has been shown to play an important role in glutamine sensing and cancer cell survival (*Reid et al, 2013*).

Due to its important role in cell signaling, it is of great interest to identify further substrates of PP2A. It is however notable that tyrosine phosphatases (PTPs) and PSTPs use different catalytic mechanisms for hydrolysis of the target phosphate. While PTPs form covalent thiol-phosphate intermediates with their substrates in the course of the reaction *(Denu and Dixon, 1995),* PSTPs only use a single step reaction without an intermediate product *(Barford, 1996).* The combinatorial complexity and the transient nature of the reaction make it difficult to detect PSTP substrates, resulting in the problem that many substrates of PP2A are still unknown (Virshup . The novel method presented in this study is aimed at identifying such PP2A substrates, or other transient protein interactions, which are hard to detect otherwise

1.2. Using the preScission™ assay to detect protein-protein interactions

1.2.1. Detecting mammalian protein-protein interactions (PPIs)

Protein-protein interactions (PPIs) constitute a field of major interest for research due to their importance in the majority of cellular processes. Protein interactomics, the field of research associated with mapping protein interactions, enhances our understanding of protein function and organization. Such knowledge is particularly important for human health, since aberrations in protein interaction patterns often lead to disease phenotypes (as reviewed by *Lievens et al, 2009*). Therefore, methods that reliably identify interactions between mammalian proteins are sought for.

Biochemical methods to detect PPIs commonly involve the analysis of protein complexes purified from cell lysates. However, systems that detect interactions within living cells preserve spatial and temporal resolution and are thus often preferable (*Fernández-Suárez et al, 2008*).

The yeast-2-hybrid system (*Fields et al, 1989*), a popular genetic interaction mapping technology, has been used successfully to map interactions between mammalian proteins of interest in yeast (*Venkatesan et al, 2009*). Many PPIs, however, can only be detected in their native cellular context, as they may require modifications or structural alterations of the interacting proteins (*Lievens et al, 2009).* Application of the yeast-2-hybrid in mammalian cells, a method named mammalian-2-hybrid *sensu stricto,* has for example led to the discovery of the transforming growth factor-β-dependent interaction of small body size/mothers against decapentaplegic homolog 2 and 4 proteins (SMAD2 and SMAD4) with cyclic adenosine monophosphate response element binding protein (CREB binding protein/CBP) (*Topper et al, 1998*). This method, however, fails to capture the dynamics of protein-protein interactions, and may lack sensitivity to detect many transient interactions.

Several protein complementation assays (PCAs) have been developed in an attempt to resolve these shortcomings. The β-lactamase assay, for example, benefits from high detection sensitivity and is able to generate a quantifiable signal, allowing to track stable phosphorylation-dependent interactions such as the ones between CREB and CBP (*Spotts et al, 2002*). In classic PCAs, reporter proteins themselves are reconstituted upon protein-protein interaction. In a related highly sensitive approach named the split-tobacco etch virus assay (split-TEV), reconstituted proteolytic activity liberates a reporter protein, which can further amplify the signal by acting as an enzyme or as a transcription factor (*Wehr et al, 2006*). This signal amplification enables the assay to potentially capture transient interactions, although the irreversibility of reporter activation compromises the assay's ability to analyze interaction dynamics (*Lievens et al, 2009).*

In principle, systems that rely on resonance energy transfer between fluorescent or bioluminescent proteins fused to the proteins of interest allow real-time analysis of protein interactions. Such systems have been used to monitor the ligand-induced interaction between G-protein coupled receptors (GPCRs) and G-proteins (*Gales et al, 2005; Hein et al, 2005*), however, using these methods is technically demanding and requires optimization for every tested case (*Lievens et al, 2009)*.

Recently, development of an easy-to-use 2-hybrid approach named Bio-ID (*Roux et al, 2012*) has provided a possibility to identify PPIs in a less demanding fashion. However, this system suffers from its lack of sensitivity in differentiating between proximal and interacting proteins, resulting in many false-positive results when it comes to identifying transient PPIs.

M-Track, a novel two-hybrid approach, enables analysis of transient PPIs in *Saccharomyces cerevisiae* (*Zuzuarregui et al, 2012*). However, M-Track relies on the action of human histone lysine 9 methyltransferase (HKMT) SUV39H1 to prove protein-protein interactions. Due to endogenous SUV39H1 activity present in mammalian cells, as opposed to *S. cerevisiae*, this system is limited in its ability to detect PPIs in mammalian cells.

Here we present the first steps towards establishing a novel 2-hybrid system aimed at detecting transient PPIs with high sensitivity in mammalian cells.

1.2.2. Model of the preScission™ assay

In this study, I worked towards establishing a novel method for detecting protein-protein interactions (PPIs). This method, named the preScission™ assay, relies on proteolysis of a target substrate to confirm protein-protein interactions (concept based on a discussion with Frank McCormick). The figure below outlines the approach (Figure 2).

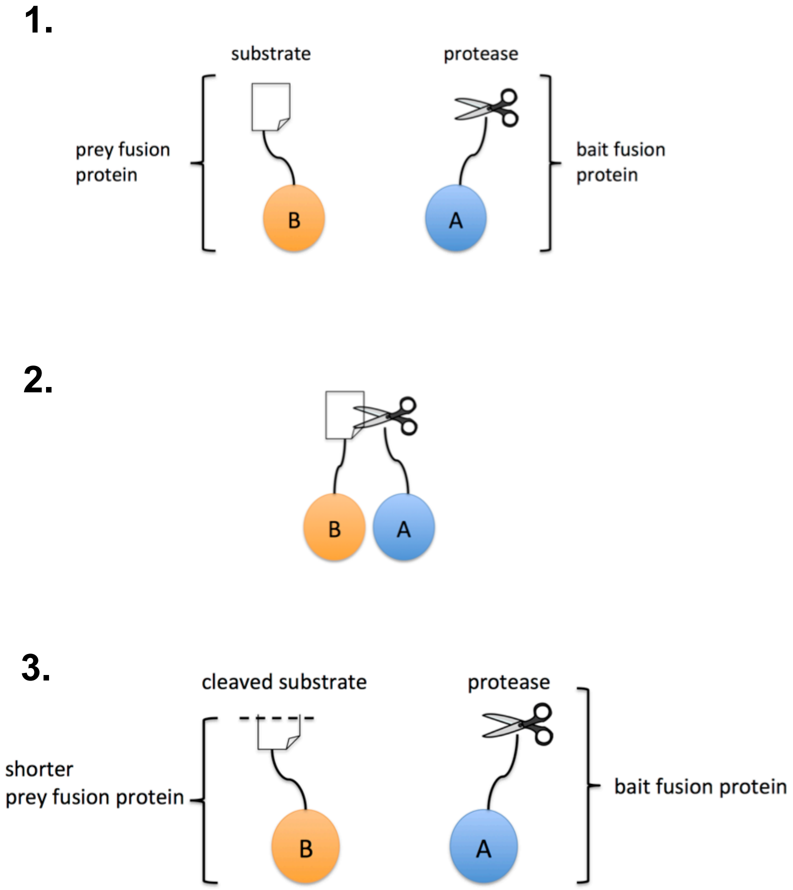

Figure 2: Model of the preScission assay

1: A protein of interest (A=bait) is fused to a preScission protease. This construct acts as a bait fusion protein. A putative interaction partner (B=prey) is fused to a preScission substrate, together forming the prey fusion protein.

2: Upon coexpression in mammalian cells, protein A interacts with B. In the process, the preScission protease is brought into close proximity of its substrate, promoting cleavage.

3: Accumulation of cleaved prey fusion protein, detectable via western blot, suggests an interaction between A and B.

Our aim was to test whether the system was able to detect stable PPIs between PP2A-Cα and PP2A-B55α and subsequently move on to identify transient interactions in further studies. Therefore, we expressed „bait“ and „prey“ fusion proteins in human embryonic kidney cells. The „bait“ fusion constructs, on the one hand, contained the preScission™ protease fused via a glycine linker to a PP2A-B55α subunit (bait = A). The „prey“ fusion constructs, on the other hand, contained a preScission™ substrate site, C3S6, fused via a glycine linker to the PP2A-Cα subunit (prey = B). (Figure 3). Our model proposed that when the Cα prey interacts with the B55α bait, the preScission™ protease is brought into close proximity of its target site. This allows the protease fused to the bait to cleave the substrate fused to the prey. Analyzing the accumulation of cleaved prey fusion protein after induction of the bait fusion protein expression should therefore be an indicator of the interaction between the ectopically expressed PP2A-Cα and PP2A-Bα subunits. It is important to mention that the tested interaction is known to be stable.

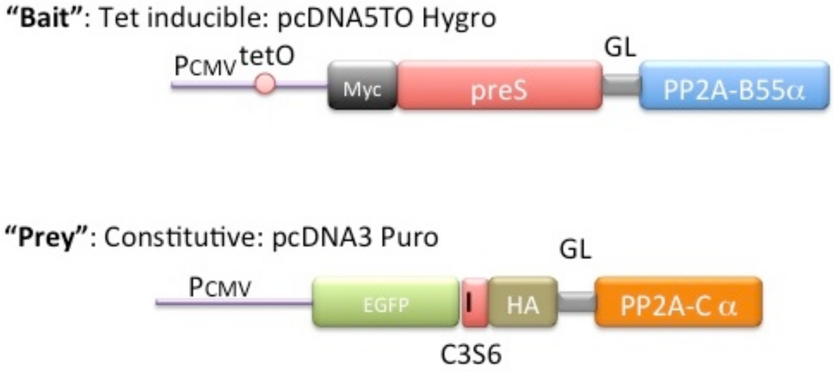
"Bait": Tet inducible: pcDNA5TO Hygro
PCMV
tetO
Myc
preS
GL
PP2A-B55α
"Prey": Constitutive: pcDNA3 Puro
PCMV
EGFP
HA
GL
PP2A-C α
C3S6

Figure 3: Expression constructs including the promoter region for the PreScission™ protease assay

A: The bait construct containing the coding sequence of a myc-tagged preScission™ protease (preS) fused via a glycine linker (GL) to the PP2A-B55α subunit (bait) under control of a tetracycline/doxycycline-inducible CMV promoter.

B: The prey construct containing the coding sequence of an enhanced green fluorescent protein (EGFP) followed by the preScission™ substrate (C3S6), a hemagglutinin tag (HA), a glycine linker (GL) and the PP2A-Cα subunit (prey) under control of a constitutive CMV promoter.

1.2.3. Structure and function of Human rhinovirus type 14 3Cpro/ PreScission™ protease

Human rhinoviruses, members of the family picornaviridae, possess a single stranded positive-sense RNA genome consisting of 7.2 -8.5 kbp. Many RNA viruses, including Human rhinovirus type 14, use proteolytic processing of a large precursor polyprotein as part of their replication strategy. By doing so, they exploit several evolutionary advantages such as a reduced genomic content as well as the potential to circumvent constraints of the mechanisms of transcriptional and translational regulation by the host cell. (*Kräusslich and Wimmer, 1988; Kay and Dunn, 1990; Lawson and Semler, 1990*).

In picornaviridae, the proteolytic steps involved in processing the polyprotein can be divided into three categories: the release of the capsid precursor P1 by protease 2A, autocatalytic cleavage in the VP0 protein and, the most abundant of all, processing involving the 3C protease (*Matthews et al, 1994*). $3C^{pro}$, a 182 amino acid protein, is predicted to cleave its polyprotein at six specific Gln-Gly junctions and possibly also at one Gln-Ala and one Glu-Gly junction (*Stanway et al, 1984*). Interestingly, it is itself a product of autocatalytic cleavage from the polyprotein. The majority of $3C^{pro}$ proteins are covalently attached to $3D^{pol}$ throughout the viral infection. Together, they fulfill a variety of functions crucial to viral replication, such as assisting in circularization of the viral genome (*Herold and Andino, 2001*) and initiating translation elongation by facilitating uridylylation of the viral VPg primer (*Yang et al, 2004*).

The mechanism of substrate proteolysis mediated by picornaviral $3C^{pro}$ relies on a cysteine residue found in the motif Gly-X-Cys-Gly-Gly at the active site of the protease. In human rhinovirus type 14, this cysteine (Cys-146) forms a catalytic triad together with a histidine (His-40) and a glutamic acid (Glu-71) (*Matthews et al, 1994*). These residues are located in a long shallow groove surrounded by two six-stranded ß-barrels, which constitute the two domains of the 3C protease (Figure 4). Structurally and probably mechanistically, this picornaviral cysteine protease is related to trypsin-like serine proteases, substituting cysteine for serine as the nucleophile at the active site.

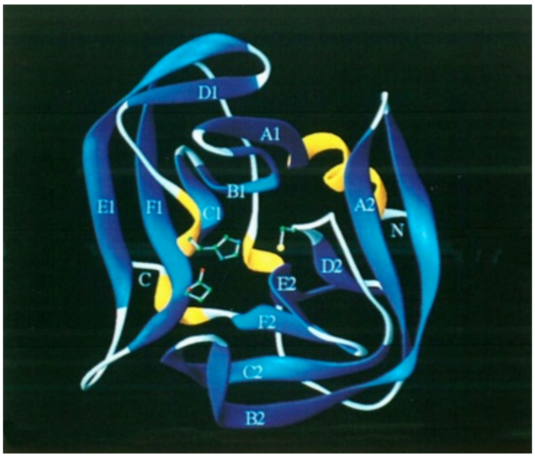

Figure 4: Ribbon drawing of $3C^{pro}$
"ß-strands are blue and the helical secondary structures yellow. Also shown are side chain positions of the three members of the catalytic triad, Cys-146, His-40 and Glu-71." (direct quotation from *Matthews et al, 1994. Reprinted with kind permission from the Elsevier publishing company.*) N = N-terminus, C = C-terminus, beta strands are labelled A1 through F2.

By tagging $3C^{pro}$ with a glutathione-S-transferase tag (GST-tag), Walker et al created a fully functional fusion protein that is easily purified via its affinity for glutathione and detectable on a western blot with an anti-GST antibody (*Walker et al, 1994*). This GST-tagged $3C^{pro}$ was named the preScission™ protease.

1.2.4. *In vitro substrate binding to Human rhinovirus type 14 3Cpro*

In vitro biochemical experiments have demonstrated the ability of purified $3C^{pro}$ to cleave a variety of short peptide substrates (*Long et al, 1989; Cordingley et al, 1990*). Long et al have suggested a minimal substrate sequence required for effective cleavage consisting of residues P_5-Val/Thr-P_3-P_2-Gln-*Gly-Pro (asterisk marks the cleavage site). Cordingley et al state that, while retaining a residue at position P_5 resulted in a better substrate by an order of magnitude, a minimum substrate consisting of only 6 amino acids ranging from P4 to P2' is sufficient. Interestingly, the rate of substrate cleavage determined in the experiments by Long and Cordingley varied by several orders of magnitude, depending largely on the identity of crucial residues at P4, P1' and P2' and on residues flanking the minimum core sequence. *In vitro* experiments (*Cordingley et al, 1990*) have also demonstrated complete specificity to the Gln-Gly scissile bond, casting doubt on the idea by Stanway et al that Gln-Ala and Glu-Gly junctions are cleaved *in vivo* (*Stanway et al, 1984*). Alternatively, this could perhaps suggest that factors other than the primary substrate sequence contribute to proteolysis in vivo (*Cordingley et al, 1990*).

A model for the binding of a substrate to $3C^{pro}$ has been constructed by superposing the related trypsin/Bowman-Birk-inhibitor complex on the crystal structure of $3C^{pro}$ and subsequent energy minimization (*Matthews et al, 1994*, Figure 6).

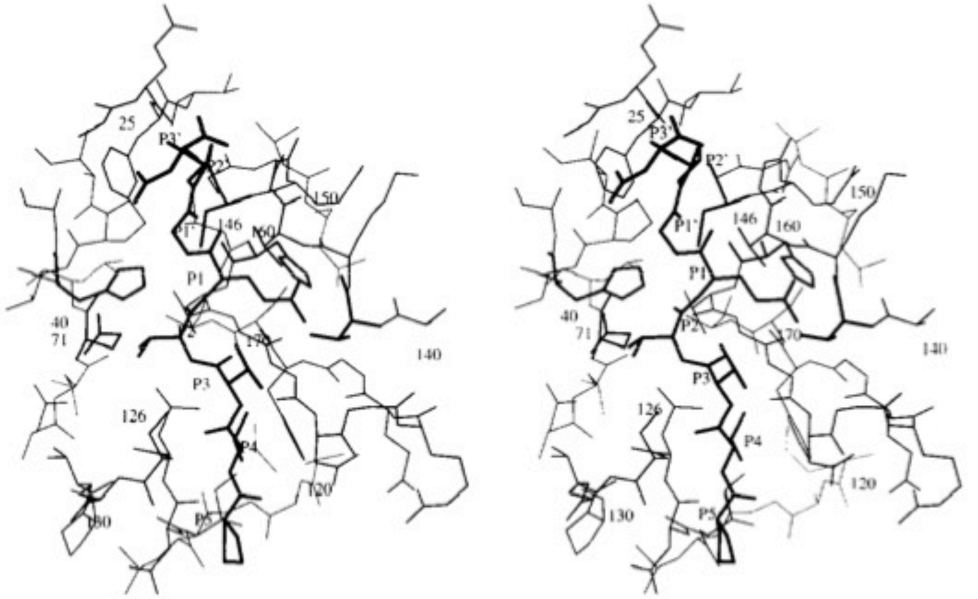

Figure 6: "Stereo representation of a model for an 8 amino acid synthetic peptide substrate of sequence PVVVQ*GPN bound to $3C^{pro}$. Residues 40, 71, 141, 146 and 160 as well as the peptide substrate are drawn with thick bonds." (direct quotation from *Matthews et al, 1994. Reprinted with kind permission from the Elsevier publishing company.)*

As Matthews and colleagues suggest (*Matthews et al, 1994)*, the substrate is assumed to bind in an elongated cleft, where the glutamine side chain at position P_1 engages in hydrogen bonding with two highly conserved residues of the enzyme, Thr-141 and His-160. P_2 is positioned in a spacious cavity, allowing even bulky amino acid side chains to be accommodated. The side chains of the residues P_3 and P_5 point away from the surface of the protease, which may serve as an explanation for the observation that a wide variety of residues are tolerated at these positions. The amino acid positioned at P_4 must have a small and relatively hydrophobic side chain to be accommodated by the hydrophobic side chains of residues Ile-124, Leu-126 and Phe-169 of the protease. Interestingly, the model suggests that the glycine and proline residues located at P'_1 and P'_2 turn the substrate towards another canyon, which has no structural counterpart in serine proteases. Therefore, it is assumed that the glycine at P'_1 is needed because of main chain conformational requirements and not to avoid potential steric clashes of larger side chains with nearby protein residues.

A noteworthy feature of the 3C protease is the loop comprising residues 140-146. This loop displays a high mobility, which Matthews and colleagues suggest could be reduced upon substrate binding (*Matthews et al, 1994)*. This feature might explain the high K_m values that have been determined even for the best synthetic $3C^{pro}$ peptide substrates by the Long and Cordingley groups. Moreover, this feature makes $3C^{pro}$ a promising candidate for detecting PPIs using our preScission™ assay, where we believe a high K_m is required, a hypothesis that is based on the properties of the HKMT used to detect transient PPIs in the M-Track assay. In this study, we aimed at comparing the kinetic parameters of two preScission™ substrates, which we named C3S5 ($3C^{pro}$ substrate 5) and C3S6 ($3C^{pro}$ substrate 6). Kinetic parameter values of C3S5, consisting of the amino acid sequence LEVLFQ*GP, were unknown. For C3S6, consisting of amino acids RPVVVQ*GP, a K_m of 3,1 mM and a V_{max} of 5,0 $\mu mol * min^{-1} * mg^{-1}$ had been determined (*Long et al, 1989)*.

1.3. Kinetic considerations for the preScission™ assay

In this study, we used the preSission protease in combination with substrate C3S6, We believed that the proposed kinetic properties of the enzymatic reaction, that is a low affinity coupled with a high turnover, are beneficial for detecting short-lived PPIs. Low affinity, on the one hand, ensures that the substrate is not cleaved extensively by the enzyme independently of an interaction between the proteins of interest. High turnover on the other hand, increases the chance of detecting short-lived interactions. Of all the tested synthetic peptides, $3C^{pro}$ displayed the lowest affinity towards C3S6, while maintaining a high turnover, which made it the most promising candidate for the preScission™ assay (*Cordingley et al, 1990 and Long et al, 1989*).

Estimating kinetic parameters such as affinity and turnover is important to understand the mechanism of the preScission™ assay. We wanted to determine the unknown kinetic parameters of the preScission™ reactions using various substrates as well as to confirm the data provided in the publications by Long and Cordingley. By doing so, we also wanted to identify further substrates of the preScission™ protease in the future, whose kinetic parameters might be more suited for detecting transient PPIs.

1.3.1. Principles of Michaelis-Menten Kinetics

In this study, we work under the assumption that the proteolysis reaction mediated by the preScission™ protease follows Michaelis-Menten kinetics. Leonor Michaelis and Maud Menten published a mathematical model to describe the kinetics of non-allosteric enzymatic reactions with a single substrate (*Michaelis and Menten, 1913*). It has been widely used in biochemical studies to determine kinetic parameters ever since. The model is able to mimic the experimental observation that the rate of change of product concentration depends on the concentration of substrate in a non-linear way. For their model, Michaelis and Menten assumed that when enzyme is added to substrate, they together form an enzyme-substrate complex, [ES], as a transition state of the reaction. Subsequently, the enzyme, which is not consumed by the reaction, releases the product. Britton Chance later experimentally confirmed the existence of [ES] (*Chance, 1943*). The reaction is described as follows:

$$E+S \underset{k'_1}{\overset{k_1}{\rightleftharpoons}} [ES] \underset{k'_2}{\overset{k_2}{\rightleftharpoons}} [EP] \underset{k'_3}{\overset{k_3}{\rightleftharpoons}} E+P$$

The rate of each step of the reaction depends on kinetic constants, termed k. Note that every step of the enzymatic reaction is in principle reversible. k_1 describes the association of the enzyme and substrate. k_2 describes the conversion of substrate to product. The dissociation of the enzyme-product complex is described by k_3. The rates for the corresponding reverse reactions are named k'_1, k'_2 and k'_3. When working with the Michaelis-Menten model, several assumptions have to be made and specified conditions have to be met. Most importantly, the rates have to be measured at the beginning of the reaction under conditions when far more substrate than enzyme is present. Under these conditions, the reaction behaves as if it were irreversible, as there is essentially no product present that could be converted back to substrate, so k_3 and k'_3 are assumed to be equal to zero. The chemical equation can then be simplified as follows:

$$E+S \underset{k'_1}{\overset{k_1}{\rightleftharpoons}} [ES] \overset{k_2}{\rightarrow} P+E$$

The rate constant k_2 in this equation is also known as the turnover number (k_{cat}) (*Briggs and Haldane, 1925*). Note that k_{cat} is commonly but erroneously referred to as a number although it is in fact a rate (i.e. "a measure, quantity or frequency, typically one measured against another quantitiy or measure", *Oxford Dictionaries, 2013*) and should therefore be addressed as "turnover rate" or "turnover frequency" (*Boudart, 1995*). In a popular approach, it is assumed that the concentration of the transition complex does not change on the time-scale of product formation (*Briggs and Haldane, 1925*). Mathematically, this leads to the following description (*Keener et al, 2004*):

$$\upsilon = \frac{d[P]}{dt} = \frac{V_{max}[S]}{K_m + [S]}$$

and

$$V_{max} = k_{cat}[E]_0$$

where "v" is the rate at which the product [P] is formed, V_{max} is the maximum reaction velocity, K_m is the Michaelis constant, [S] is the substrate concentration, k_{cat} is the turnover number and $[E]_0$ is the concentration of enzyme.

The Michaelis constant, K_m, is described as the substrate concentration at which the reaction rate is at half-maximum. In a common simplification, K_m is interpreted as an inverse measure of enzyme-substrate affinity, where a small K_m corresponds to a high affinity and a large K_m to a low affinity (*Lehninger et al, 2005*). It is notable that the quasi-steady state approximation is only valid if

$$\epsilon_m = \frac{[E]_0}{[S]_0 + K_m} \ll 1$$

Therefore, it holds true when the substrate concentration far exceeds the enzyme concentration or when the K_m is very large (*Murray, 2002; Segel and Slemrod, 1989*). Interestingly, the Michaelis and Menten model does not take pH dependence into consideration, making it one of the most practical models to date (*Gunawardena, 2012*).

The value of k_{cat}/K_m is often used as a measure of how efficiently an enzyme converts substrate into product. Kinetic parameters of enzymes can vary widely, resulting in a large range of catalytic efficiencies (*Mathews et al, 1999*). In principle, it is possible for two enzymes to have the same k_{cat}/K_m value, but different substrate affinities (K_m) and turnover numbers (k_{cat}). Therefore, it is important to consider each of the kinetic parameters individually when investigating enzymatic mechanisms.

1.3.2. Determining kinetic parameters of Michaelis-Menten enzymatic reactions

The method to determine kinetic parameters typically consists of running a series of enzyme assays at varying substrate concentrations. By measuring the velocity of the reaction at an early stage, one can obtain values approximating the initial velocity of the reaction, $v_{0.}$ At this early stage, it is assumed that the enzyme-substrate complex has formed, but that the substrate concentration is constant. This fulfills the requirement of both the equilibrium and the quasi-steady-state approximation. By plotting the initial reaction rate against the substrate concentration, one can observe that the rates asymptotically approach a maximum value, V_{max}. This manifests itself in a graphical representation as a hyperbolic curve from which the kinetic parameters can be obtained via non-linear regression (*Murray, 2002*).

The most accurate way of performing non-linear regression is via computational analysis. Graphical methods of linearisation are useful for visualization but distort the error structure of the data (*Greco et al, 1979*). Lineweaver and Burk developed one linearisation technique that is commonly used in the literature (*Lineweaver and Burk, 1934*). In this representation, both ratios of the Michaelis-Menten equation are reciprocated, yielding

$$\frac{1}{V} = \frac{K_m + [S]}{V_{max}[S]} = \frac{K_m}{V_{max}} \frac{1}{[S]} + \frac{1}{V_{max}}$$

Graphically, this changes the hyperbolic curve to a straight line with the equation y= mx * c (Figure 8).

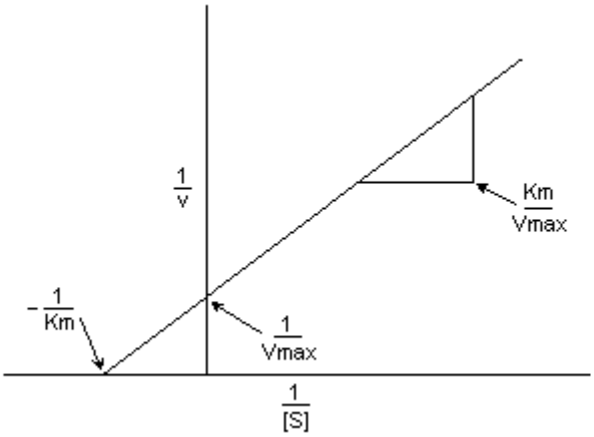

Figure 8: Lineweaver-Burk plot. The gradient of the curve denotes K_m/V_{max}. The point where the line intercepts the y-axis is equivalent to $1/V_{max}$ and the x-intercept represents $-1/K_m$. (©Diberri, CC-BY-SA-3.0, GFDL)

As measurements cannot be taken at a negative substrate concentration, the x-intercept is an extrapolation of the measurements taken at positive substrate concentrations. Therefore, the Lineweaver-Burk plot can provide false estimates of V_{max} or K_m because the importance of measurements at low substrate concentrations is skewed. (*Dowd and Riggs, 1964*; *Tseng et al, 1990*). Therefore, computationally derived non-linear regression is the preferable method for calculating kinetic constants.

1.3.3. Enzyme Assays - Types and Uses

In vitro enzyme assays are vital for studying enzyme kinetics. One way of classifying enzyme assays is by their continuity of measurement.

Continuous assays, on the one hand, give constant reading of enzyme activity and include widely used methods such as spectrophotometric, calorimetric, chemiluminescent and fluorometric assays (*Bergmeyer, 1974*). Fluorometric assays rely on a change in fluorescence when a substrate is converted into product. The use of this assay is restricted to fluorescent substrate compounds and can suffer from interference caused by impurities and instability of the fluorescent compound. However, such assays are in general more sensitive than most spectrophotometric approaches (*Passonneau, 1993*).

In discontinuous enzyme assays, on the other hand, samples are taken from the enzymatic reaction at intervals and analyzed for their product formation or substrate consumption using radiometric or chromatographic assays, for example. Depending on the approach used, these methods can achieve great sensitivity (*Churchwella et al, 2005*). Both the Long as well as the Cordingley group used a reverse phase chromatographic approach to determine kinetic parameters of the cleavage reaction involving $3C^{pro}$ and short synthetic peptide substrates (*Long et al, 1989; Cordingley et al, 1990).* Here I describe the use of a fluorometric assay as well as a novel discontinuous assay to determine the kinetic parameters of the preScission™ reaction.

1.4. Using a Förster Resonance energy transfer (FRET) enzyme assay to determine kinetic parameters of preScisson reactions

1.4.1. Mechanism of FRET

In this study, we used a FRET-based approach to try to determine kinetic parameters of the preScission™ proteolytic reaction. FRET is a quantum mechanical process first described by Theodor Förster (*Förster, 1948*). It involves the direct radiationless transfer of energy from a donor to an acceptor chromophore. In general, four conditions must be fulfilled for FRET to occur: First, the emission spectrum of the donor must overlap with the absorption spectrum of the acceptor. Second, the donor and acceptor molecule must be in close proximity, in a range of approximately one to ten nanometers. Third, the emission dipole moment of the donor, the absorption dipole moment of the acceptor as well as their separation vectors must be in a mutual orientation. Fourth, the donor molecule must have a sufficiently high quantum yield (*Periasamy, 2001*). In FRET, the donor chromophore is first brought to an excited state. When returning to its original state, the chromophore transfers energy to a nearby acceptor chromophore through non-radiative dipole - dipole coupling (*Helms and Volkhard, 2008*). According to the Förster equation, FRET efficiency (E) is inversely proportional to the sixth power of the distance between the donor and the acceptor.

$$E = \frac{1}{1 + (r/R_0)^6}$$

This feature makes FRET sensitive to very small gaps between the chromophores. However, the sensitivity rapidly decreases for gaps exceeding the Förster distance (R_0), at which the transfer efficiency between the donor and the acceptor is 50%. The Förster distance is the distance at which half of the energy of the donor is transferred to the acceptor (*Harris, 2010*). FRET has many applications in modern biochemistry. Its main use is to study molecular dynamics of protein-protein interactions, protein-DNA interactions and protein conformational changes. One popular way to measure FRET efficiency is to measure the intensity of the acceptor emission (*Clegg, 2009*).

When the donor is in close proximity to the acceptor, the acceptor emission increases due to intermolecular FRET. Separating the donor from the acceptor results in a decrease of FRET, but an increase of donor emission.

1.4.2. Using fluorescent proteins to study FRET

Fluorescent proteins are commonly used as donor and acceptor molecules in FRET. Many of the currently available proteins are derivatives of the green fluorescent protein (GFP) first isolated from the jellyfish *Aequorea victoria* by Shimomura and colleagues (*Shimomura et al, 1962*). In vivo, GFP is excited by aequorin, which is a bioluminescent protein of the jellyfish (reviewed by *Tsien, 1998*). Aequorin binds Ca^{2+} ions, which induce a conformational change in the protein, leading to oxidation of its prosthetic group coelenterazine. When the excited molecule relaxes to the ground state, energy of this relaxation is transferred to GFP, which in turn undergoes an excitation and relaxation reaction, resulting in the emission of green light (*Morise et al, 1974*).

Purified wild-type GFP has a major excitation peak at 395 nanometers and a second minor peak at 475 nanometers. Two point mutations (S65T and F64L) introduced by Heim and Thastrup respectively improved the spectral characteristics of GFP and allowed its practical use in mammalian cells (*Heim et al, 1995; Thastrup et al, 2001*). This new protein, named EGFP, displayed increased photostability and fluorescence, a shift of the major excitation peak to 488 nm and a high folding efficiency at 37 °C.

Further mutations in the EGFP protein resulted in a variety of color mutants (*Heim and Tsien, 1996),* subsequent optimizations yielded the enhanced versions of the proteins used in this study, an enhanced cyan fluorescent protein and an enhanced yellow fluorescent protein (*Clontech, 2002*). ECFP has its major excitation peak at 434 nm and its major emission peak at 477 nm. The excitation peak of EYFP, on the other hand, is at 514 nm and the emission peak at 527 (*Patterson et al, 2001*). Due to the overlap in the emission spectrum of ECFP and the absorption spectrum of EYFP, these two fluorophores constitute a suitable pair for FRET analysis.

In this study, we attempted to determine kinetic parameters of preScission™ reactions by using a FRET approach that involves the fusion of ECFP and EYFP fluorophores to a preScission™ substrate. Mitra et al were the first to fuse two fluorophores with overlapping emission/absorption spectra to opposite ends of a protease substrate sequence. Upon addition of the protease, they noted a decrease in FRET (*Mitra et al, 1996).* Felber and colleagues adopted this approach, fusing CFP to YFP with various protease substrate sequences (*Felber et al, 2004*). In their study, they determined optimum conditions for expression of CFP-YFP fusion proteins in *E.coli*. Furthermore, they provided conclusive data on the optimal pH (8.5) and buffer salt concentrations (20mM) during FRET measurement, showing that both factors have a significant influence on FRET efficiency. Interestingly, the efficiency was hardly influenced by temperature in the range of 4°C to 37°C. The CFP-YFP system also worked efficiently with substrate linkers consisting of up to 25 amino acids, which bridge a distance of up to 5 nanometers between the two fluorophores. Longer linkers were, however, not tested in their study. Using increasing concentrations of CFP-YFP fusion proteins, they determined that FRET is relatively stable in a range of 0.05 µM to 25 µM, but slightly increases at higher concentrations. They suggest that intermolecular FRET could account for this problem, possibly due to dimerization of CFP and/or YFP. GFP, for example, is known to dimerize at concentrations greater than 100 µM (*Mitra et al, 1996*), suggesting a similar behaviour of the closely related cyan and yellow fluorescent protein.

In addition to establishing appropriate FRET conditions, Felber et al showed that the decrease of FRET efficiency upon addition of the protease correlates with the reaction velocity. Therefore, they were able to deduce kinetic parameters of the reaction. As a measure of FRET efficiency, they used the ratio between the emission measured at 528 nm (YFP emission peak) and 485 nm (CFP emission peak) upon excitation at 440 nm (close to CFP absorption peak). Uncleaved CFP-substrate-YFP fusion proteins showed the following FRET characteristics. 1) The CFP emission of these proteins was decreased compared to CFP alone due to energy transfer to YFP. 2) YFP emission was increased due to YFP excitation by the proximal CFP. Separation of CFP and YFP by protease cleavage of the substrate linker eliminated FRET. This was indicated by a decreased FRET ratio, which approximated the value of an unconjugated mixture of CFP and YFP of the same concentration. To analyze enzyme kinetics, they incubated enzyme ro CFP-substrate-YFP at a ratio of 1:30 to

1:60. The substrate concentration in the experiments was far below the estimated K_m. By continuously recording the change in FRET ratio over time, Felber et al were able to calculate k_{cat}/K_m ratios of several enzyme substrate pairs, using the following formula, assuming first-order Michaelis-Menten conditions:

$$\frac{-dS}{dt} = \frac{k_{cat}}{K_m}\,[E_t][S]$$

In this formula, -dS/dt refers to the velocity of substrate conversion; E_t and S refer to total enzyme and initial substrate concentration respectively. To validate the system, the increase of CFP emission was compared to the amount of cleaved CFP-substrate-YFP, determined via densitometric analysis of coomassie-stained SDS-PAGE. There was an excellent correlation between fluorescence appearance at 485 nm and CFP-substrate-YFP hydrolysis. The authors also suggest that, in principle, the K_m of enzymatic reactions could be detected directly. For a confident estimate of V_{max}, the highest tested substrate concentrations should far exceed K_m. However, as stated before, intermolecular FRET could interfere with the measurements when trying to determine FRET efficiency at high substrate concentrations.

1.5. Using a discontinuous enzyme assay coupled with in-gel western detection to determine enzymatic activity

In addition to the FRET approach, I attempted to determine kinetic parameters of the preScission™ reaction by using a discontinuous enzyme assay method. I took samples of a proteolytic reaction at specified time points and separated the product from the substrate via SDS-PAGE. I subsequently analysed the accumulation of product via an in-gel western blotting approach using fluorescently-labeled antibody probes for detection.

In general, horseradish peroxidase-coupled enhanced chemiluminescence is an often-used technique for detecting proteins on western. Although the technique has a high sensitivity and is easy to use, it has several limitations. The enzyme/substrate kinetics inherent to the process can compromise the quantification of proteins on a western blot because of the limited linear range of the detection and the limited reproducibility of measurements (*Schutz-Gschwender et al, 2004*).

An alternative to chemiluminescence is the use of fluorescently-labeled antibody probes for western detection. Several studies have described the use of antibodies directly conjugated to fluorophores such as Cy3, Cy5, fluorescein and PBXL (*Amersham 2001; Fradelizi et al, 1999; Gingrich et al, 2000; Morseman et al, 1999*). Because no enzymatic reaction is involved in detecting fluorescence, these methods offer the potential for an improved linearity and accuracy of quantification. A significant drawback of these fluorophores, however, is that they are activated in the visible light range. This significantly decreases the sensitivity of the method, as biomolecules as well as western blot membranes are likely to have substantial autofluorescence in the visible light region, leading to extensive background signals. Interestingly, this autofluorescence is much lower in the near-infrared region of the spectrum (*Patonay et al, 1991; Sowell et al, 2001).* Schutz-Gschwender et al describe the use of two IR fluorophores coupled to secondary antibodies to detect proteins on a western blot using a laser imager as a detector (*Schutz-Gschwender et al, 2004).* They report several advantages of this system over chemiluminescence such as a wide quantitative linear range, high sensitivity and a low blot-to-blot variation. Even when compared to studies using visible fluorophores (*Gingrich et al, 2000*), this method yielded 200-400-fold higher detection sensitivity.

Unfortunately, the process of western blotting itself suffers from inherent drawbacks that introduce errors into the quantification process. Proteins that have a high molecular weight, or that are hydrophobic or have post-translational modifications may transfer inefficiently from gel to membrane. Low molecular weight proteins, on the other hand, may transfer extensively, causing them to pass through the membrane (*Henderson et al, 1992*). Detection of proteins in-gel, directly after electrophoresis, removes these problems, as it obviates the blotting step. Using the system developed by LI-COR biosciences, proteins have been identified in-gel with relatively little effort and high sensitivity (*Schutz-Gschwender et al, 2004).* Under appropriate conditions, this method is capable of detecting proteins down to the nanogram range with relatively little noise/background. The infrared scanner read-out allows quantification of the proteins of interest, although the authors of the protocol caution that in-gel detection may not always be quantitative (*Odyssey in-gel western detection protocol, 2006*). Furthermore, it must be considered that gel loading and handling may still introduce errors or cause variations from blot to blot.

In this study, we use the Odyssey in-gel western approach to study the enzyme kinetics of preScission™/substrate reactions.

1.6. Aim of the thesis

The primary aim of this thesis was to develop a novel preScission™ protease-based approach to detect transient interactions in mammalian cells. According to our model of the assay based on the results obtained from M-Track (*Zuzuarregui et al, 2012*), enzyme-substrate reactions with high K_m and k_{cat} values are favorable for detecting transient protein-protein interactions.

Therefore, the first aim of the study was to determine the kinetic parameters of preScission™ reactions with the hope of identifying a substrate with the desired properties. I applied two techniques to do this: A FRET-based approach and a discontinuous enzyme assay coupled with in-gel western blotting.

To test the method, I tried to confirm the stable interaction between two subunits of mammalian protein phosphatase 2A, named PP2A-B55α and PP2A-Cα, aiming at identifying transient interactions in further studies. The preScission™ protease and one of its substrates, C3S6, functioned as an enzyme/substrate pair in this assay. The subsequent step was therefore to test whether the kinetic parameters of the preScission™/C3S6 reaction were suitable for detecting protein-protein interactions such as the ones between PP2A-B55α and PP2A-Cα in mammalian cells.

2. Materials and methods

2.1. Working with Bacteria

2.1.1. Solutions and Media

LB-medium: 5g Tryptone (AppliChem #A1553); 2.5g Yeast extract (AppliChem #A1552); 2.5g NaCl; Dissolve in 500ml ddH$_2$O, autoclave immediately and store at RT.

LB-agar plates: 5g Tryptone; 2.5g Yeast extract; 2.5g NaCl; 7.5g Agar (AppliChem #A0949); Dissolve in 500ml ddH$_2$O, autoclave immediately, cool to 50°C, add appropriate antibiotics, pour plates and store plates at 4°C.

Ampicillin-stock (100x) (Gerbu #1046): Dissolve 10mg/ml in ddH$_2$O. Filter sterilize through a membrane filter with a pore size of 0.2µm and store aliquots at -20°C.

Chloramphenicol-stock (1000x) (Serva #16785): Dissolve 34mg/ml in 96% ethanol and store at -20°C.

200mM IPTG-stock: Dissolve 9.35g IPTG in 200ml of ddH$_2$O and store aliquots at -20°C.

Bacterial strains:

XL1blue: *recA1 endA1 gyrA96 hsdR17 supE44 relA1 lac [F΄proAB lacIqZΔM15 Tn10 (TetR)*]. The bacterial strain is tetracycline resistant.

Rosetta(DE3)pLysS: *F΄ompThsdSB(rB-mB-) gal dcm lacYI(DE3) pLysSRARE (CamR).* The bacterial strain is chloramphenicol resistant.

2.1.2. Growth of bacteria:

Bacterial strains were grown in LB-medium or on LB-agar plates at 37°C. For XL1blue, the medium contained 100µg/ml ampicillin. For Rosetta(DE3)pLysS, the medium contained 100 µg/ml ampicillin and 25µg/ml chloramphenicol.

2.1.3. Transformation of XL1-blue competent Escherichia coli

XL1-blue competent *E.coli* cells were thawed on ice. 90 μl of this suspension were gently mixed with 10 μl of ligated plasmid suspension (contains approximately 50ng plasmid DNA), incubated on ice for approximately 30 minutes and then plated on pre-warmed LB-amp-plates (100 μg/ml). The plates were incubated at 37 °C overnight and subsequently stored at 4 °C.

2.1.4. Freezing/thawing of bacteria:

For freezing, 200μl of glycerol and 800µl of bacterial overnight culture were mixed thoroughly and stored at -80°C. For thawing, the freezing stock was scraped with a pipette tip and the scraped material was inoculated in 5ml of LB-medium including the appropriate antibiotics o/n at 37°C on a shaker.

2.1.5. Bacterial expression of fusion proteins

Rosetta - competent *E.coli* cells were thawed on ice. 100 μl aliquots were mixed with 500ng plasmid and incubated on ice for 20 min. After a heat-shock at 45°C for 1 min, 1 ml of LB without antibiotics was added and the solution was incubated for 1 hour at 37°C while shaking. Subsequently, the solution was mixed with 4 ml LB with ampicillin (100μg/ml) and chloramphenicol (25μg/ml) and incubated over night at 37°C while shaking. The following day, the mixture was diluted 1:50 in LB with ampicillin and chloramphenicol to the requested volume and grown to an OD_{600} of 0.5. Subsequently, IPTG was added to induce the expression of the protein of interest and the cells were grown under the following conditions that were established before and allowed a high protein yield: For the expression of CFP and YFP, the medium was supplemented with 1 mM IPTG and the cells were grown at 37°C for 3 hours. For "CFP-YFP" and all "CFP-substrate-YFP" proteins, the optimum conditions were 0.1 mM IPTG, and incubation at 22°C over night. An uninduced sample always served as a control. Proteins were subsequently extracted and purified (see 2.4.4. "Purification of bacterially expressed proteins")

2.2. Working with DNA

2.2.1. Solutions

50x TAE: 484g Tris (2M); 114ml acetic acid, 200ml 0.5M EDTA pH 8.0; Dissolve and fill up to 2l.

1x TAE: 20 mM Tris acetate and 20 mM Tris base, 1mM EDTA

6x DNA loading dye (Fermentas #R0611): 4M Urea, 50% (w/v) Sucrose, 50mM EDTA ph 7.0, 1% w/v Bromphenol blue

GeneRuler 1kb plus DNA Ladder (Thermo Scientific #SM1334)

Mini-preparation solutions:
Solution 1: 50mM glucose, 25 mM Tris-Cl (pH 8.0), 10 mM EDTA (pH 8.0)
Solution 2: 0,2M NaOH, 1%SDS
Solution 3: 3M potassium acetate, 2M glacial acetic acid

RNAse A (Sigma #R-5125): 10mg/ml RNAse A was dissolved in 10mM sodium acetate pH5.2, heated up to 100°C for 15 minutes and cooled down to RT. The pH was adjusted by adding 0.1 volumes of 1M Tris-Cl pH7.4 and aliquots were stored at -20°C.

2.2.2. Minipreparation: QIAprep™ Spin Miniprep Kit (Qiagen #27106)

An overnight culture was prepared by inoculating 4-6 ml of LB medium + Ampicillin (100 μg/μl) with a single colony picked from a freshly streaked plate. Isolation of DNA was then performed according to the manufacturer´s protocol.

2.2.3. *Plasmid DNA isolation using alkaline lysis*

Cells were grown and harvested via centrifugation as described in the minipreparation protocol above. The resulting pellet was then resuspended in 250 μl of pre-cooled Miniprep-solution 1, then 250 μl of Miniprep-solution 2 was added and the solution was mixed by inverting the tube 4-6 times. 350 μl of pre-cooled Miniprep-solution 3 were then immediately added and thoroughly mixed by inverting the tube another 4-6 times. The lysate was cleared by centrifugation at 13.000 rpm for 10 minutes. DNA was precipitated by mixing 700 μl of the supernatant with 500 μl isopropanol and subsequent incubation at room temperature for at least 30 minutes. The suspension was then centrifuged at 14.000 rpm for 15 minutes, the supernatant was discarded and the pelleted DNA was washed by adding 500 μl of 70% ethanol and subsequent centrifugation for 5 minutes at 14.000 rpm. To remove any residual ethanol, the supernatant was thoroughly discarded and the pellet was incubated at 37 °C with the microcentrifuge lid open to allow evaporation. The pellet was then resuspended in 50 μl of H_20 with pre-added RNAse (20μg/ml) and stored at -20 °C.

2.2.4. *Plasmid Midi preparation using PureYield™ Plasmid Midiprep System (Promega #252219)*

For large amounts of plasmid DNA preparation the Pure Yield™ Plasmid Midiprep System kit was used. The guidelines provided by the supplier´s protocol were used.

2.2.5. *Restriction Digest*

For every μg of DNA, 1 – 5 units of the requested restriction enzyme were used to digest the plasmid. 10x enzyme buffer, 100x BSA, H_2O and restriction enzyme were added in an Eppendorf tube to a total volume of 100 μl for a preparative digest or 30 μl for an analytical digest. The resulting solution was gently mixed and incubated at the requested temperature for approximately 1 hour (analytical digest) or overnight (preparative digest). The solution was subsequently mixed with appropriate amounts of loading dye. The result of the digest was analyzed via separating the fragments on an agarose gel.

2.2.6. Gel Elution: Promega SV Gel and PCR-clean-up System

Gel elution was performed according to the manufacturer´s protocol. DNA was eluted in 30μl nuclease-free water. Eluted DNA was stored at -20 °C.

2.2.7. Agarose Gel-electrophoresis for Gel Elution

Appropriate amounts of agarose were mixed with 100ml 1x TAE and 5 μl Ethidiumbromide (0,5 ug/ml). Samples were mixed with 6x loading buffer. The gel was then run at approximately 100 volts until the bands were sufficiently separated. The results were then analyzed with a UV transilluminator.

2.2.8. Plasmids

The following table lists the plasmids used in this study. Please refer to the respective plasmid maps in the appendix for details on the cloning procedure.

Vector	**Cloned by**
pYM30	Janke C. et al, 2004
pyM39	Janke C. et al, 2004
pB'-his NP stop	Ingrid Mudrak
pB'-his CFP mixed	Wolfgang Hintringer
pB'-his YFP	Wolfgang Hintringer
pB'-his CFP-YFP	Wolfgang Hintringer
pB'-his CFP-C3S5-YFP	Wolfgang Hintringer
pB'-his CFP-C3S6-YFP	Wolfgang Hintringer
pB'-his CFP-C3S5gly-YFP	Wolfgang Hintringer
pB'-his CFP-C3S6gly-YFP	Wolfgang Hintringer
pcDNA3puro-EGFP-C3S6	Wolfgang Hintringer
pcDNA3puro-EGFP-C3S6-HA-GL	Wolfgang Hintringer
pcDNA3puro-EGFP-C3S6-HA-GL-B55α	Wolfgang Hintringer
pcDNA3puro-EGFP-C3S6-HA-GL-p36	Wolfgang Hintringer
pcDNA5to-myc-preScission™_new_stop-GL-NP	Wolfgang Hintringer
pcDNA5to-myc-preScission™-GL-B55α	Ingrid Frohner

2.2.9. *PCR (Polymerase Chain Reaction)*

PCRs were performed by mixing 1 unit of Phusion HF Polymerase, Phusion HF-buffer, 0.3mM dNTPs, 5 pmol/µl primer (forward and reverse), 2-4 ng DNA as template and ddH$_2$O to a total volume of 50 μl. The following conditions were selected for amplifying the DNA of interest: 98 °C 30 sec, followed by 35 cycles of 95 °C for 30 seconds (denaturing step), 55 °C for 15 seconds (annealing step) and 72 °C for 15 seconds (extension step). PCR ends with an extension step at 72°C for 10 minutes and subsequent cooling to 4°C.

The following table comprises the list of primers used for PCR amplification. In-frame start codons are highlighted. Please refer to the referenced plasmid map in the appendix for details.

PCR primer	**Nr.**	**5' - 3'**	**Plasmid reference**
NcoI CFP2_fw	1491	AGTCCC**ATG**GGTAGCAAGGGCGAGGAGC	pB'His-CFP, pB'His-CFPmixed
SphI BamHI CFP_r	1462	AGTCGCATGCCGTGGATCCCTTGTACAGCTCGTC	pB'His-CFPmixed
SphI CFP_r	1465	AGTCGCATGCCTTGTACAGCTCGTCC	pB'His-CFP
BamHI HpaI SalI YFP_fw	1463	AGTCGGATCCGTTAACGTCGACAGCAAGGGCGAGGAGC	pB'His-YFPmixed
NcoI YFP2_fw	1492	AGTCCCATGGGTAGCAAGGGCGAGGAGC	pB'His-YFP
SphI YFP_r	1467	AGTCGCATGCCTTGTACAGCTCGTCC	pB'His-YFP, pB'His-YFPmixed
EcoRI-Kozak-EGFP_F	1181	ATCCGGAATTCGCCACC**ATG**GTGAGCAAG	pcDNA3puro EGFP-C3S6
Kpn1_C3S6_EGFP_R	1541	ATCGGGGTACCCGGGCCCTGCACCACCACCGGGCGCTTGTACAGCTCGTCCATG	pcDNA3puro EGFP-C3S6

2.2.10. *Annealing of Oligonucleotides and 5´-end Phosphorylation*

Equimolar amounts (100 pmol of each) of complementary oligonucleotides (Sigma Aldrich) were mixed in PCR-tubes in a total volume of 40μl and subsequently heated for four minutes at 95 °C on a PCR block and cooled down to room temperature. For ligation to each other or to a dephosphorylated vector, oligos were subsequently phosphorylated at their 5' ends. 320 ng of annealed oligonucleotides were then mixed with 5 μl 10x phosphonucleotide-kinase buffer, 10 units phosphonucleotide-kinase T4 polymerase, ATP was added to a final concentration of 5 nM ATP and H$_2$O was added to a final volume of 50 μl. The solution was incubated for 30 minutes at 37 °C to allow 5'-end phosphorylation to occur, then immediately incubated at 62 °C to inactivate the kinase.

2.2.11. Ligation

First, Nanodrop was used to determine the concentration of the plasmid DNA. 100 ng of plasmid DNA was mixed with phosphorylated oligonucleotides at a molar ratio of 1:3 and 1:6 and 2μl of 10x T4-Ligase buffer, 0.5 U of T4 ligase and H_2O to a final volume of 20 μl was added. Ligation was performed by incubating the samples over night at 4 °C or alternatively for at least 30 minutes at room temperature. The following table compiles the oligonucleotides used for ligation in this study. In-frame stop codons are highlighted. Please refer to the appendix to find a summary of the cloning strategy for each individual plasmid.

Oligonucleotide	**Nr.**	**5'-3' sequence**	**Plasmid reference**
C3S5_s	1476	GATCCCTGGAAGTGCTGTTTCAGGGCCCGC	pB'His-CFP-C3S5-YFP
C3S5_as_new	1542	TCGAGCGGGCCCTGAAACAGCACTTCCAGG	pB'His-CFP-C3S5-YFP
C3S6_s	1500	GATCCCGCCCGGTGGTGGTGCAGGGCCCGC	pB'His-CFP-C3S6-YFP
C3S6_as_new	1544	TCGAGCGGGCCCTGCACCACCACCGGGCGG	pB'His-CFP-C3S6-YFP
C3S6_gly_left_s	1502	GATCCGGTGGCGGTGGCTCTGGAGGTGGTGGGTCCCGCCCGGTGGTG	pB'His-CFP-C3S6gly-YFP
C3S6_gly_left_as	1503	GCACCACCACCGGGCGGGACCCACCACCTCCAGAGCCACCGCCACCG	pB'His-CFP-C3S6gly-YFP
C3S6_gly_right_s	1504	GTGCAGGGCCCGGGTGGCGGTGGCTCTGGAGGTGGTGGGTCCC	pB'His-CFP-C3S6gly-YFP
C3S6_gly_right_as_new	1545	TCGAGGGACCCACCACCTCCAGAGCCACCGCCACCCGGGCCCT	pB'His-CFP-C3S6gly-YFP
C3S5_gly_left_s	1506	GATCCGGTGGCGGTGGCTCTGGAGGTGGTGGGTCCCTGGAAGTGCTGT	pB'His-CFP-C3S5gly-YFP
C3S5_gly_left_as	1507	TGAAACAGCACTTCCAGGGACCCACCACCTCCAGAGCCACCGCCACCG	pB'His-CFP-C3S5gly-YFP
C3S5_gly_right_s	1508	TTCAGGGCCCGGGTGGCGGTGGCTCTGGAGGTGGTGGGTCCC	pB'His-CFP-C3S5gly-YFP
C3S5_gly_right_as_new	1543	TCGAGGGACCCACCACCTCCAGAGCCACCGCCACCCGGGCCC	pB'His-CFP-C3S5gly-YFP
Kpn HA Gly HindIII_s	1181	ATATCCCTATGACGTCCCGGACTATGCAGGTGGCGGTGGCTCTGGAGGTGGTGGGTCCA	pcDNA3puro EGFP-C3S6-HA-GL
Kpn HA Gly HindIII_as	1182	AGCTTGGACCCACCACCTCCAGAGCCACCGCCACCTGCATAGTCCGGGACGTCATAGGGATATGTAC	pcDNA3puro EGFP-C3S6-HA-GL
pyx-new-stop_s	1045	GATCC**TAA**CTGACTAGGTCGACGATATCCTCGAGG	pcDNA5to-myc-preScission™_new stop-GL
pyx-new-stop_as	1046	CTAGCCTCGAGGATATCGTCGACCTAGTCAG**TTA**G	pcDNA5to-myc-preScission™_new stop-GL

2.2.12. DNA sequencing

DNA (final concentration = 100 ng/μl) and Primer solutions (final concentration = 1.4 μM) were mixed. Sequencing was performed by LGC genomics. The table below provides a list of primers used for sequencing plasmids. Please refer to the plasmid maps in the appendix for details.

Sequencing primer	**Origin/Nr.**	**5' - 3'**	**used for sequencing of**
pcDNA3.1-R binds 82 bp (pcDNA3) or 55 bp (pcDNA5) downstream of stop codon	LGC genomics	TAGAAGGCACAGTCGAGGCT	all pcDNA3 and pcDNA5 vectors
CMV-F binds 138 bp (pcDNA3) or 230 bp (pcDNA5) upstream of start ATG	LGC genomics	CGCAAATGGGCGGTAGGCGTG	all pcDNA3 and pcDNA5 vectors
pb'His-forward new binds 21 bp upstream of start ATG	523	CTCTAGAAAGGAGGTACGATC	pb'His-CFP, pB'His-YFP
pb'His-reverse binds 76 bp downstream of stop codon	482	GAAGACAGTCATAAGTGCGG	pb'His-CFP, pB'His-YFP
CFP_fw binds 209 bp downstream of start ATG	1539	TGACCACCCTGACCTGG	pB'His-CFP-YFP, pB'His-CFP-substrate-YFP
YFP_r binds 523 bp upstream of stop codon	1540	ACGCCGTAGCCGAAGG	pB'His-CFP-YFP, pB'His-CFP-substrate-YFP

2.3. Working in Tissue Culture

2.3.1. Solutions and Media

10xPBS: 1.37M NaCl; 27mM KCl; 43mM Na_2HPO_4 ; 14mM KH_2PO_4. Dissolve in ddH_2O, adjust to pH 7.4 and autoclave.

DMEM (Gibco #31660-083): Dissolve one package in 5l ddH_2O and stir for 30min until completely dissolved. Add 30g $NaHCO_3$, stir until completely dissolved and add ddH_2O up to 10l. Filter sterilize through a membrane filter (0.2µm) and make aliquots of 450ml. Store at 4°C. Add glutamine, if stored longer than 2 weeks.

Trypsin- EDTA (TE): Dissolve 250mg Trypsin in 25ml 10xPBS and add water to a total of 245ml. Stir for 2 hours. Add 5ml 1% Na-EDTA (pH 7.4), mix and filter sterilize through a membrane filter (0.2µm). Store aliquots of 10ml at –20°C.

Blasticidin (Invitrogen #R210-01): Dissolve 50mg in 20ml ddH_2O, filter sterilize through a membrane filter (0.2µm), aliquot and store at –20°C. Use at a concentration of 5 µg/ml for HEK293Trex.

Hygromycin B (Calbiochem #400049): Dissolve 50mg/ml in ddH_2O, filter sterilize through a membrane filter (0.2µm). Use at a concentration of 200 µg/ml for HEK293Trex.

Puromycin (Sigma #P-7255): Dissolve 100mg Puromycin in 10ml ddH_2O, filter sterilize through a membrane filter (0.2µm), aliquot and store at –20°C. Use at a concentration of 1µg/ml for HEK293Trex.

Doxycycline (Sigma #D-9891): Dissolve 10mg in 10ml ddH_2O, filter sterilize through a mem- brane filter (0.2µm), aliquot and store at –20°C. Use at a concentration of 1µg/ml for HEK293Trex.

AB: 0.6g Penicillin-G; 1g Streptomycin-sulfate; 10ml 10x PBS. Add H_2O to 100ml, filter sterilize through a membrane filter (0.2µm) and store 5ml aliquots at -20°C. Use at a concentration of 100 U/ml penicillin and 100 ug/ml streptomycin-sulfate for HEK293Trex.

DMSO (Dimethylsulfoxide, Applichem #A3672.0250)

Tet-free FCS (fetal calf serum, Gibco #4023696J): Store 50ml aliquots at -20°C.

HEK293Trex: human embryonic kidney cell line, stably expressing the Tet-repressor (kindly provided by Stefan Strack, *Strack et al, 2004*)

2.3.2. Tissue Culture: Cultivation and Propagation of HEK293Trex cells

HEK293-TRex cells were grown at 37 °C in Dulbecco's modified eagle medium (DMEM) with 10% tetracycline-free fetal calf serum. All media were supplemented with penicillin (100 units/ml), and streptomycin (100μg/ml). All cells expressing the tet-repressor were grown in medium containing blasticidin (20μg/ml). Cells containing a pcDNA5to vector were selected by adding hygromycin to the medium (200 μg/ml), while pcDNA3puro cells (cloned by Ingrid Mudrak) were selected by adding puromycin (1μg/ml). All cells were cultivated at 37 °C in an atmosphere containing 7,5% CO_2. Cells were split when they had grown to 80% confluence according to the following protocol: First, the medium was carefully removed. The cells were then washed with 2-3 ml PBS. The cells were detached from the plate by adding TE at 37 °C for one minute. The cells were then carefully resuspended in 10 ml growth medium and subsequently 1 ml of this suspension was added to a fresh dish containing 9 ml growth medium + relevant antibiotics (1:10 split).

2.3.3. Tissue Culture: Freezing/thawing of HEK293Trex cells

Cells were prepared for freezing via centrifugation at 1200 rpm for 5 minutes, removal of the medium and careful resuspension in 500 μl of pre-cooled FCS + 10% DMSO on ice. The suspension was then transferred to cryo-tubes (50 μl per tube) and stored in liquid nitrogen. For re-thawing of the cells, the cryo-tubes were shortly incubated in a 37°C water bath. The liquid suspension was then quickly diluted in 8ml DMEM and the cells were subsequently pelleted via centrifugation. After discarding the supernatant, the cells were resuspended in the appropriate volume of medium and plated on petri dishes.

2.3.4. *Transfection of mammalian cells using Lipofectamine 2000 (Invitrogen #11668- 027)*

HEK-Trex cells were grown in DMEM + 10% FCS with appropriate selective antibiotics as indicated in section 2.3.2. 1x10^6 cells were seeded on 6-well tissue culture dishes supplemented with DMEM + 10%FCS without antibiotics the day before transfection. 6µl of Lipofectamine 2000 was diluted in serum-free DMEM to a final volume of 250 μl and incubated at room temperature for 5 minutes. 4 μg of plasmid DNA was mixed with 250 μl serum free DMEM. Both solutions were mixed carefully and incubated together at room temperature for 20 minutes. Cells were washed with 1xPBS and supplemented with 2ml of DMEM + 10%FCS lacking selective antibiotics. The transfection mix was added to the medium and cells were incubated at 37 °C. Medium was changed after 7 hours. Efficiency of the transfection for vectors coding for GFP was assessed via fluorescence microscopy. Mixed or single clones were grown by seeding appropriate amounts of cells onto petri dishes supplemented with DMEM + 10%FCS. Medium was changed after 7 hours to contain penicillin and streptomycin. After 2 days, cells were split for selecting single clones and mixed clones and further relevant selection antibiotics were added (since resistance gene expression could be too low at earlier time points). For mixed clone selection, cells were split 1:3-1:5 onto 10 cm dishes. For single clone selection, cells were split 1:500-1:1000 onto 15 cm dishes Upon colony formation, single colonies were transferred to separate wells on 24-well dishes and subsequently expanded to 10 cm dishes in medium.

2.3.5. *CASY Cell Concentration Determination*

50 μl of cell suspension was diluted in 10 ml CASYton buffer. Measurements were performed using the CASY cell counter according to the manufacturer´s protocol.

2.4. Working with Proteins

2.4.1. Solutions and Media

30% Acrylamide: 292g acrylamide; 8g bisacrylamide. Fill up to 1l with ddH_2O. Add mixed-bed, ion-exchange resin (BioRad AG 501-X6) to the final solution and store in dark at 4°C.

1M Tris pH 8.8: Dissolve 242.3g Tris in 1l of ddH_2O. Adjust pH to pH 8.8 with HCl and fill up to 2l with ddH_2O, autoclave and store at 4°C.

1M Tris pH 6.8: Dissolve 60.5g Tris in $ddKH_2O$. Adjust pH to 6.8 with HCl and fill up to 500ml with H_2O, autoclave and store at 4°C.

20% SDS: Dissolve 40g SDS (Amresco #0227) in 100ml of ddH_2O, stir and slightly heat, fill up to 200ml with H_2O and store at RT.

10% APS: Dissolve 1g ammoniumperoxodisulfate (Merck #1201) in 10ml ddH_2O and store at 4°C.

TEMED (N,N,N',N'-Tetramethylenediamine, Fluka #87689)

10xRunning buffer: 250mM Tris, 1,92 M Glycine and 1% SDS in H_2O, pH 8,3, store at RT.

Transfer buffer with Methanol: 25mM Tris; 190mM Glycine; 20% (v/v) Methanol. Dissolve Tris and Glycine in H_2O and add Methanol, store at 4°C.

Ponceau S stock solution (10x): 2g Ponceau S (Serva #33429); 30g Trichloroacetic acid (Ap- pliChem #A1431); 30g Sulfosalicylic acid (Merck #1.00691). Dissolve and fill up to 100ml with ddH_2O and store at RT.

Ponceau S working solution: Dilute Ponceau S stock solution 1:10 with ddH_2O.

20% Sodium-azide (Merck #67188): Dissolve 2g sodium-azide in 10ml ddH_2O and store in the dark at 4°C.

GSD stock (3x): 335mM DTT (Gerbu #1008); 230mM (6%) SDS; 4.5M 30% Glycerol (Merck #1.04092); 20ml ddH_2O. Add a bit bromphenolblue (Amresco #0312) and a few drops 1M Tris pH 6.8 until solution appears blue. Store 2ml aliquots at -20°C. To obtain 1x GSD, dilute the stock with ddH_2O.

1% Thimerosal (Sigma #T-5125): Dissolve 0.5g Thimerosal in 50ml ddH_2O. Store in the dark at 4°C.

Prestained Protein Molecular Weight Standards (Biorad #161-0373): Store at -20°C. Use 4µl or 8µl for one lane on a small or large SDS-polyacrylamide gel, respectively.

10xPBS: 1.37M NaCl; 27mM KCl; 43mM $Na2HPO_4$; 14mM KH_2PO_4. Dissolve in ddH_2O, adjust to pH 7.4 and autoclave.

3% Non-Fat Dry Milk / blocking solution: 15g Non fat dry milk (NFDM); 50µl 20% sodium azide. Add PBS and 0.05% Tween20 to 500ml and store at 4°C.

0.5% Non-Fat Dry Milk: 2.5g Non fat dry milk (NFDM); 500µl 1% Thimerosal. Add PBS + 0.05% Tween 20 to 500ml and store at 4°C.

Ni-NTA beads (Qiagen #30410)

PMSF-stock (100x): Dissolve 0.697g PMSF (Roche #837091) in 20ml isopropanol and store aliquots of 1ml at room temperature, protected from light.

Aprotinin-stock (200x): Store aliquots of 1ml Aprotinin (Sigma #A-6012) at 4°C.

Complete (25x): Dissolve one CompleteTM Protease Inhibitor cocktail tablet (Boehringer Mannheim #1836145) in 2ml IP-Lyse buffer and store at 4°C for a maximum of 2 weeks.

0.1M Glycine buffer: Dissolve 3.76g glycine in 400ml H_2O. Adjust to pH 3.0 and add ddH_2O to 500ml. Store at 4°C.

Lysis buffer: 50 mM NaH_2 PO_4, 300 mM NaCl, 10 mM imidazole, adjust pH to 8.0 with NaOH, 1 mM PMSF, 1 mM ß-mercaptoethanol, 1 μg/ml aprotinin, 1 μg/ml leupeptin, 1 μg/ml pepstatin.

Wash buffer: 50 mM NaH_2 PO_4,300 mM NaCl, 20 mM imidazole, adjust pH to 8.0 with NaOH, 1 mM ß-mercaptoethanol, 1 μg/ml aprotinin, 1 μg/ml leupeptin, 1 μg/ml pepstatin

Elution buffer: 50 mM NaH_2 PO_4,300 mM NaCl, 250 mM imidazole, adjust pH to 8.0 with NaOH, 1 mM ß-mercaptoethanol, 1 μg/ml aprotinin, 1 μg/ml leupeptin, 1 μg/ml pepstatin

PreScission™ protease: GST-tagged human rhinovirus type 14 $3C^{pro}$, 46 kDa, stored at -20°C in glycerol at a concentration of 5 μg/μl (109 μM), kindly provided by Katharina Maderböck. Diluted in preScission™ buffer prior to use: 50 mM Tris-HCl pH 8, 150 mM NaCl, 1 mM EDTA, 1 mM DTT

Coomassie-stock: Dissolve 2.5g Coomassie (Serva #17524) in 500ml methanol, stir over night, add 500ml ddH_2O and store at room temperature.

Coomassie working solution: 30% Ethanol; 30% Coomassie-stock; 10% acetic acid; 30% ddH_2O.

Destaining solution: 30% Ethanol; 60% ddH_2O ; 10% acetic acidIP Wash: 10% glycerol; 20mM Tris pH 8.0; 135 mM NaCl. Filter sterilize through a membrane filter (0.2µm) and store at 4°C.

IP wash: 10% Glycerol, 20mM Tris-HCL ph8.0, 135mM NaCl. Filter sterilize through a membrane filter (0.2µm) and store at 4°C.

IP Lyse: IP-wash, 1 % (w/v) NP-40, 1x complete, 1x PMSF, 1x aprotinin added freshly before use.

TBS: Tris-buffered saline: 50 mM Tris and 150 nM NaCl, pH 7.6.

Fixation solution for silver staining: 10% acetic acid + 45% methanol + H_2O

Farmer's reducer: 30 mM $K_3Fe(CN)_6$ + 30 mM $Na_2S_2O_3$ $5H_20$

Silver staining solution: 0,1% silver nitrate in 100 ml H_2O

Developing solution: 0,1% Formaldehyde in 100 ml 2,5% Na_2CO_3

2.4.2. Protein Expression and Extraction from HEK293Trex cells

HEK-Trex cells pre-transfected with the relevant plasmids were grown according to the method stated above. 1x 10^6 cells were plated and expression was induced by adding 1 μg of doxycyline per ml of medium the following day. For harvesting the cells at the selected time points, the medium was removed and the cells were washed with approximately 1 ml PBS. Upon removal of the PBS, 50 μl "IP Lyse" buffer was added and the cells were scraped off the plate using pieces of autoclaved rubber. All steps were performed on ice. The lysate was subsequently transferred to a microcentrifuge tube and centrifuged at 14.000 rpm, 4°C, for 5 minutes to separate the cell debris from the soluble proteins. Protein concentration in the supernatant was then measured via the BioRad assay.

2.4.3. BioRad Assay / Protein Concentration Measurement

Pre-cooled Bio-Rad protein assay dye reagent was diluted 1:5 in H_2O. 500 μl of the solution was transferred to plastic cuvettes. After addition of 1 μl sample or lysis buffer (served as a blank), the solution was immediately mixed and incubated at room temperature for 10 minutes. The extinction was measured at a wavelength of 595 nm. Extinction values of the samples were then compared to extinction values of bovine serum albumine of known concentration. This allowed the deduction of the protein amount present in the sample.

2.4.4. Purification of bacterially expressed proteins

For culturing of bacteria refer to 2.1.5. After determining the $OD_{600,}$ the bacterial cells were then pelleted via centrifugation at 4000 rpm for 15 min at 4°C. Ice cold lysis buffer was used for resuspending the cells. The suspension was then frozen in liquid nitrogen and lysed or alternatively stored at -80°C. For lysing the cells, the bacterial suspension was thawed, transferred to 15 ml falcon tubes on ice and subjected to ultrasound sonoporation, using ultrasound pulses lasting 3x 20 seconds and 1x 30 seconds, each pulse separated by a 40 second pause on ice. To ensure complete lysis, the suspension was incubated with 1 mg/ml Lysozyme 45 minutes on ice. For checking the expression of the proteins, the samples were then centrifuged at 14.000 rpm for 15 minutes at 4°C. The supernatant was separated from the pellet and both were diluted in GSD sample buffer. Samples were analysed together with an uninduced control on 12,5% SDS-PAG, using coomassie staining as well as immunoblotting with a monoclonal α-His antibody to assess expression efficacy. For purification of the proteins, the lysed bacterial suspensions were ultracentrifuged at 43.000 rpm (100.000 g) at 4°C for 1 hour, the supernatant was loaded onto a Nickel-bead column (200μl bead suspension 1:1), which had been equilibrated with lysis buffer. Aliquots of the supernatant, the pellet and the flow-through were collected and stored at -80°C. The beads were then washed with ice-cold wash buffer using a volume corresponding to 10x the volume of the beads. To elute the proteins that remained bound to the beads, 50 μl aliquots of elution buffer containing imidazole at a concentration of 250 mM were added to the column and each aliquot was collected in a separate microcentrifuge tube. The purity and protein yield of the eluted fractions was assessed by SDS-PAGE and subsequent coomassie blue staining or western blotting using monoclonal α-His or α-GFP 2B6 antibody. When required, samples were further purified by centrifugation in a Millipore centricon with a nominal molecular weight limit of 50 kDa according to the manufacturer's protocol.

2.4.5. TCA precipitation of proteins

100 μl of 1 μM CFP, YFP and CFP-substrate-YFP protein solutions was mixed with 20 μl of 50% trichloroacetic acid. The solution was incubated on ice for 10 minutes and subsequently centrifuged at 14.000 rpm at 4°C for 10 min. After discarding the supernatant, the pellet was resuspended in 30 μl 1x GSD + 3 μl of unbuffered 1M Tris. The resulting sample was boiled at 95°C for 5 minutes and loaded onto an SDS-PAG.

2.4.6. Sodium dodecyl sulfate polyacrylamide gel electrophoresis (SDS-PAGE)

The running gel was prepared by mixing appropriate amounts of 30% Acrylamide with 1M Tris pH 8.8, 20% SDS, ddH$_2$O, 10 % APS and TEMED. The resulting solution was quickly poured into the gel caster, overlayed with isopropanol and left at room temperature until polymerization was complete. The stacking gel was prepared by mixing appropriate amounts of 30 % Acrylamide, 1M Tris pH 6.8, 20% SDS, ddH$_2$O, 10%APS and TEMED. The samples were prepared by adding 1x GSD and boiled at approximately 92 ºC for 5-10 minutes, followed by short centrifugation of the samples prior to loading. The gel was run overnight at 6-9 mA.

Separating gel

	15%	12,5%	10%
Acrylamide/Bis-acrylamide (30%)	20ml	16.7ml	13.4ml
1M Tris pH 8.8	15ml	15ml	15ml
ddH$_2$O	5ml	8.8ml	11.7ml
20% SDS	200µl	200µl	200µl
10% APS	134µl	134µl	134µl
TEMED	26µl	26µl	26µl

Stacking gel

Acrylamide/Bis-acrylamide (30%)	1.7ml
1M Tris pH 6.8	1.25ml
ddH$_2$O	7.1ml
20% SDS	50µl
10% APS	50µl
TEMED	10µl

2.4.7. Coomassie staining of gels

SDS-PA gels were stained with Coomassie staining solution for 1-2 hours, repeatedly incubated in fresh destaining solution for a total time of approximately 2 hours and dried for 3.5 hours at 80°C in a vacuum trap.

2.4.8. Silver staining of SDS-PAGE gels

Gels were shaken in fixation solution for 15 minutes at room temperature. The gel was then transferred into a freshly prepared Farmer's Reducer solution and incubated for 2 minutes while shaking. After discarding the reducing solution, the gel was washed repeatedly with ddH$_2$O until the yellow color had been completely removed. The gel was subsequently transferred into a freshly prepared silver staining solution and incubated for 15 minutes at room temperature while shaking. After a washing step with ddH$_2$O lasting 30 seconds, the gel was incubated in a 2,5% Na_2CO_3 solution for 30 seconds while shaking. To develop the silver stain, the gel was then placed into the silver stain developing solution until the staining was sufficient. To stop the reaction, an excess of 10 % acetic acid was added. After further 10 minutes of shaking at room temperature, the gel was washed with ddH$_2$O several times and subsequently dried.

2.4.9. Western Blot

Two sponges, a nitrocellulose membrane and four whatman papers were soaked in transfer buffer. The components were then assembled in the following order in a western blot cage: sponge, 2 x whatman paper, membrane, SDS-PAGE gel, 2 x whatman paper and another sponge. The cage was then put into the buffer chamber including transfer buffer and the blot was run for 3.5 hours at 500 mA, 4 ºC. To visualize whether blotting was successful, the membrane was stained with Ponceau-stain, which was subsequently washed off using dH_2O. The membrane was then incubated with blocking buffer for one hour while shaking. The blocking buffer was then discarded and the membrane was incubated with approximately 30 ml primary antibody solution (0.5% Non-Fat Dry Milk solution) for at least two hours at room temperature, or alternatively at 4°C over night, while shaking. After 3x 5 minute washing steps with 1x PBST, the membrane was subsequently incubated with approximately 30 ml secondary antibody solution (0.5% Non-Fat Dry Milk solution) for at least 1 hour while shaking. After subsequent 3x 10 minute washing steps with PBST, signals were detected using a commercially available enhanced chemiluminescence detection kit (Western Lightning ECL by Perkin Elmer or ECL select by Amersham) and photographic films (Fuji). For densitometric analysis, blots were scanned with a resolution of 600 dpi and analysed using ImageJ 1.46r software. The following table provides a summary of the antibodies used for western blotting in this study.

primary antibody	**target**	**dilution**	**type of antibody**
16B12	HA-tag	1:20.000 - 1:30.000	mouse,monoclonal (Covance)
4A6	myc-tag	1:1.000 - 1:500	mouse, monoclonal (Hombauer et al, 2007)
ß-tubulin	ß-tubulin	1:20.000	mouse, monoclonal (upstate, #05-661)
avidin-HRP	biotin	1:20.000	glycoprotein (not an antibody), Abcam
α-His	His-tag	1:10.000	mouse, monoclonal, GE healthcare
2B6	α-GFP	1:500	mouse, monoclonal (Schüchner et al, unpublished)
SAT20	PP2A-Cα subunit	1:10.000	rabbit, polyclonal, purified, Europentec #20, 3rd bleed
2H3-D10	α-GST	1:10.000	mouse monoclonal, (Roblek et al, 2010)
55 delta 237	His 55a, rat frag. 238-447	1:10.000	rabbit, polyclonal, purified, 6th bleed (Nunbhakdi-Craig et al, 2002)
α-GAPDH	α-GAPDH	1:10.000	mouse, monoclonal, Millipore

Secondary antibody	**target**	**dilution**	**type of antibody**
HRP anti-mouse	IgG, Fcγ fragment-specific	1:10.000	Goat; Jackson #115-035- 008
HRP anti-rabbit	IgG, Fcγ fragment-specific	1:10.000	Goat; Jackson #111-035- 008
IRDye 680 LT anti-mouse	IgG, Fcγ fragment-specific	1: 5.000	Goat, LI-COR Biosciences

2.4.10. *In vitro enzyme kinetic assay*

Purified substrates were diluted in preScission™ buffer to a final substrate concentration of 500 nM, 1μM, 4 μM and 16 μM and mixed with preScission™ protease at a final concentration of 109 nM in a total volume of 100 μl in microcentrifuge tubes. The solutions were incubated at room temperature. 45μl aliquots were removed after 90 and 180 minutes, 22,5 μl 3x GSD was added and the solution was immediately boiled at 95 °C for 5 minutes to stop the enzymatic reaction. All samples were subsequently serially diluted to a substrate concentrations of 250 nM with 1x GSD and shortly boiled again in a total volume of 50 μl. 18

μl of each dilution, corresponding to 170 ng of CFP-substrate-YFP protein, was loaded onto small 0.75 mm-thin SDS-PAG which were subjected to in-gel western blotting.

2.4.11. *LI-COR™ in gel western*

In-gel western blots were performed according to the manufacturer's protocol (*LI-COR™ Biosciences, 2006)*. For optimal results, primary antibody anti-GFP 2B6 was diluted 1:100 in 5% BSA in PBS and incubated together with a small SDS-PAG at 4°C for 24 hours while shaking. After washing, the gel was incubated for another 24 hours with secondary antibody IRDye 680 LT (Odyssey) diluted 1:5000 in 5% BSA in PBS, while being protected from light. Scanning of the gel was performed using the Odyssey LI-COR infrared scanner at an appropriate intensity, the focus offset was set to half of the gel thickness (0.375 mm). To remove residual background, the gels were incubated in PBS at 4°C in the dark for up to three days prior to rescanning. Densitometric quantification was performed using the LI-COR™ Odyssey software. Cleaved product signals were quantified in both the 0h (background) and 3h time point samples, using manual background setting. Upon subtraction of background, concentration of the accumulated product after 3h was derived by comparing to the signal intensity of uncleaved substrate of known concentration at time point 0. Values were multiplied by the corresponding dilution factor. Rates (μM/h) were calculated from each progress curve using Microsoft Excel™. Substrate concentration on the x-axis was plotted against velocity on the y-axis. Kinetic parameters K_m and V_{max} were derived via computerized least-squares fitting of the data using a non-linear GRG module provided by the "Solver"-tool of Microsoft Excel™. For a concise explanation of the method please refer to http://src.sfasu.edu/~avk/BTC560/HOW%20TO.htm (Date: 29.01.2013)

2.4.12. *Co-Immunoprecipitation*

Cells were grown on 15cm dishes, expression was induced by incubating the cells with doxycycline for 21 hours. Subsequently, the medium was removed and the cells were carefully washed with PBS and IP-wash solution After adding 500μl IP Lyse + protease inhibitors (aprotinin, complete and PMSF), the dishes were incubated for 15 min at 4°C while shaking. The resulting lysate and cell debris were subsequently scraped off the dishes and transferred to Eppendorf tubes. After centrifugation, 10 min at 4°C, 15.000 rpm, the supernatant was transferred to a fresh Eppendorf tube. Protein concentration was measured using the BioRad-assay and IP-Lyse was added to equilibrate to the requested protein concentration. Lysates were either stored at -80°C or immediately subjected to immunoprecipitation. 60μl of a 1:1 suspension of cross-linked myc-beads (4A6) was added to one half (= 250 μl) of the lysate, while 60 μl of a 1:1 suspension of cross-linked HA beads (12CA5) was added to the other. The solutions were then incubated at 4°C for 1 hour and 20 min while shaking and subsequently centrifuged for 1 min at 1000 rpm, 4°C. The supernatant was stored at -80°C and the beads were carefully washed with 1ml IP-Lyse + protease inhibitors. Finally, the beads were washed 3 times with TBS. The beads were then resuspended in 50μl 1x GSD and loaded onto an SDS-PAGE gel.

2.4.13. Determination of kinetic parameters using FRET

For determining kinetic parameters of the proteolytic reaction between the preScission™ protease and its substrates, purified GST-tagged preScission™ protease stored in glycerol (by Katharina Maderböck) was diluted in preScission™ buffer (50 mM Tris-HCl pH 8, 150 mM NaCl, 1 mM EDTA, 1 mM DTT). "CFP-substrate-YFP" protein dilutions were were pipetted into wells of 96-well microplates and mixed with preScission™ dilution or with 10 μl preScission™ buffer (control) to a final preScission™ concentration of 109 nM or 1.09 μM and a final substrate concentration of 1 μM, 4 μM, 8 μM and 16 μM. Measurements were made at time intervals of 0, 1, 60, 90 and 180 minutes using a VICTOR™ microplate reader. To measure a change in FRET, samples were excited at 430 nm (excites predominantly CFP, lamp energy setting was 7000) and emission was measured at 460 nm (near CFP emission peak) and at 535 nm (near YFP emission peak). The resulting values were analyzed and compared using Microsoft Excel. The background value (substrate + buffer) was subtracted from each sample at the concomitant time point.

3. Results

The main aim of this thesis was to develop a novel mammalian two-hybrid approach similar to the M-Track approach (*Zuzuarregui, 2012*), but using a preScission™ protease reaction instead of an HKMT reaction to detect transient protein-protein interactions. Based on the results from M-Track, we hypothesized that an enzymatic reaction with a high affinity and a high turnover would be beneficent for this purpose. Therefore, a first approach was to determine kinetic parameters of preScission™ reactions.

3.1. Determining kinetic parameters of the preScission™ reaction

To be able to find optimal kinetic parameters for the preScission™ assay, I aimed at constructing various recombinant proteins that included preScission™ recognition sequences ready for testing via FRET and in-gel western blotting. I cloned preScission™ substrate recognition sequences of interest, named C3S5 and C3S6 as well as C3S1gly and C3S6gly, into a bacterial expression vector (see Materials and Methods and Appendix for details). The preScission™ substrate sequences in these vectors were flanked by an ECFP sequence on their N-terminus and an EYFP sequence on their C-terminus. Six N-terminal His tags were introduced at the ECFP-N-terminus to allow subsequent affinity purification via Ni^{2+-}beads (Figure 1). Vectors coding for His-ECFP only, His-EYFP only and an uncleavable "His-ECFP-EYFP" fusion protein lacking a substrate recognition sequence served as controls. For readability, His-ECFP-substrate-EYFP proteins are henceforth also referred to as CFP-substrate-YFP or simply by their substrate name.

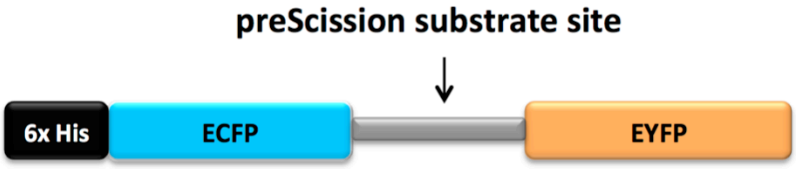
preScission substrate site
6x His
ECFP
EYFP

Figure 1: **Cartoon depicting the design of the "His-ECFP-substrate-EYFP" proteins.** Proteins consist of 6 His-tags at the N-terminus, followed by an enhanced cyan fluorescent protein (ECFP) linked via a preScission™ substrate site to an enhanced yellow fluorescent protein (EYFP).

I expressed CFP, YFP, CFP-YFP, CFP-C3S5-YFP, CFP-C3S6-YFP, CFP-C3S5gly-YFP and CFP-C3S6gly-YFP in *E.coli* cells. Expression of all proteins of interest was most efficient in the "Rosetta -" *E.coli* strain. The highest yield of soluble CFP only and YFP only was achieved by inducing the expression with 1mM IPTG and incubating the cells at 37°C for three hours. "CFP-YFP" or "CFP-substrate-YFP" proteins were best expressed by adding 0.1mM IPTG and incubating the bacteria over night at 22°C (for an example see Figure 2).

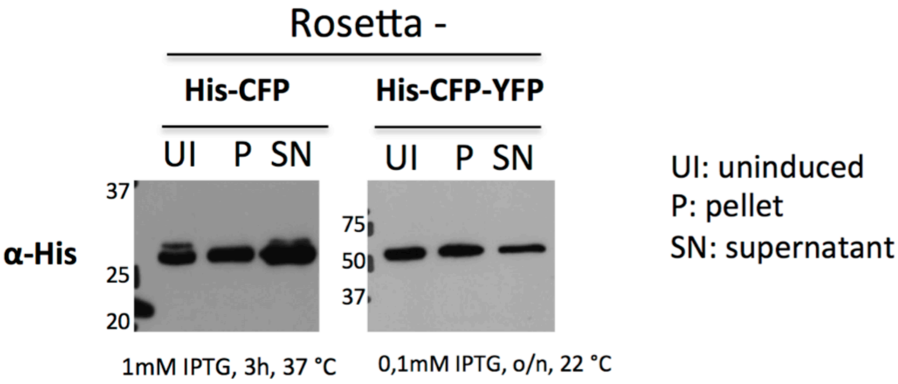
Rosetta -
His-CFP
His-CFP-YFP
UI P SN
UI P SN
37
25
20
75
50
37
α-His
UI: uninduced
P: pellet
SN: supernatant
1mM IPTG, 3h, 37 °C
0,1mM IPTG, o/n, 22 °C

Figure 2: "Rosetta minus" competent *E.coli* cells were transformed with pB'His expression plasmids coding for the proteins of interest. Expression and solubility of the recombinant proteins was analysed by 12,5% SDS-PAGE and immunoblotting, using an α-His antibody for detection. The figure shows the results for recombinant His-ECFP (28 kDa) and His-ECFP-EYFP (55 kDa) proteins expressed under the indicated conditions.

I extracted the proteins, purified them from the soluble fraction by affinity chromatography using Ni^{2+}-beads and assessed the purity of the eluted fractions by SDS-PAGE and coomassie staining, as well as via immunoblotting and probing with anti-His and anti-GFP 2B6 monoclonal antibodies, which recognize the His-tag and the ECFP/EYFP epitopes respectively (as an example see Figure 3).

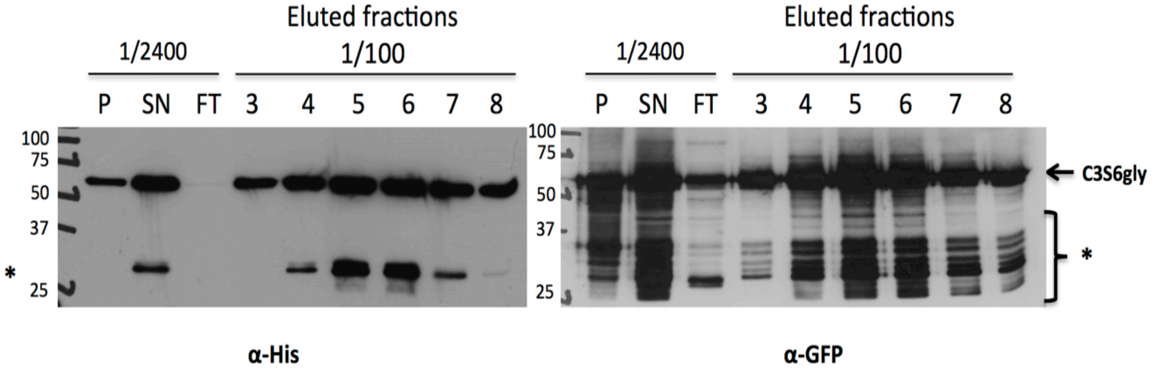

Figure 3: **Purification of recombinant proteins.**
Recombinant proteins were expressed in and purified from "Rosetta minus" *E.coli* strain assessed for purity via 12.5% SDS-PAGE. 1/2400 of the pellet (P), supernatant (SN) and flow-through (FT) was loaded. 1/100 of the eluted fractions 3-8 was loaded. The figure shows the result of His-ECFP-C3S6gly-EYFP purification as an example. The blots were incubated with monoclonal antibodies against α-His (left) or α-GFP (right). Asterisk marks degradations in the sample.

Upon elution from the Nickel column, some of the samples displayed impurities, presumably protein degradations that arose during the purification process. I tried to remove remaining impurities by pooling the cleanest fractions and subjecting them to membrane filtration (cut-off = 50 kDa) via centrifugation (see Materials and Methods, 2.4.4). Densitometric analysis of the proteins on a coomassie-stained SDS-PA gel was used to calculate the concentration of the recombinant proteins of interest (Figure 4).

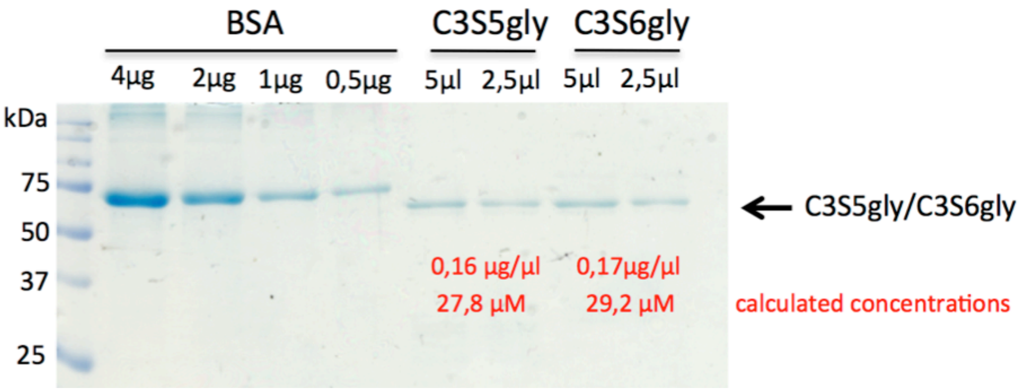
BSA
C3S5gly
C3S6gly
4µg
2µg
1µg
0,5µg
5µl
2,5µl
5µl
2,5µl
kDa
75
50
37
25
C3S5gly/C3S6gly
0,16 µg/µl
27,8 µM
0,17µg/µl
29,2 µM
calculated concentrations

Figure 4: **Coomassie staining of recombinant proteins separated by SDS-PAGE.** Recombinant proteins were expressed in "Rosetta minus" *E.coli* strain and purified via affinity chromatography and membrane filtration. 5μl and 2.5μl of the samples were loaded on a 12.5 % SDS-PAGE. Bovine serum albumine (BSA) of known concentration was used as a standard. Concentration of the samples was determined via coomassie staining and densitometric analysis of band intensity compared to the BSA standard by analysing scanned images with a resolution of 600 dpi using the ImageJ software. This figure shows the amounts of His-ECFP-C3S5gly-EYFP ("C3S5gly", 57kDa) and His-ECFP-C3S6gly-EYFP ("C3S6gly", 57 kDa) calculated based on the comparison of band intensity to the BSA-standard.

3.1.1. Using a Förster Resonance energy transfer (FRET) enzyme assay to determine kinetic parameters of preScisson reactions

Upon dilution in preScission™ buffer, I tested whether the purified proteins displayed the expected fluorescent properties. To do this, I diluted the proteins in preScission™ buffer to a concentration of 1 µM and incubated them with or without preScission™ protease for one hour at room temperature prior to analyzing their fluorescent spectra (Figure 5).

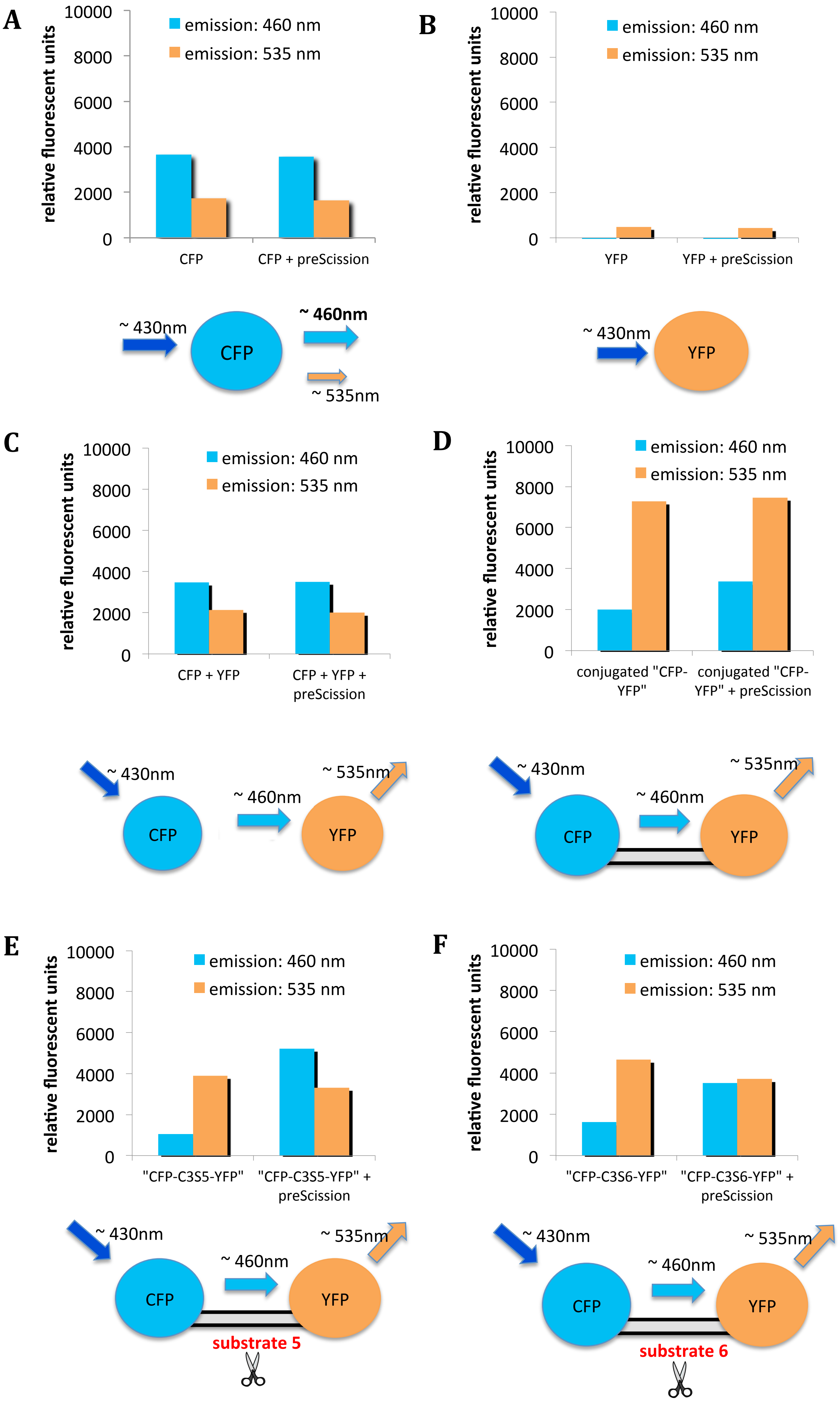
A
relative fluorescent units
10000
8000
6000
4000
2000
0
emission: 460 nm
emission: 535 nm
CFP
CFP + preScission
~ 430nm
CFP
~ 460nm
~ 535nm
B
relative fluorescent units
10000
8000
6000
4000
2000
0
emission: 460 nm
emission: 535 nm
YFP
YFP + preScission
~ 430nm
YFP
C
relative fluorescent units
10000
8000
6000
4000
2000
0
emission: 460 nm
emission: 535 nm
CFP + YFP
CFP + YFP + preScission
~ 430nm
~ 460nm
~ 535nm
CFP
YFP
D
relative fluorescent units
10000
8000
6000
4000
2000
0
emission: 460 nm
emission: 535 nm
conjugated "CFP-YFP"
conjugated "CFP-YFP" + preScission
~ 430nm
~ 460nm
~ 535nm
CFP
YFP
E
relative fluorescent units
10000
8000
6000
4000
2000
0
emission: 460 nm
emission: 535 nm
"CFP-C3S5-YFP"
"CFP-C3S5-YFP" + preScission
~ 430nm
~ 460nm
~ 535nm
CFP
YFP
substrate 5
F
relative fluorescent units
10000
8000
6000
4000
2000
0
emission: 460 nm
emission: 535 nm
"CFP-C3S6-YFP"
"CFP-C3S6-YFP" + preScission
~ 430nm
~ 460nm
~ 535nm
CFP
YFP
substrate 6

Figure 5: **Fluorescence properties of recombinant proteins.**
Proteins were diluted in preScission™ buffer to a concentration of 1 μM. Buffer (control) or 1.09 μM preScission™ protease was added to a final volume of 100 μl and samples were incubated for one hour at room temperature. Emission was measured at 460 nm (cyan), which is close to the ECFP emission peak, as well as at 530 nm (orange), which is close to the EYFP emission peak, upon excitation at 430 nm, which is close to the ECFP absorption peak. **A-F**: Fluorescent spectra of unconjugated His-ECFP (A), unconjugated His-EYFP (B), a mixture of 1 μM His-ECFP and 1 μM His-EYFP (C), conjugated His-ECFP-EYFP negative control (D), His-ECFP-C3S5-EYFP (E) and His-ECFP-C3S6-EYFP (F).

The purified proteins displayed characteristic fluorescent properties in vitro, consistent with the findings of Felber and colleagues (*Felber et al, 2004*). Upon exciting purified CFP at a wavelength of 430 nm, which is close to the CFP absorption peak (434 nm), emission was mainly detected at 460 nm, which is close to the CFP emission peak (477 nm) (A), with only minor background YFP emission due to spectral overlap. When excited at 430 nm, purified YFP showed almost no emission at 530 nm, which is close to its emission peak of 527 nm (B). A mixture of both CFP and YFP results in roughly the addition of the two separate emission intensities (C). Upon exciting 1 µM solutions of purified "CFP-YFP" (D) at 430nm, emission from the samples was primarily measured at 530 nm, which is close to at the YFP emission peak, the characteristic feature of FRET. The same was true for the CFP-substrate-YFP proteins (E+F) in absence of the protease. Neither purified CFP nor YFP nor a mixture of both showed this characteristic high YFP emission, indicating that it resulted from resonance energy transfer between the two covalently linked fluorophores. Upon addition of preScission™ protease to a final concentration of 1.09 µM and incubation of the solutions for one hour at room temperature, FRET decreased significantly in the CFP-substrate-YFP samples. Simultaneously, CFP emission increased, approaching values similar to an unconjugated CFP/YFP mixture, indicating proteolysis of the protein. Emission of the "CFP only" and "YFP only" and "CFP-YFP" fusion proteins, on the other hand, was not influenced by the addition of protease. The 530/460 nm emission ratio can be used as an indicator of FRET efficiency. After one hour of incubation with protease, the CFP-C3S5-YFP sample showed a 6.1-fold lower FRET ratio compared to the untreated sample, while the CFP-C3S6-YFP sample showed only a 2.6-fold lower FRET ratio (Figure 6). This suggests that the CFP-C3S5-YFP sample was cleaved more efficiently.

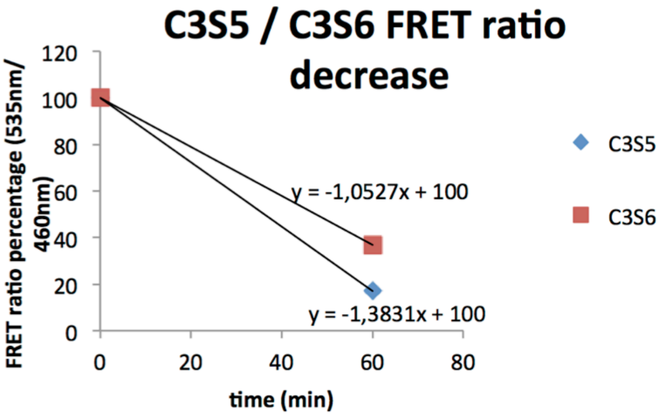

Figure 6: **Graphical representation of the decrease in FRET efficiency over time.** The x-axis denotes the time of incubation with 1.09 μM preScission™ protease. The y-axis denotes the decrease in FRET efficiency ratio percentage when comparing the untreated control (0 min) to the preScission™-incubated sample (60 min).

Based on their data, Felber et al proposed that the drop of FRET ratio over time is proportional to the rate of substrate cleavage. To confirm this, I compared the change in fluorescence to the amount of hydrolyzed CFP-substrate-YFP in samples incubated under the same conditions in parallel and evaluated the results via SDS-PAGE and subsequent coomassie staining (Figure 7).

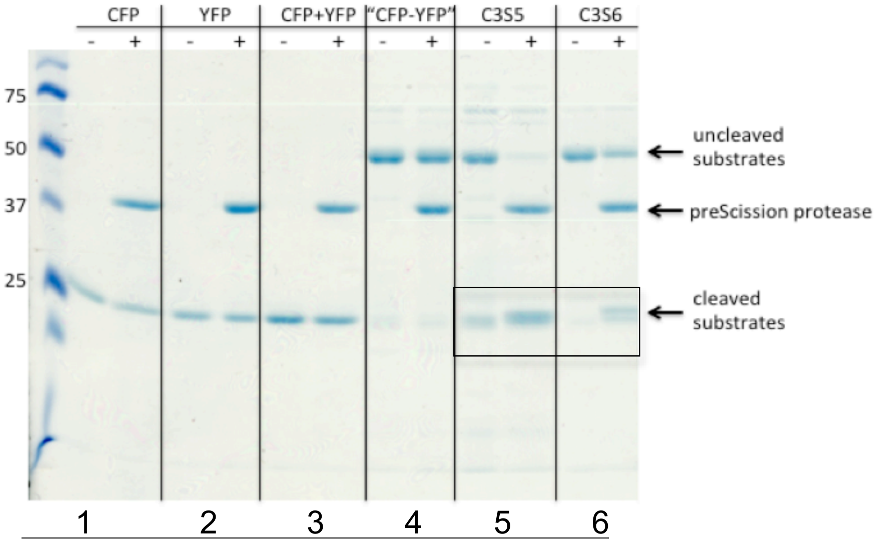

Figure 7: **Cleavage analysis of recombinant proteins.** Substrate proteins were diluted in preScission™ buffer to a concentration of 1 μM. Buffer (control) or 1.09 μM preScission™ protease was added to a final volume of 100 μl and samples were incubated for one hour at room temperature. Upon TCA precipitation (100μl samples + 10% TCA), the precipitates were loaded and analysed via 12.5% SDS-PAGE and coomassie blue staining. CFP = unconjugated His-ECFP (28 kDa); YFP = unconjugated His-EYFP (28 kDa); CFP + YFP = a a mixture of 1 μM His-ECFP and 1 μM His-EYFP; "CFP-YFP" = conjugated His-ECFP-EYFP negative control (55kDa); C3S5 = His-ECFP-C3S5-EYFP (uncleaved: 56 kDa, N-terminal cleavage product: 29 kDa, C-terminal cleavage product: 27 kDa); C3S6 = His-ECFP-C3S6-EYFP (uncleaved 56 kDa, N-terminal cleavage product: 29 kDa, C-terminal cleavage product: 27 kDa), preScission™ 46 kDa.

The experiment showed that FRET decrease coincided with CFP-substrate-YFP hydrolysis. Purified CFP, YFP, a mixture of both (CFP+YFP) and conjugated CFP-YFP remained uncleaved (Fig. 7, lane 1-4). CFP-C3S5-YFP (C3S5) was almost fully cleaved after one hour under the tested conditions, as could be judged by the accumulation of cleavage product and the depletion of uncleaved substrate (Fig. 7, lane 5). CFP-C3S6-YFP (C3S6) was not completely cleaved, supporting the result of the FRET assay that C3S5 was cleaved more efficiently than C3S6 (Fig. 7, lane 6).

In a subsequent silverstaining experiment I evaluated the influence of various parameters on substrate cleavage to be able to find optimal and reproducible conditions for enzyme cleavage assays. These parameters included enzyme concentration, temperature, duration of incubation and the influence of protease inhibitors on proteolysis. (Figure 8)

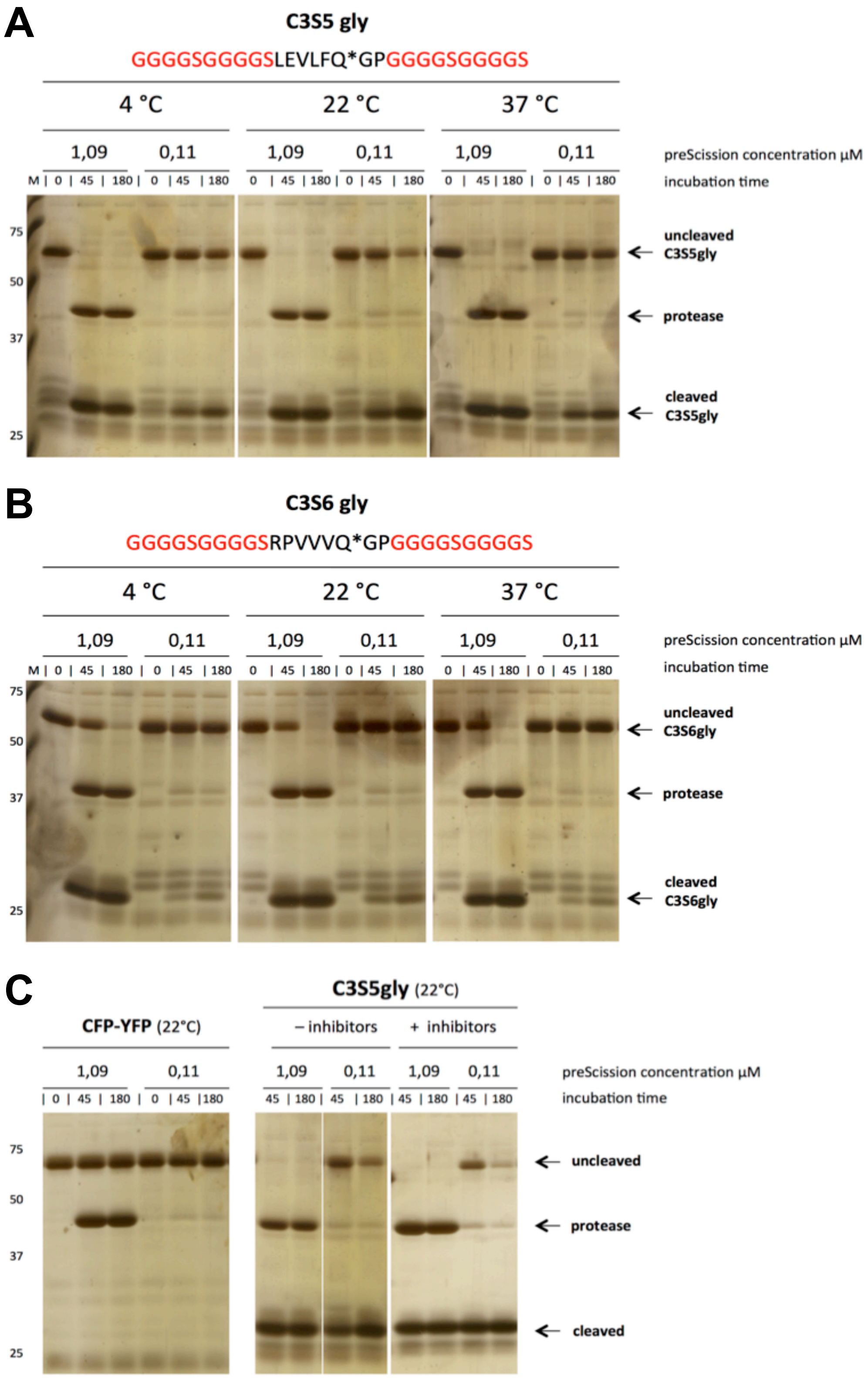
A
C3S5 gly
GGGGSGGGGSLEVLFQ*GPGGGGSGGGGS
4 °C
22 °C
37 °C
1,09
0,11
1,09
0,11
1,09
0,11
preScission concentration µM
M | 0 | 45 | 180 | 0 | 45 | 180
0 | 45 | 180 | 0 | 45 | 180
0 | 45 | 180 | 0 | 45 | 180
incubation time
75
50
37
25
uncleaved C3S5gly
protease
cleaved C3S5gly
B
C3S6 gly
GGGGSGGGGSRPVVVQ*GPGGGGSGGGGS
4 °C
22 °C
37 °C
1,09
0,11
1,09
0,11
1,09
0,11
preScission concentration µM
M | 0 | 45 | 180 | 0 | 45 | 180
0 | 45 | 180 | 0 | 45 | 180
0 | 45 | 180 | 0 | 45 | 180
incubation time
75
50
37
25
uncleaved C3S6gly
protease
cleaved C3S6gly
C
CFP-YFP (22°C)
C3S5gly (22°C)
– inhibitors
+ inhibitors
1,09
0,11
1,09
0,11
1,09
0,11
preScission concentration µM
| 0 | 45 | 180 | 0 | 45 | 180
45 | 180 | 45 | 180 | 45 | 180 | 45 | 180
incubation time
75
50
37
25
uncleaved
protease
cleaved

Figure 8: **Determining optimal conditions for preScission™ reactions in vitro.**
Substrate proteins were diluted in preScission™ buffer to a concentration of 1 µM. Buffer (0) or preScission™ protease was added to a final concentration of 1.09 µM or 109 nM. Samples were incubated for 45 or 180 minutes at 4°C, 22°C or 37 °C. 1.7 µg substrate was loaded and analysed by 12.5 % SDS-PAGE and silver staining. **A:** His-ECFP-C3S5gly-EYFP fusion protein (uncleaved: 57 kDa, N-terminal cleavage product: 29kDa, C-terminal cleavage product: 28 kDa) **B:** His-ECFP-C3S6gly-EYFP fusion protein. (uncleaved: 57 kDa, N-terminal cleavage product: 29kDa, C-terminal cleavage product: 28 kDa) **C left:** His-ECFP-EYFP fusion protein (55 kDa) **C right**: His-ECFP-C3S5gly-EYFP fusion protein diluted in buffer without (-) or with (+) protease inhibitors aprotinin, pepstatin and leupeptin (all 1µg/ml).

Upon incubation for 180 minutes without protease ("0" Fig. 8 A-C), the proteins remained uncleaved, indicating that the proteins were stable under the tested conditions. Upon addition of protease, the C3S5gly substrate (Fig. 8 A) was cleaved more efficiently than the C3S6gly substrate (Fig. 8 B), as could be judged by the accumulation of cleavage product and the depletion of uncleaved substrate over time (45, 180). The protease hydrolyzed both substrates most efficiently at room temperature (22°C) as compared to 4°C and 37°C. In addition, proteolysis of the substrates was significantly reduced upon dilution of the protease to 0,11 µM when compared to 1,09 µM. The negative control, a CFP-YFP fusion protein, was uncleavable under all tested conditions (Fig. 8 C). Protease inhibitors such as aprotinin, leupeptin and pepstatin at low concentrations (1µg/ml) did not have a significant influence on C3S5gly substrate cleavage under the given conditions. These inhibitors are usually added to the preScission™ buffer to ensure protein stability. According to the manufacturer's protocol (*PreScission™ Protease, GE healthcare, Version AA, 06/2011),* 1 µM leupeptin a as well as 0,3 µM aprotinin failed to inhibit preScission™ protease activity by more than 20%. However, I chose not to add inhibitors in further experiments because they are in principle capable of influencing kinetic parameters of an enzymatic reaction (*Cornish-Bowden, 1995*).

In order to be able to calculate the kinetic parameters K_m and k_{cat}, one has to run a series of enzyme assays at varying substrate concentrations, using a surplus of substrate in order to calculate the inital velocity of the reaction under Michaelis-Menten conditions. To determine the velocity of the reaction, CFP and FRET emission was measured at several intervals at 22 nM protease concentration (0, 60, 90 and 180 minutes). In this study, we measured C3S5 and C3S6 substrate concentrations ranging from 1 µM to 16 µM. As a negative control, 1 µM CFP-YFP was used. As a positive control, 1 µM C3S6 was incubated with 1.09 µM protease. FRET efficiency ratios were determined for all samples and compared to vehicle-treated controls. (Figure 9).

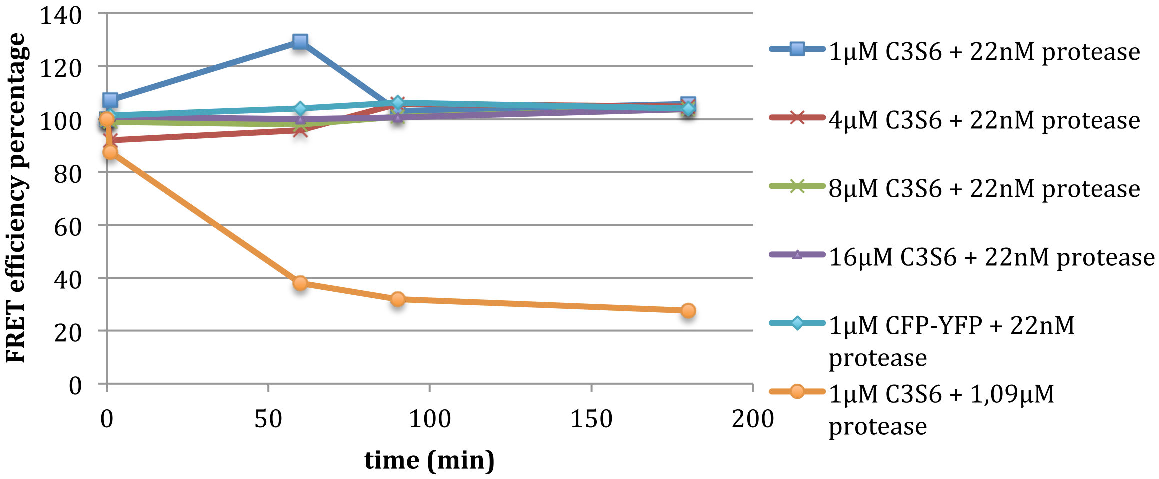

Figure 9: **Changes in FRET efficiency were not detected at low enzyme concentrations.** FRET efficiency ratios (535nm/460nm emission) were determined for recombinant His-ECFP-C3S6-EYFP proteins for 1μM (blue); 4μM (red); 8μM (green); 16μM (purple), incubated with 22nM preScission™ protease, ECFP-EYFP 1μM (cyan) incubated with 22nM protease and C3S6 1μM (orange) incubated with 1,09μM protease, for 0,1, 60, 90 and 180 minutes. All values were normalized to vehicle-treated controls.

Upon addition of preScission™ protease to a final concentration of 22 nM, none of the C3S6 samples showed a substantial change in FRET efficiency (Fig. 9, blue, red, green, purple). FRET efficiency of the "CFP-YFP" negative control also did not change upon incubation with 22nM protease (Fig. 9, cyan). However, 1μM C3S6 substrate incubated with 1.09 μM protease resulted in decrease of FRET over time (Fig. 9, orange). After 60 minutes, the FRET efficiency ratio of this sample had dropped to 38 percent of the vehicle-treated control, similar to the drop in FRET efficiency shown in Figure 6. After a further 30 minutes, the ratio dropped to 32 percent and continued to decrease down to 28 percent of the vehicle-treated control after a further 90 minutes. In conclusion, the results suggest that potential changes in FRET upon incubation with 22nM protease were not detectable under the tested conditions, presumably due to low protease activity and limited sensitivity of the system. Using a higher enzyme concentration of 1.09 μM, however, results in detectable, nonlinear FRET decrease over the course of 180 minutes. Assuming that the decrease in FRET corresponds to substrate cleavage, these results suggest that the velocity of proteolysis decreases over time, presumably because of substrate depletion and/or product inhibition. In the positive control sample there was, however, no surplus of substrate compared to enzyme. The determined velocity, even for the shortest tested interval, can therefore not be assumed to fulfill Michaelis-Menten criteria and therefore does not correspond to the initial reaction velocity under conditions where the substrate is present in excess. I was therefore unable to calculate the kinetic parameters of the preScission™/C3S6 proteolytic reaction under the given conditions.

3.1.2. Using a discontinuous enzyme assay coupled with in-gel western detection to determine kinetic parameters of preScission™ reactions

An *in vitro* cleavage assay in combination with in-gel western blotting was used as a second approach to determine kinetic parameters of the preScission™ proteolytic reaction. The aim of the approach was to quantify the accumulation of cleaved substrate over time with an infrared scanner (Odyssey) and corresponding imaging software, using a 2B6 anti-GFP primary antibody and an Odyssey IR-Dye 680 LT secondary antibody for detecting the substrate. In a first set of experiments, I dertermined the quantifiable linear range of substrate detection (Figure 10)

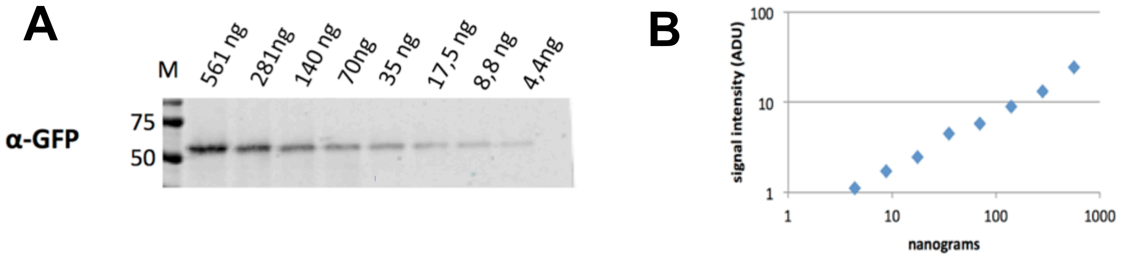

Figure 10: **Determining the linear range of substrate detection using in gel western blot.** **A:** His-ECFP-C3S6-EYFP was serially diluted (561 - 4,4 ng) and analysed by 10% SDS-PAGE and in-gel western blotting using the α-GFP 2B6 primary antibody and the Odyssey 680 LT secondary antibody. **B:** Log-log plot of the quantification via densitometric analysis. The x-axis denotes nanograms of protein loaded, the y-axis denotes the signal intensity of the bands (arbitrary densitometric units, ADU).

Under these conditions, the minimum quantifiable linear range of substrate detection stretched from 4.4 ng to 281 ng, since 561 was not found to be reproducibly in the linear range. Upon further dilution (data not shown), proteins were detectable down to 69 pg, but were out of the quantifiable linear range. I subsequently analyzed differences in cleavage efficiency between C3S5 and C3S6 using the aforementioned method (Figure 11).

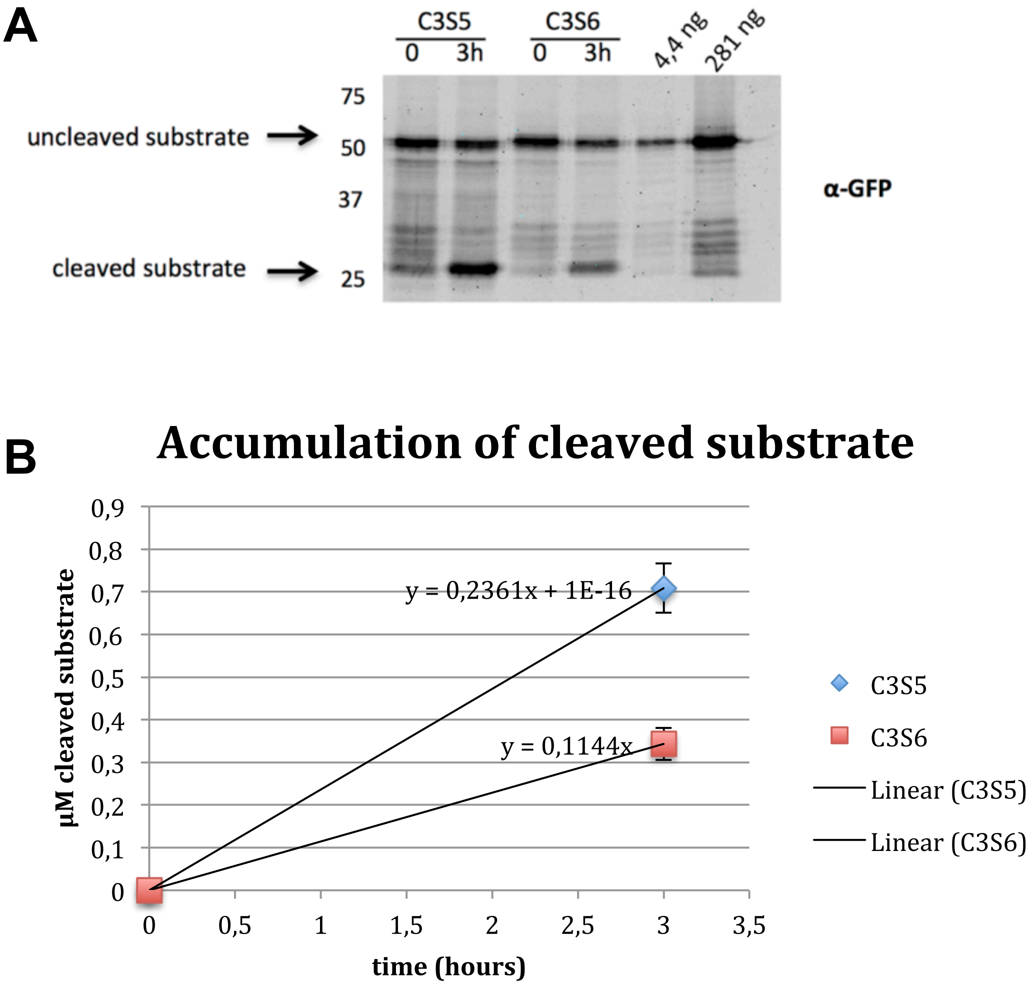

His-ECFP-C3S5-EYFP is cleaved more efficiently than His-ECFP-C3S6-EYFP. Substrate proteins were diluted in preScission™ buffer to a concentration of 1 μM. Buffer (0) or preScission™ protease was added to a final concentration of 1,09 μM. Samples were incubated at room temperature for 3 hours. **A:** 170 ng of substrate was loaded of each condition and 4,4 ng and 281 ng of untreated C3S6 was loaded to show the lower and upper limit of the quantifiable linear range and analysed by 10 % SDS-PAGE and in-gel western blotting using the α-GFP 2B6 primary antibody and the Odyssey 680 LT secondary antibody. **B:** Densitometric analysis of the blot. The x-axis denotes the duration of incubation with protease. The y-axis denotes the concentration of cleaved substrate in μM. The slope of the trendline denotes the reaction rate (μM/h). Average rates are shown, standard deviations for C3S5=0,0581; C3S6=0,0379. P-value: 0,043 in a two-tailed t-test assuming unequal variances, N=3.

When 1 µM of substrate was incubated with 1.09µM of protease for 3 hours, the rate of accumulation of cleaved substrate was found to be 2-fold higher for C3S5 compared to C3S6. Furthermore, the experiment showed that cleaved substrate accumulated to a quantifiable amount under the tested conditions.

Subsequently, I aimed at determining the initial velocities at varying substrate concentrations (500 nM, 1 µM, 4µM and 16 µM) under Michaelis-Menten conditions in order to be able to calculate the kinetic parameters. In order to be able to quantify substrates of a wide range of concentrations on the same blot, all samples were diluted to an equal concentration prior to loading and fixed amounts of protein (170 ng) were loaded. To calculate the reaction rates I subsequently analysed the signal intensity and multiplied each value with the corresponding dilution factor (see Materials and Methods for details). By assuming that the gradient of protein accumulation over 180 minutes corresponded to the initial velocity of the enzymatic reaction (V_0), the kinetic parameters of the reaction were determined by plotting the reaction rate against the substrate concentration (Figure 12).

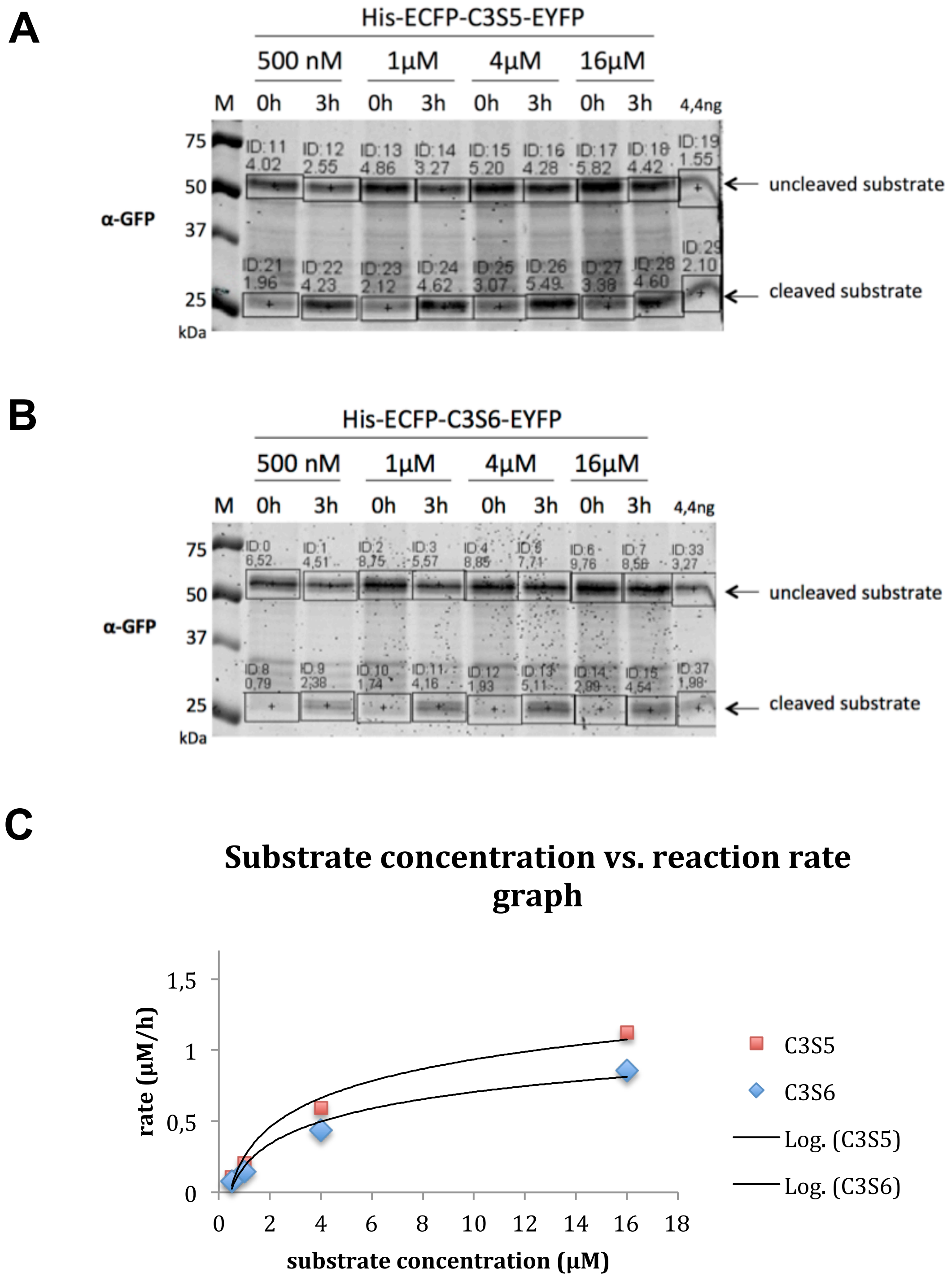

Figure 12: **Differential reaction rates of C3S5 and C3S6 under Michaelis Menten conditions.**

A+B: Proteins were diluted in preScission™ buffer to different concentrations (500 nM, 1 µM, 4 µM, 16 µM). Buffer (0) or preScission™ protease (3h) was added to a final concentration of 109 nM. Samples were incubated for 180 minutes at 22°C. 168 ng of total substrate was loaded and analysed via 12,5 % SDS-PAGE and LI-COR™ in-gel western blotting using the α-GFP 2B6 primary antibody and the Odyssey 680 LT secondary antibody. 4,4 ng of C3S6 was loaded as control **C:** Substrate concentration vs. reaction rate plot of the accumulation of cleaved His-ECFP-C3S5-EYFP or His-ECFP-C3S6-EYFP. Least-square fit values (red), K_m and V_{max} were calculated by non-linear regression of the measured rates (blue) according to the Michaelis-Menten equation. Logarithmic trendlines were added for visualization.

Figure 12 shows differential accumulation of cleaved His-ECFP-substrate-EYFP for different concentrations of substrate (500 nM, 1 µM, 4 µM, 16 µM) when incubated with 109 nM protease (Fig.12 A+B). Densitometric analysis of the accumulation of cleaved substrate (Fig.12 C) revealed that the rate of proteolysis increased asymptotically towards a maximum rate (V_{max}) with increasing substrate concentration. Non-linear regression determined V_{max} to be approximately 1.59 µM/h for C3S5 and 1.23 µM/h for C3S6. The K_m of the reaction was 6.62 µM for C3S5 and 7.13 µM for C3S6, indicating a slightly lower affinity of the protease to the latter substrate. K_{cat} was calculated from V_{max}. Assuming a single catalytic site in the protease, each preScission™ molecule can cleave a maximum of only 0.0041 molecules of C3S5 per second (equals approximately 0,25 per minute) and 0.0031 molecules of C3S6 per second (equals approximately 0,19 per minute) at saturated conditions. This suggests a very low specific activity of the protease under the tested conditions. 4.4 ng of C3S6 was loaded as a control on each blot to show the lower limit of the quantifiable linear range (Fig 12 A+B, 4.4 ng). The ratio of k_{cat} to K_m was therefore 37 nM^{-1} min^{-1} for C3S5 and 26 nM^{-1} min^{-1} for C3S6. The signal for the cleaved substrate of the 500 nM C3S6 sample was excluded from quantification since the value was outside of the linear range (Fig. 12 B). When analyzing samples taken after 90 minutes of incubation with protease, accumulated cleaved substrate signals were too low for reliable quantification (data not shown). In a separate in-gel analysis, equal volumes of samples were loaded without prior dilution to the same substrate concentration. However, densitometric analysis revealed that this approach exceeded the linear detection range of the antibody (data not shown). All in all, the results provided estimates of the kinetic parameters of the preScission™ reaction for the two tested substrates. Substrate C3S6 has a higher Michaelis constant but a lower maximal velocity compared to substrate C3S5. Therefore, it also has a slightly lower turnover number than C3S5. We believed that these parameters made substrate C3S6 the preferable choice for the preScission™ assay due to its higher K_m, therefore being useful for detecting transient protein-protein interactions in mammalian cells. To confirm the values that were obtained in the in-gel analysis, further repetitions of the experiment are needed to obtain statistical significance of the data. Further experiments ranging to higher substrate concentrations should also be performed.

3.2. Using the preScission™ assay to detect protein-protein interactions

To test whether the preScission™ protease assay in combination with substrate C3S6 is suitable for detecting PPIs in principle, I attempted to detect the stable interaction between the catalytic subunit PP2A-Cα and the regulatory subunit PP2A-B55α. Ingrid Frohner, a postdoctoral fellow in the lab, had previously cloned a vector expressing the recombinant bait fusion protein ("pcDNA5TO-myc-preScission™-GL-B55α") and established single HEK293-Trex cell clones expressing the protein. I transfected cells of one of these clones, 14A1, either with a vector coding for the recombinant prey fusion protein ("pcDNA3-EGFP-C3S6-HA-GL-p36), or with a vector coding for a negative control ("pcDNA3-EGFP-C3S6-HA-GL-B55α") (see Materials and Methods + Appendix for cloning procedures). Since no homoligomerization between B55α subunits has yet been observed, we believed that the EGFP-C3S6-HA-GL-B55α could serve as a negative control, an idea that is further evaluated in results section 3.3. I cultivated mixed clones and tested the clones for expression of the proteins. I compared the expression and hydrolysis of the prey fusion protein to a clone previously established by Ingrid Frohner, which expressed the preScission™-B55 protein and a prey that had been fused to the C3S5 substrate (C3S5-p36) (Figure 13). While the bait fusion protein was constitutively expressed, expression of the prey fusion proteins and the negative control was doxycycline inducible.

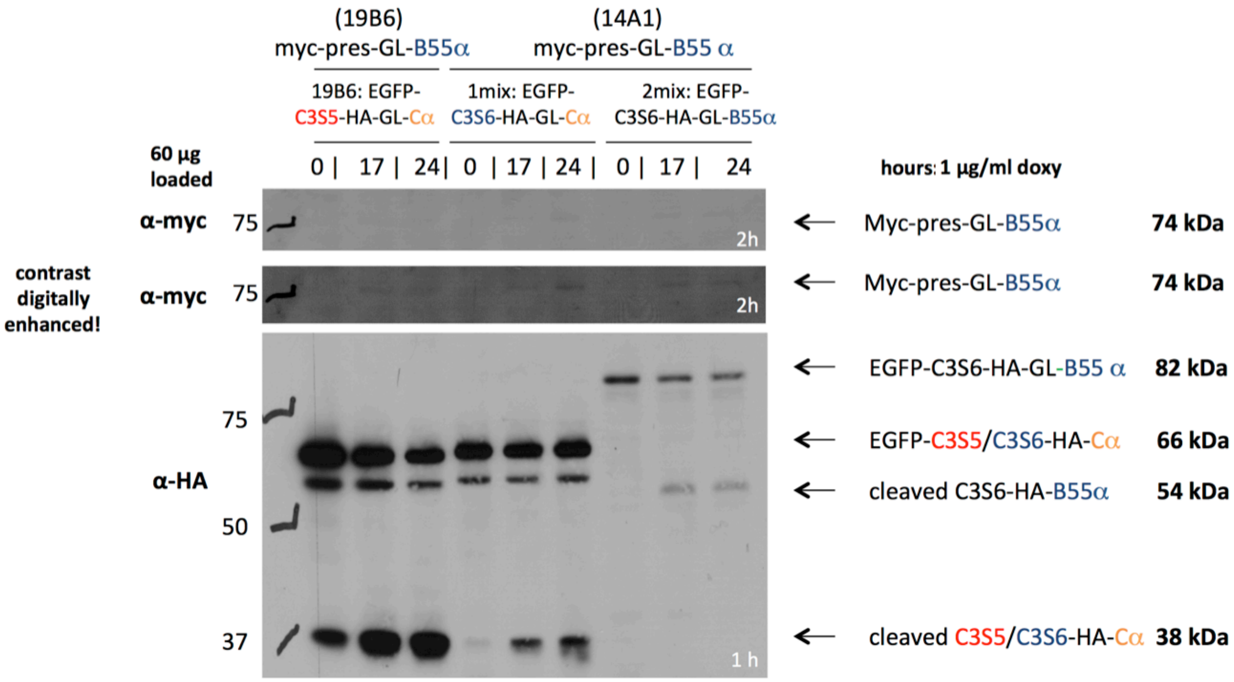
(19B6)
myc-pres-GL-B55α
(14A1)
myc-pres-GL-B55 α
19B6: EGFP-
C3S5-HA-GL-Cα
1mix: EGFP-
C3S6-HA-GL-Cα
2mix: EGFP-
C3S6-HA-GL-B55α
60 µg
loaded
0 | 17 | 24 | 0 | 17 | 24 | 0 | 17 | 24
hours: 1 µg/ml doxy
α-myc
75
2h
Myc-pres-GL-B55α
74 kDa
contrast
digitally
enhanced!
α-myc
75
2h
Myc-pres-GL-B55α
74 kDa
α-HA
75
50
37
1 h
EGFP-C3S6-HA-GL-B55 α
82 kDa
EGFP-C3S5/C3S6-HA-Cα
66 kDa
cleaved C3S6-HA-B55α
54 kDa
cleaved C3S5/C3S6-HA-Cα
38 kDa

Figure 13: Cleavage and expression of preScission™ cleavage site-containing proteins differs in several HEK-Trex mixed clones.
Native whole cell lysates were prepared from HEK-Trex cell clones 19B6 (single clone), 1mix and 2mix (both mixed clones) in which bait expression was induced for 17 and 24 hours with 1μg/ml doxycycline. Untreated cells were used as controls (0). 60μg of protein was loaded. Samples were analyzed by 12.5% SDS-PAGE, immunoblotted and incubated with monoclonal antibodies against myc (4A6) and HA (16B12). The myc-blot in the center panel is a digitally enhanced version of the blot shown in the uppermost panel, achieved. Brightness parameters were altered by -45 while contrast parameters were altered by -65 using GraphicConverterX V. 6.7.4 software. Text in the bottom right corner of each panel indicates the exposure time. Densitometric prey quantification of was performed by analyzing 1h and a 30 sec exposures (data not shown) of the HA blot.

Expression of the myc-preScission™-GL-PP2A-B55α protein was observable in all three cell lines upon doxycycline treatment, however, quantification of bait expression was unfeasible due to low expression. Initial expression of the prey fusion protein was approximately 2,4 times higher 19B6 than in 1mix (Fig 13, αHA). After 24 hours of incubation with doxycycline, approximately 73% of the C3S5-containing prey fusion protein had been cleaved in 19B6. In contrast, only 44% of the C3S6-containing prey fusion protein had been cleaved in 1mix. The EGFP-C3S6-HA-GL-PP2A-B55α protein, however, was also cleaved to a comparable extent: After 24 hours, 44% of this control had been cleaved, although initial expression was at least 2,7 times lower compared to EGFP-C3S6-HA-GL-PP2A-Cα in 1mix. Assuming no B55α dimerization, this suggests that the substrates could be cleaved to some extent independently of an interaction between the B55α and the Cα subunit. The results hint that a C3S5-containing prey fusion protein is cleaved more efficiently than a C3S6-containing prey fusion protein, although differing prey expression levels could have skewed the results.

It was desirable to quantify the extent of proteolysis that is mediated by the preScission proteases' inherent affinity to its own substrate, which is therefore independent of bait/prey interaction. Therefore, I cultivated and tested single clones that constituted an additional negative control by transfecting wild type HEK293-Trex cells with two plasmids simultaneously: one plasmid coding for the prey fusion protein (“pcDNA3-EGFP-C3S6-HA-GL-p36”) as well as one plasmid coding for a doxycycline-inducible myc-preScission™ without an interaction partner of PP2A-Cα (“pcDNA5TO-myc-preScission™-GL"). This control was used to determine unspecific background proteolysis in order to assess the applicability of the preScission™ assay. Furthermore, I cultivated single clones expressing the recombinant bait and prey fusion proteins (Figure 14) In the cells transfected with bait B55α and prey Cα fusion proteins (Fig. 14, 1A1-1A5), expression of "myc-preScission™-GL-B55α" could be observed in all clones upon doxycycline addition, although expression was very difficult to detect even after a 2 hours exposure of the blot. The "EGFP-C3S6-HA-GL-PP2A-Cα" protein was expressed in clones 1A1, 1A2 and 1A5. In these clones, the prey fusion protein was cleaved upon inducing expression of the bait fusion protein, although expression and cleavage in 1A5 was approximately three times lower compared to 1A1 and 1A2 (Fig. 14, 1A1+, 1A2+, 1A5+). In the cells transfected with vectors coding for the bait "myc-preScission™-GL-B55α" and the prey "EGFP-C3S6-HA-GL-PP2A-B55α" protein (2C1-2C6), expression of the bait fusion protein was detected upon doxycycline treatment in clones 2C2, 2C4 and 2C6 and expression of the prey in clones 2C1 and 2C4. The expression of prey "EGFP-C3S6-HA-GL-PP2A-B55α" protein was twofold in 2C4 compared to 2C1, upon doxycycline treatment, prey proteins were cleaved in both clones (cleavage of 2C1 is visible on a longer exposure, data not shown)..

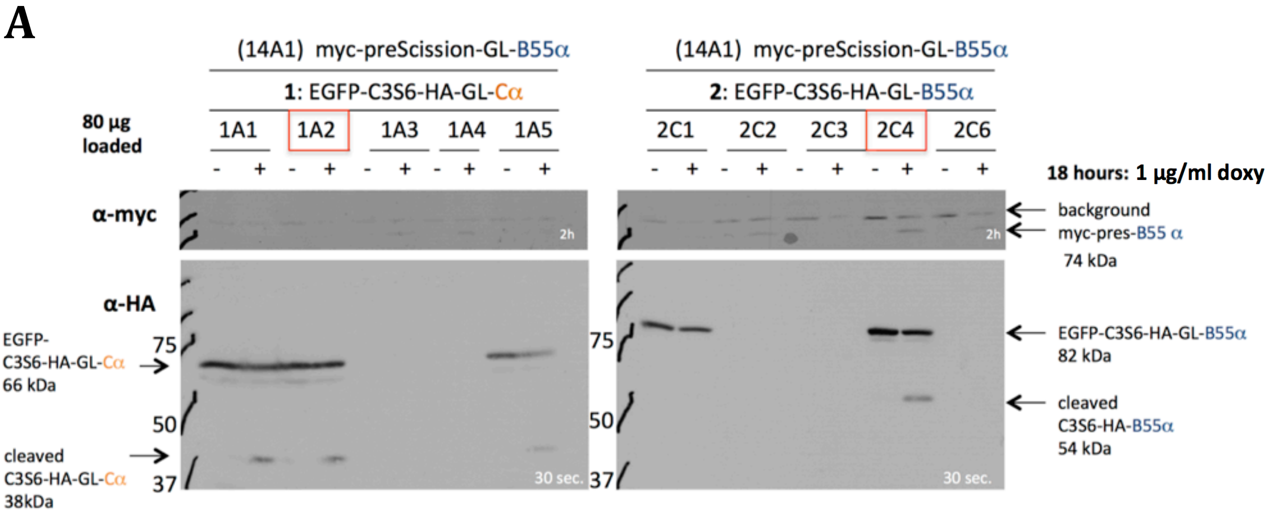
A
(14A1) myc-preScission-GL-B55α
1: EGFP-C3S6-HA-GL-Cα
80 µg loaded
1A1
1A2
1A3
1A4
1A5
(14A1) myc-preScission-GL-B55α
2: EGFP-C3S6-HA-GL-B55α
2C1
2C2
2C3
2C4
2C6
18 hours: 1 µg/ml doxy
α-myc
2h
α-HA
EGFP-C3S6-HA-GL-Cα 66 kDa
75
50
37
cleaved C3S6-HA-GL-Cα 38kDa
30 sec.
background
myc-pres-B55 α 74 kDa
EGFP-C3S6-HA-GL-B55α 82 kDa
cleaved C3S6-HA-B55α 54 kDa

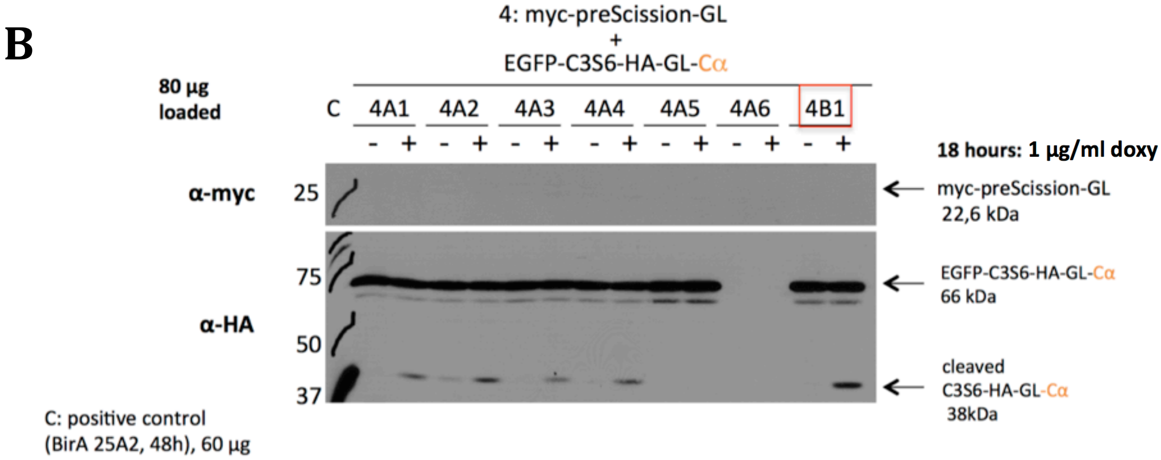
B
4: myc-preScission-GL + EGFP-C3S6-HA-GL-Cα
80 µg loaded
C
4A1
4A2
4A3
4A4
4A5
4A6
4B1
18 hours: 1 µg/ml doxy
α-myc
25
α-HA
75
50
37
myc-preScission-GL 22,6 kDa
EGFP-C3S6-HA-GL-Cα 66 kDa
cleaved C3S6-HA-GL-Cα 38kDa
C: positive control (BirA 25A2, 48h), 60 µg

Figure 14: **Expression analysis of transfected bait and prey fusion proteins in several HEK-Trex single clones.**

Native whole cell lysates were prepared from HEK-Trex cells 18h post doxycycline induction (+). Untreated cells were used as controls (-). **A**: Clones 1A1-1A5 were tested for the expression of the bait fusion protein (myc-preScission™-GL-PP2A-B55α) and the prey fusion protein (EGFP-C3S6-HA-GL-PP2A-Cα). Clones 2C1-2C6 were tested for the expression of the bait fusion protein (myc-preScission™-GL-PP2A-B55α) and the prey EGFP-C3S6-HA-GL-PP2A-B55α protein. 80µg of protein was loaded. **B:** Clones 4A1-4B1 were tested for expression of the bait myc-preScission™-GL protein and of the prey fusion protein (EGFP-C3S6-HA-GL-PP2A-Cα). 120µg of protein was loaded. Samples were analyzed by 12.5% SDS-PAGE on 2 separate gels, immunoblotted and incubated with monoclonal antibodies against HA (16B12) and myc (4A6). Clones that were used in further experiments are marked in red.

In the cells that were simultaneously transfected with plasmids coding for "myc-preScission™-GL" and "EGFP-C3S6-HA-GL-PP2A-Cα", expression of the "myc-preScission™-GL" protein could not be detected in any of the clones (Fig.14, 4A1-4B1), "EGFP-C3S6-HA-GL-PP2A-Cα" expression, however, was observed in all except clone 4A6. Interestingly, this prey fusion protein was cleaved in the doxycycline-treated cells of clones 4A1, 4A2, 4A3, 4A4 and most notably in 4B1, in which cleavage was on average approximately 2,3-fold higher compared to the other clones of transfection 4. This not only suggested that the "myc-preScission™-GL" protein was expressed upon incubation with doxycycline in these clones, but also that it could mediate proteolysis of the substrate, even though it lacked a cognate binding partner of PP2A-Cα. Therefore, this provided further evidence that the prey fusion protein could be hydrolyzed to some extent independently of an interaction between PP2A-B55α and PP2A-Cα. This unspecific cleavage constituted a background signal in the preScission™ assay. It was therefore necessary to quantify this background signal to be able to assess whether the preScission™ assay proposed in this study was able to detect the interaction between the proteins of interest, or whether the rate of proteolysis was mainly dependent on the affinity of the protease to its substrate, C3S6. To be able to do this, I needed to detect, quantify and compare bait and prey levels. I therefore subsequently attempted to confirm the expression of the "myc-preScission™-GL" protein in clone 4B1 and compare it to the expression level of the "myc-preScission™-GL-B55α" bait fusion protein.

Since the expression of the "myc-preScission™-GL" bait protein could not be detected in any of the five single clones, I increased the detection efficiency of the immunoblotting approach by loading 195µg instead of 120µg of 4B1 lysate onto a 15% SDS-PAGE and used a higher primary antibody concentration (1:500) as well as super-ECL for detection. I loaded 65 µg of 1A2 lysate onto a 10% gel in order to be able to compare the expression level of "myc-preScission™-GL" in 4B1 to the level of "myc-preScission™-GL-B55α" expression in clone 1A2 (Figure 16).

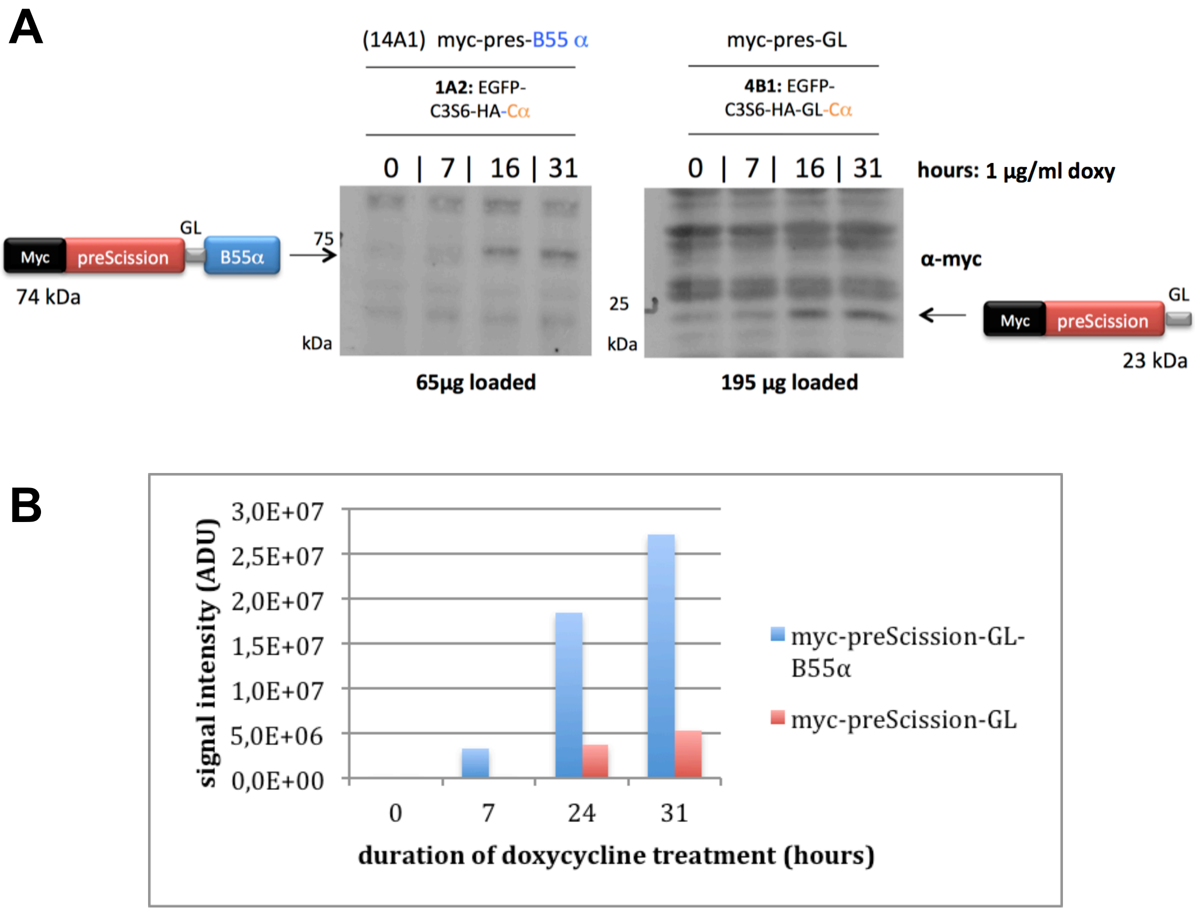

Figure 16: Comparison of the expression levels of "myc-preScission™-GL-PP2A-B55α" and "myc-preScission™-GL".
Native whole cell lysates were prepared from HEK-Trex cell clones 1A2 and 4B1 after 7, 16, or 31 hours of doxycycline induction. Cells incubated for 31h without treatment (0) served as a negative control. Samples were analyzed by 10% SDS-PAGE (1A2) or via 15% SDS-PAGE (4B1), blotted onto the same membrane and incubated with monoclonal α-myc 4A6 antibody. 1A2 lysate containing 65 μg of protein and 4B1 lysate containing 195 μg of protein were loaded. **B:** Densitometric quantification of the expression levels on a 10 second exposure. The x-axis denotes the duration of doxycyline induction. The y-axis denotes the values of band signal intensity normalized to protein amount after having subtracted background values from time point 0 (arbitrary densitometric units, ADU). "myc-preScission™-GL-PP2A-B55α" expression is depicted in blue. "myc-preScission™-GL" expression is depicted in red.

Taking into consideration that three times more protein was loaded for 4B1 compared to 1A2, densitometric analysis of the immunoblot in figure 16 revealed that expression of the "myc-preScission™-GL" protein in clone 4B1 was on average 5-fold lower at the quantifiable time points (24 and 31 hours) than "myc-preScission™-GL-B55α" expression in clone 1A2.

Having determined the levels of myc-preScission™-GL expression, I subsequently chose one suitable clone of each transfection (1A2, 2C4 and 4B1) and compared the accumulation of hydrolyzed prey fusion protein upon 7, 16, 24 and 30 hours of doxycycline treatment. According to our model, accumulation of hydrolyzed prey fusion protein in clone 1A2 that exceeds the background proteolysis detectable in the controls 2C4 and 4B1 would provide evidence for the interaction between the ectopically expressed PP2A-B55α and PP2A-Cα subunits (Figure 17).

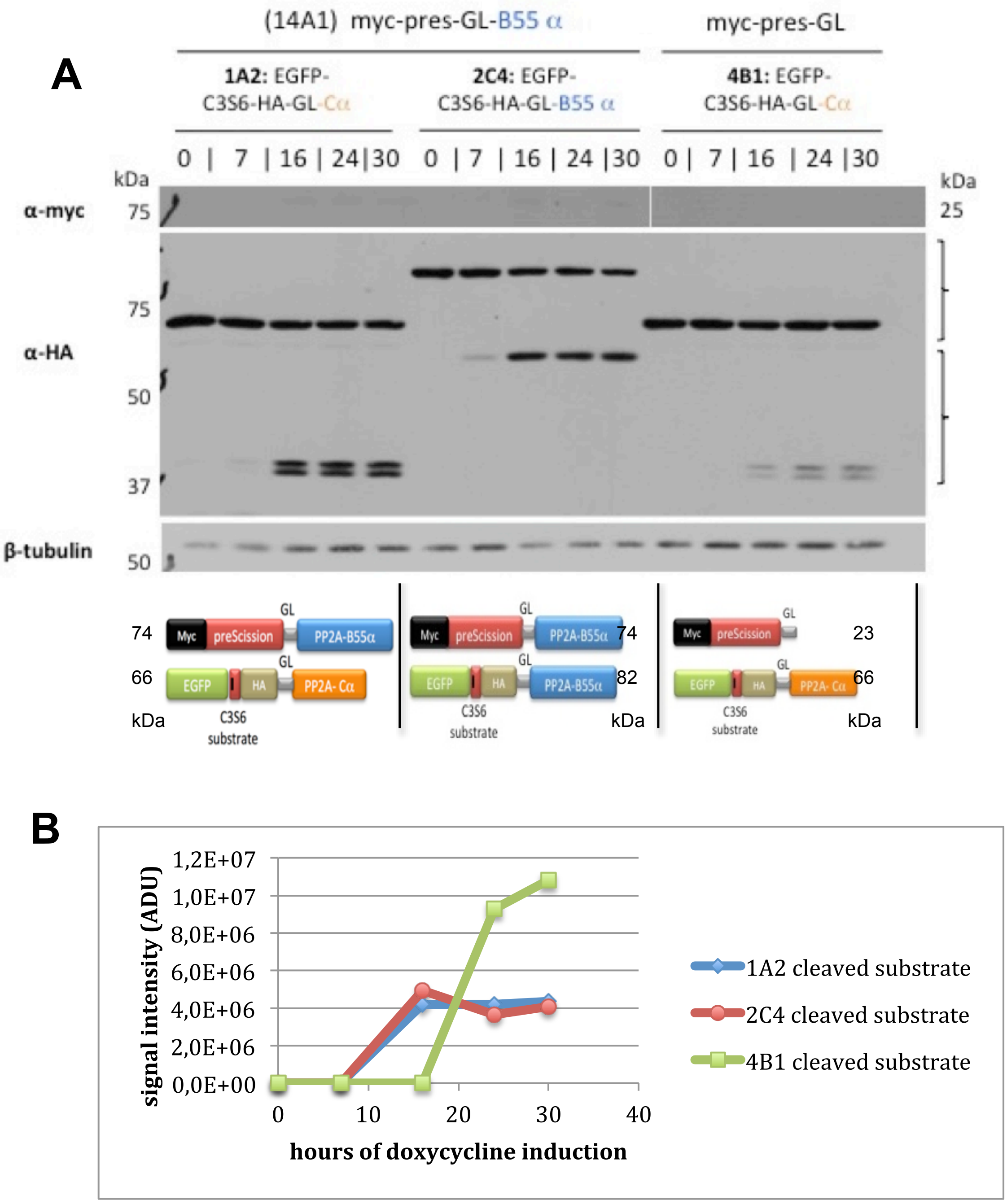

Figure 17: **PreScission™ timecourse assay for the detection of stable PPIs.**
Native whole cell lysates were prepared from HEK-Trex 1A2, 2C4 and 4B1 clones 7, 16, 24 or 30h post doxycycline induction or after 30h incubation without treatment (0). **A:** Samples were analyzed by 12,5% SDS-PAGE on two gels, immunoblotted and incubated with monoclonal antibodies against HA (16B12) and myc (4A6). For the HA-blot, 81 μg of protein was loaded, for the myc-blot, 195 μg of protein was loaded. The HA blot was reincubated with monoclonal antibody against β-tubulin to provide a loading control. **B:** Quantification of the accumulated cleavage products ("cleaved prey") via densitometric analysis of a one-minute exposure of the HA-blot. The x-axis denotes the duration of doyxycline induction. The y-axis denotes the signal intensity of the bands corresponding to the cleavage products. Their values were normalized to the signal strength of prey fusion protein expression at the corresponding time points. For normalization, "myc-preScission™-GL" expression was assumed to be five times lower than "myc-preScission™-GL-B55α (arbitrary densitometric units, ADU).

The preScission™ assay (A) showed that in clone 1A2, the prey fusion protein (visible on the HA blot) was cleaved upon induced expression of the bait fusion protein (myc blot). However, the negative control in clone 2C4, EGFP-C3S6-HA-GL-PP2A-B55α, was also cleaved to a similar extent and time-dependent manner. The expression level of the bait fusion protein in clone 2C4 was presumably similar to the one in clone 1A2, although it needs to be cautioned that quantifications of bands of such a low intensity is prone to error. Therefore, C3S6 was cleaved to approximately the same extent in clones 1A2 and 2C4, indicating that the myc-preScission™-GL-PP2A-B55α bait did not distinguish between substrates fused to PP2A-B55α or PP2A-Cα. Expression of the "myc-preScission™-GL" protein was not detected in clone 4B1. However, it is reasonable to assume that the expression of the protein was similar to the expression in the assay shown in figure 16, where it was on average five times lower than expression of the "myc-preScission™-GL-B55α" protein. Assuming a five-fold lower expression of the "myc-preScission™-GL" protein compared to the "myc-preScission™-GL-PP2A-B55α" protein, the cleavage efficiency was more than two-fold higher in this negative control. Taking this into consideration, the results suggested that the preScission™ protease alone was able to substantially cleave the substrate C3S6 independently of an interaction between the PP2A subunits. By comparing proteolysis in 1A2 to 2C4 and 4B1, it is therefore not possible to deduce that the catalytic Cα and the regulatory B55α subunit of PP2A interacted despite the fact that the endogenous B and C subunits are known to exist in a stable complex.

One possible explanation for the results obtained in the preScission™ assay could be that the affinity of the preScission™ protease to its own substrate, C3S6, is too high to allow the detection of PPIs. However, another interpretation would be that the bait B and prey C subunit fusion proteins did not assemble into stable PP2A holoenzymes because the preScission™ and EGFP parts impair assembly, leaving only the background proteolysis to be detected in the assay. On the other hand, it is also possible that the controls that were used in the preScission™ assay were not appropriate for defining a true background signal. The myc-preScission™-GL protein in clone 4B1, for example, was significantly smaller in size than the true bait fusion protein, since it lacked a B55α subunit. It is conceivable that due to steric hindrance, the B55α subunit on the bait fusion protein inhibited the protease from cutting its substrate on the prey fusion protein. In this case, the proteolysis efficiency would have been biased towards the negative control. Furthermore, it is an intriguing possibility that PP2A-B55α regulatory subunits could oligomerize in vivo. Although no such B55α-B55α interactions have yet been discovered, this possibility could lead to wrong interpretation of the results, where it is assumed that the recombinant proteins in clone 2C4 did not bind to each other.

3.3. Evaluating the preScission™ assay

3.3.1. Co-Immunoprecipitations of recombinant fusion proteins

To resolve the uncertainties of stable complex formation and PP2A-B55α homooligomerization, I attempted to co-immunoprecipitate the myc-tagged bait and the HA-tagged prey fusion proteins using cross-linked myc- and HA-beads (Figure 18).

Recombinant fusion proteins as well as endogenous PP2A subunits were expressed in all cells and prey fusion proteins were cleaved upon doxycycline treatment in cells expressing the protease (Fig. 18, Lys). In general, the results show that since the bait expression was very low, no immunoprecipitated myc-tagged bait and, most likely as a consequence, no co-immunoprecipitated prey fusion protein could be detected in any of the clones (Fig. 18, myc-IP). However, substantial amounts of both HA-tagged B55α and Cα-containing prey fusion proteins were immunoprecipitated. Again, co-immunoprecipitated bait fusion protein could not be detected, presumably due to low expression, but detection was also hampered by unspecific smear signals on the blot, presumably due to a cross-reaction between the beads and the myc-4A6 antibody (Fig. 18, HA-IP).

Endogenous Cα subunits co-immunoprecipitated with HA-prey B55α fusion protein (clone 2C4, but not in 1A2, 4B1 and 10B2). Endogenous B55α subunits, on the other hand, co-immunoprecipitated exclusively with HA-prey Cα fusion protein (clones 1A2, 4B1 and 10B2, but not in 2C4).

A

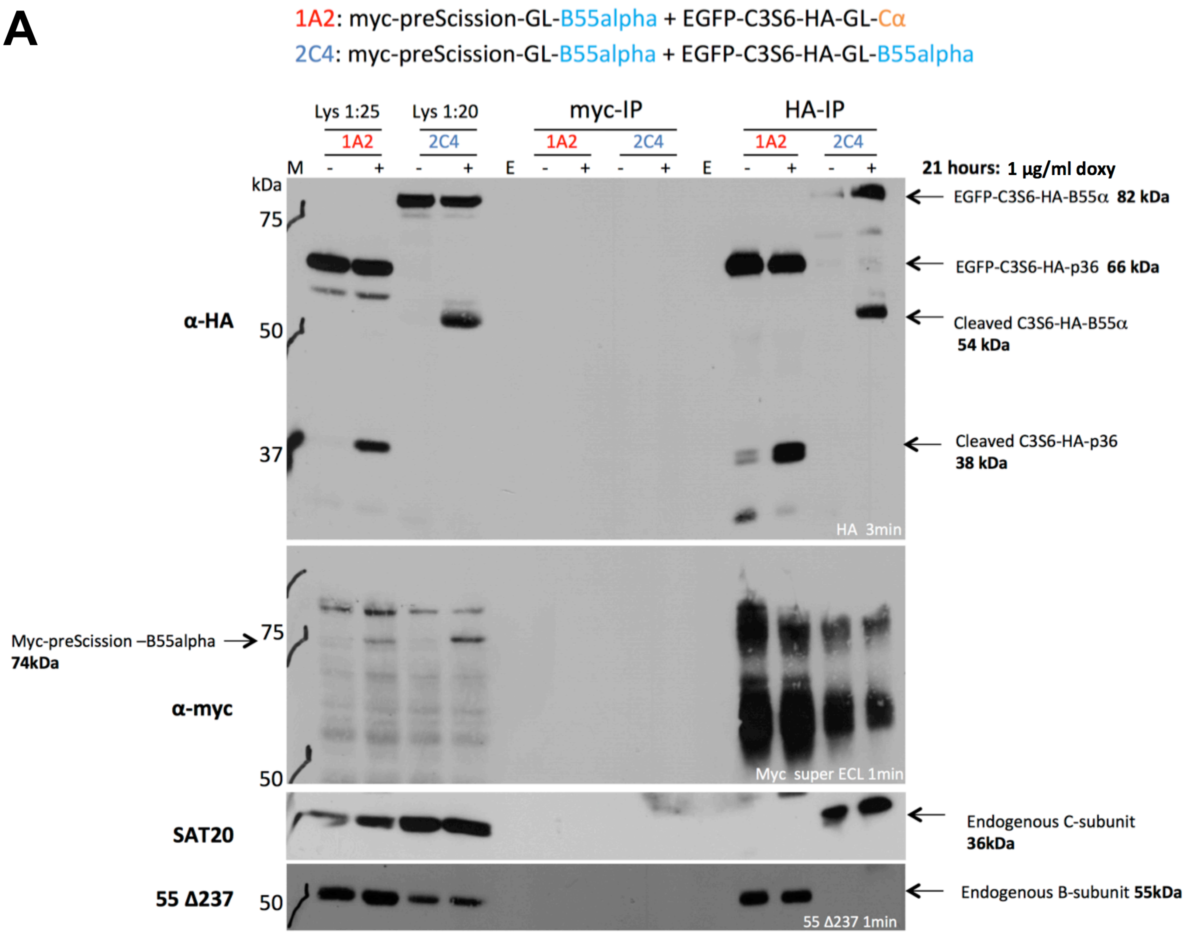
1A2: myc-preScission-GL-B55alpha + EGFP-C3S6-HA-GL-Cα
2C4: myc-preScission-GL-B55alpha + EGFP-C3S6-HA-GL-B55alpha
Lys 1:25
Lys 1:20
myc-IP
HA-IP
1A2
2C4
1A2
2C4
1A2
2C4
M - + - + E - + - + E - + - +
21 hours: 1 µg/ml doxy
kDa
75
50
37
α-HA
EGFP-C3S6-HA-B55α 82 kDa
EGFP-C3S6-HA-p36 66 kDa
Cleaved C3S6-HA-B55α 54 kDa
Cleaved C3S6-HA-p36 38 kDa
HA 3min
Myc-preScission –B55alpha 74kDa
75
α-myc
50
Myc super ECL 1min
SAT20
Endogenous C-subunit 36kDa
55 Δ237
50
Endogenous B-subunit 55kDa
55 Δ237 1min

B

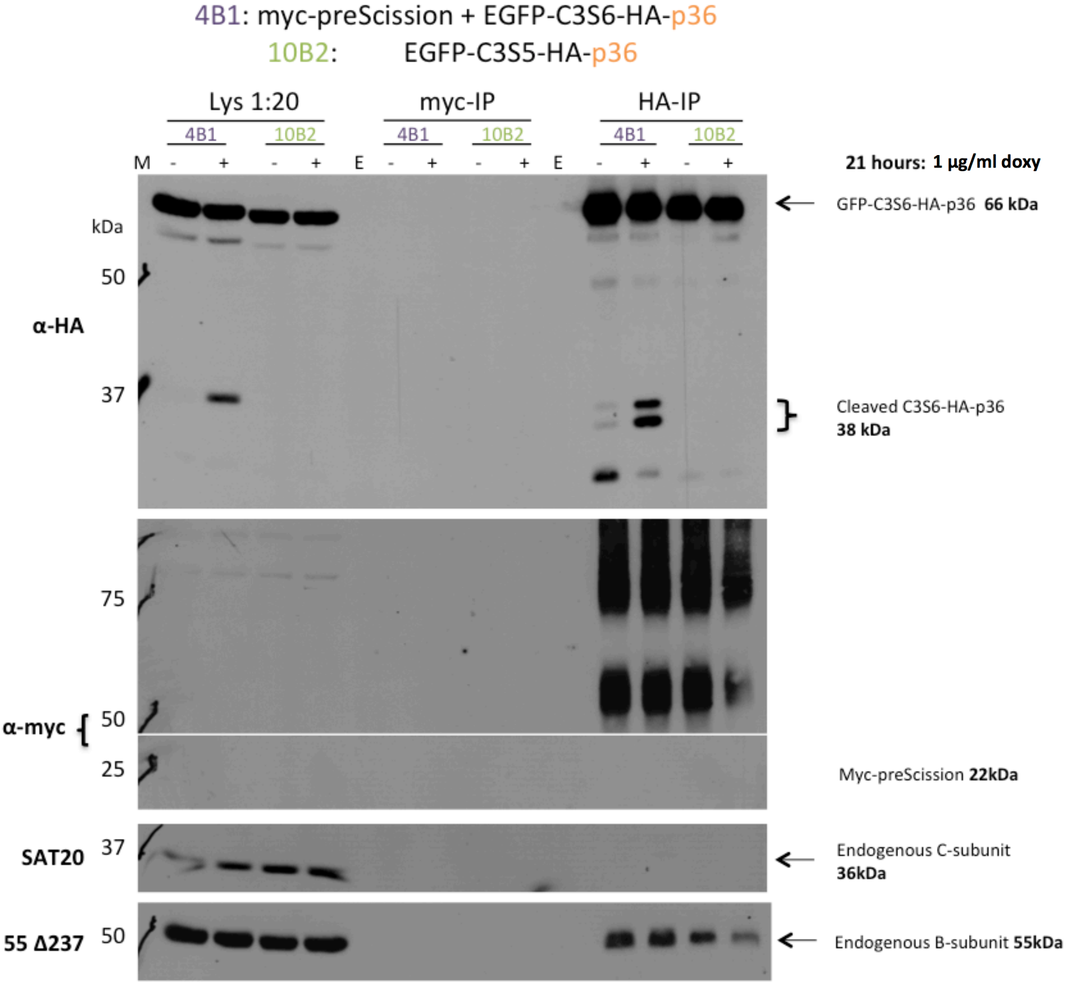
4B1: myc-preScission + EGFP-C3S6-HA-p36
10B2: EGFP-C3S5-HA-p36
Lys 1:20
myc-IP
HA-IP
4B1
10B2
4B1
10B2
4B1
10B2
M - + - + E - + - + E - + - +
21 hours: 1 µg/ml doxy
kDa
50
37
α-HA
GFP-C3S6-HA-p36 66 kDa
Cleaved C3S6-HA-p36 38 kDa
75
α-myc
50
25
Myc-preScission 22kDa
SAT20
37
Endogenous C-subunit 36kDa
55 Δ237
50
Endogenous B-subunit 55kDa

Figure 18: **Co-immunoprecipitation analysis of bait and prey fusion proteins.**
Native whole cell lysates were prepared from HEK-Trex cells 21 hours post doxycycline induction (+) or after 21 hours without treatment (-). One twentieth of the lysate was loaded as control (Lys 1:20). Only one twenty-fifth of the lysate was loaded for 1A2 by mistake (Lys 1:25). One half of the remaining lysate was incubated with myc beads (myc-IP) while the other half was incubated with HA beads (HA-IP) prior to loading. Samples were analyzed by 12.5% SDS-PAGE, immunoblotted and incubated with monoclonal antibodies against myc (4A6), HA (16B12) and polyclonal antibodies against PP2A-Cα (SAT 20) and PP2A-Bα (55Δ237).

All in all, the immunoprecipitations suggested that the prey fusion proteins are in principle capable of complex formation with endogenous PP2A subunits. Furthermore, they indicate that B55α subunits presumably do not form stable homooligomers since endogenous B55α subunits did not co-immunoprecipitate with prey B55α-fusion proteins. Therefore, clone 2C4 most likely constituted a valid negative control in the preScission assay.

While "EGFP-C3S6-HA-GL-PP2A-B55α" expression was clearly detected using the 55 Δ 237 antibody (data not shown, clone 2C4), expression of the 74 kDa "preScission-B55α" bait fusion protein was only detected with the myc-antibody (clones 1A2+ and 2C4+). This suggests that the expression level of the bait fusion protein was much lower than the one of the "EGFP-C3S6-HA-GL-PP2A-B55α" protein. To compare the expression of bait and prey fusion proteins to the expression levels of endogenous PP2A-B55α and Cα subunits, I subsequently analysed a twentieth of the lysate used for the IP in figure 18 (Figure 19).

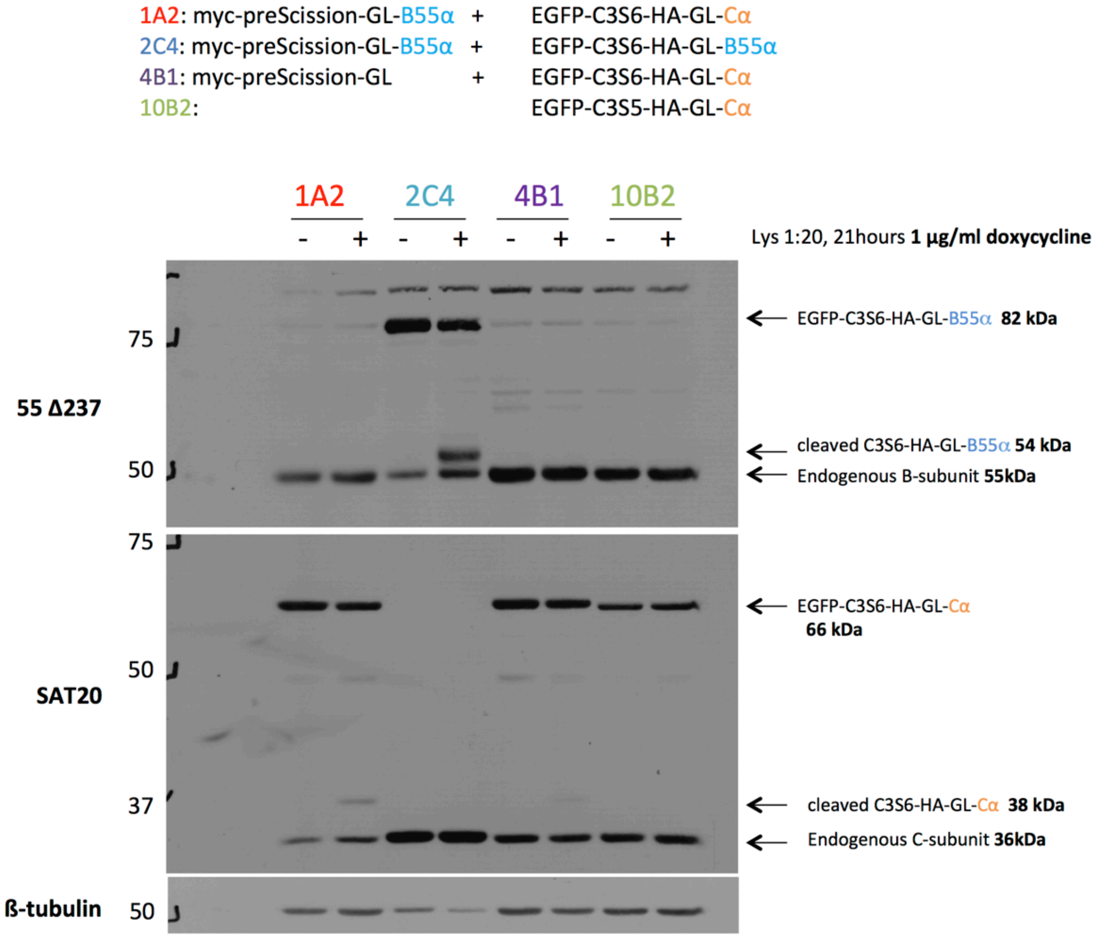
1A2: myc-preScission-GL-B55α + EGFP-C3S6-HA-GL-Cα
2C4: myc-preScission-GL-B55α + EGFP-C3S6-HA-GL-B55α
4B1: myc-preScission-GL + EGFP-C3S6-HA-GL-Cα
10B2: EGFP-C3S5-HA-GL-Cα
1A2
2C4
4B1
10B2
- + - + - + - +
Lys 1:20, 21hours 1 µg/ml doxycycline
55 Δ237
75
50
EGFP-C3S6-HA-GL-B55α 82 kDa
cleaved C3S6-HA-GL-B55α 54 kDa
Endogenous B-subunit 55kDa
SAT20
75
50
37
EGFP-C3S6-HA-GL-Cα 66 kDa
cleaved C3S6-HA-GL-Cα 38 kDa
Endogenous C-subunit 36kDa
ß-tubulin
50

Figure 19: **Expression of endogenous and ectopically expressed proteins.** Native whole cell lysates were prepared from HEK-Trex cells 21 hours post doxycxycline induction (+). Untreated cells were lysed after 21 hours incubation as controls (-). One twentieth of the lysate was loaded (Lys 1:20). Samples were analyzed by 12.5% SDS-PAGE, immunoblotted and incubated with polyclonal antibodies against PP2A-Cα (SAT 20), PP2A-Bα (55Δ237) and ß-tubulin (loading control).

Again, expression of the 74 kDa "preScission-B55α" bait fusion protein was not detected using the 55Δ237 antibody (clones 1A2+ and 2C4+). In clone 2C4, expression of "EGFP-C3S6-HA-GL-PP2A-B55α" was however approximately 14-fold higher than endogenous PP2A-B55α. The SAT20 blot shows that expression of prey Cα-subunit fusion proteins was on average only 1,7-fold higher compared to the endogenous Cα subunits in clones 1A2, 4B1 and 10B2. Taking unequal loading into account, endogenous C-subunit levels were at least 3,5-fold higher in 2C4 compared to the other clones. This is consistent with the observation that the level of PP2A expression is tightly regulated (*Baharians and Schönthal, 1998*). Therefore, an ectopically expressed Cα-subunit presumably led to the downregulation of endogenous Cα.

3.3.2. Evaluating the preScission™ assay by inhibiting bait and prey interaction

The idea that the prey fusion protein is cleaved independently of an interaction between PP2A-B55α and PP2A-Cα was further tested by a preScission™ timecourse in which I treated the cells with okadaic acid (OA), which inhibits PP2A catalytic activity, decreases PP2A methylation and has been suggested to cause disassembly of PP2A complexes. Therefore, adding okadaic acid to the cells concomitantly to doxycycline treatment should decrease cleavage of the substrate by the preScission™ protease, if the proteolytic reaction depends on the interaction of bait and prey. DMSO-treated cells served as a vehicle control. I compared the proteolysis of the substrate in clone 1A2 to the accumulation of cleaved product in clone 4B1, which expressed the "myc-preScission™-GL" protein. The MAP kinase kinase ERK is a target of PP2A (*Sontag et al, 1993*). When PP2A is inhibited, ERK is phosphorylated and active (*Alessi et al, 1995).* Therefore I checked the phosphorylation status of ERK with a monoclonal anti-p44/42 antibody to confirm the inhibition of PP2A by okadaic acid. α-GAPDH served as a loading control (Figure 20).

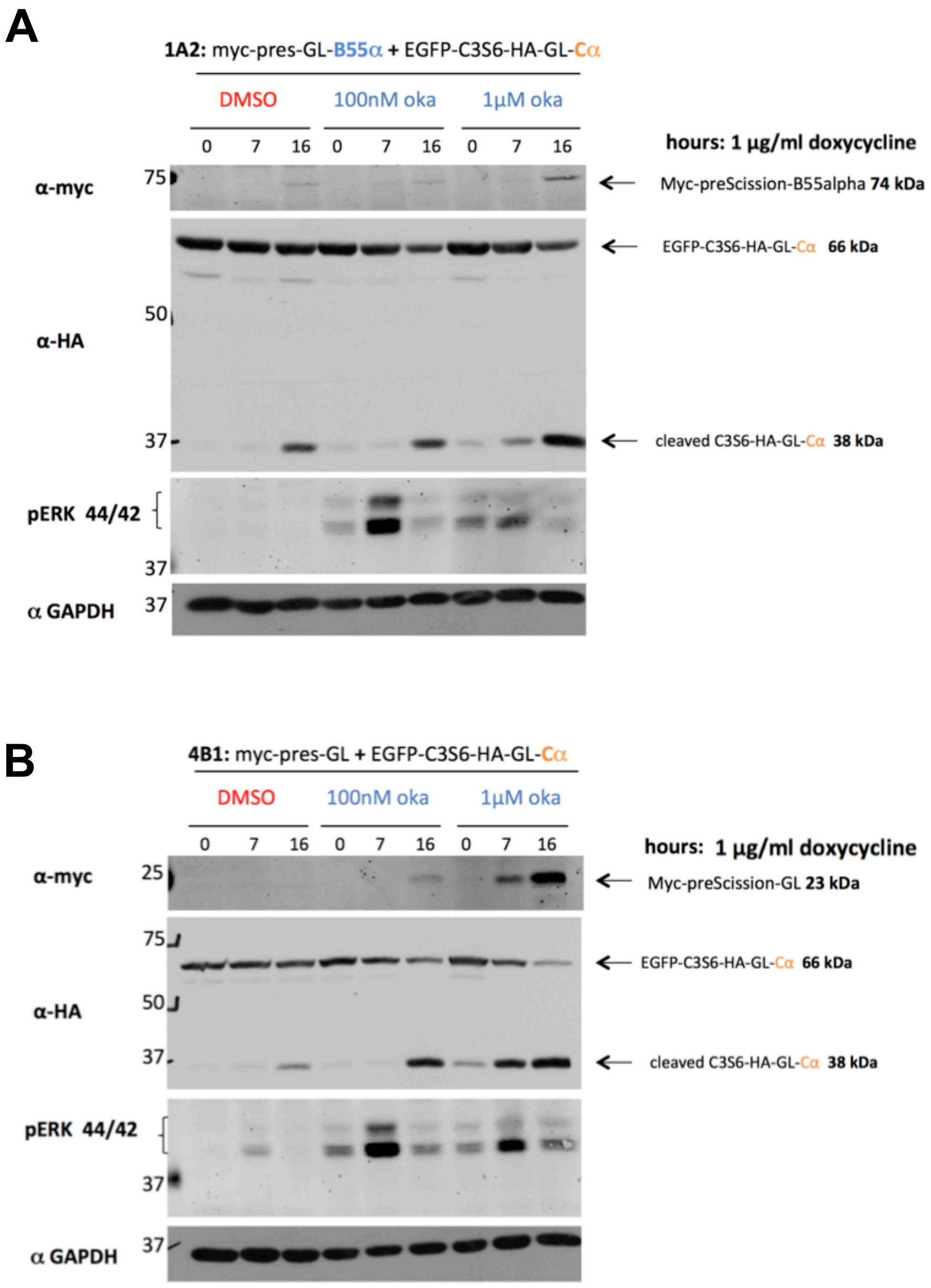
A
1A2: myc-pres-GL-B55α + EGFP-C3S6-HA-GL-Cα
DMSO
100nM oka
1μM oka
0 7 16 0 7 16 0 7 16
hours: 1 μg/ml doxycycline
α-myc
75
Myc-preScission-B55alpha 74 kDa
EGFP-C3S6-HA-GL-Cα 66 kDa
50
α-HA
37
cleaved C3S6-HA-GL-Cα 38 kDa
pERK 44/42
37
α GAPDH
37
B
4B1: myc-pres-GL + EGFP-C3S6-HA-GL-Cα
DMSO
100nM oka
1μM oka
0 7 16 0 7 16 0 7 16
hours: 1 μg/ml doxycycline
α-myc
25
Myc-preScission-GL 23 kDa
75
EGFP-C3S6-HA-GL-Cα 66 kDa
50
α-HA
37
cleaved C3S6-HA-GL-Cα 38 kDa
pERK 44/42
37
α GAPDH
37

Figure 20: **Inhibition of PP2A assembly shows that substrate proteolysis is independent of B55α and Cα interaction.**

Native whole cell lysates were prepared from HEK-Trex cells 7 and 16 hours after doxycycline treatment. Cells were treated with DMSO or okadaic acid (100nM oka or 1μM oka) one hour prior to doxycycline induction. As controls, cells were lysed after 17 hours of treatment with DMSO or okadaic acid in growth medium lacking doxycycline (0). 195μg or 150μg of protein was loaded on two 10% SDS-PA gels, immunoblotted and incubated with monoclonal antibodies against α-myc (4A6) and α-HA (16B12) on one membrane or pERK (p44/42) and α-GAPDH on the other. **A:** Clone 1A2 expressed the bait and the prey fusion proteins (myc-preScission™-GL-PP2A-B55α, and EGFP-C3S6-HA-GL-PP2A-Cα). **B:** Clone 4B1 expressed a myc-preScission™-GL protein and the prey fusion protein (EGFP-C3S6-HA-GL-PP2A-Cα).

Incubation with doxycycline for 7 or 16 hours in clone 1A2 (Figure 20, A, myc) led to cleavage of the substrate (A, HA) in the cells treated with DMSO, 100nM okadaic acid or 1 µM okadaic acid. Interestingly, preScission™ expression and substrate hydrolysis was higher in the samples treated for 17 hours with 1µM okadaic acid and for 16 hours with doxycycline than in vehicle treated samples. Prolonged treatment with okadaic acid at a high concentration might therefore have enhanced expression or stability of the protease. The exact mechanism for this is elusive. pERK was hyperphosphorylated in the oka-treated samples, most notably in the cells incubated for 8 hours with 100nM okadaic acid and for 7 hours with doxycycline.

This indicated that okadaic acid inhibited PP2A catalytic activity, however the prey substrate was still cleaved in the cells treated with okadaic acid. More notably, it was cleaved to the same extent in the samples incubated with 100 nM okadaic acid and the DMSO-treated controls, where preScission™ expression was similar. This indicated that the substrate was most probably cleaved independently of PP2A-Cα and PP2A-B55α interaction. The results for clone 4B1 (Figure 20, B) support these findings. The substrate was similarly cleaved in the clone expressing a "myc-preScission™-GL" protein, which confirmed that proteolysis of the prey fusion protein is independent of an interaction between the B55α and Cα subunit. This insinuates that cleavage of the prey fusion protein is solely dependent on the affinity of the preScission™ to the substrate C3S6.

4. Discussion

The goal of this study was to develop a novel approach using the preScission™ protease to detect transient protein-protein interactions in mammalian cells. To find an optimal preScission™ substrate for the assay, I first attempted to determine kinetic parameters of preScission™ reactions *in vitro*. I was unable to determine these parameters using FRET due to limited sensitivity of the method under the tested conditions. I succeeded to provide estimates of the parameters using a discontinuous enzymatic assay approach coupled to in-gel western blotting. In mammalian cells, the preScission™ assay was however unable to detect PPIs between PP2A subunits, presumably due to high levels of endogenous PP2A subunits, inhibition of PP2A assembly due to steric hindrance or high inherent affinity of the protease to its own substrate.

4.1. Determining kinetic parameters of the preScission™ reaction

In this study, recombinant His-ECFP-substrate-EYFP proteins were successfully cloned, expressed and purified for subsequent kinetic analysis of the preScission™ protease reaction. Residual impurities were detected in the sample after affinity purification. These impurities could not be completely removed via membrane filtration, potentially influencing FRET and in-gel measurements in the subsequent experiments. Further purification of the samples via HPLC was not performed due to the risk of dimerization of the fluorescent molecules at high concentrations (*Mitra et al, 1996*).

The purified proteins displayed characteristic fluorescent properties *in vitro* consistent with the findings of Felber and colleagues (*Felber et al, 2004*). FRET decrease coincided with CFP-substrate-YFP hydrolysis. However, the attempt to determine kinetic parameters under Michaelis-Menten conditions was unsuccessful. When using a low enzyme concentration (22 nM), no changes in FRET were observed in any of the tested samples. This was possibly due to lack of sensitivity of the equipment to measure subtle changes in FRET. For a confident estimate of the kinetic parameters, the highest tested substrate concentrations should far exceed K_m. Previous studies suggest a high K_m of 3.1 mM for substrate C3S6 (*Long et al, 1989*). However, we only tested substrate concentrations up to 16 µM. The reason for this is that CFP and YFP run the risk of dimerizing at concentrations exceeding 100 µM (*Mitra et al, 1996; Felber et al, 2004*). This might lead to precipitation of the proteins or intermolecular FRET, causing background signals in the assay. Alternatively, an increase of sensitivity of the assay could be achieved by choosing filters that allow more specific stimulation or emission measurements of the fluorescent proteins, thereby optimizing the excitation conditions and emission measurements. Further studies should aim at optimizing FRET conditions in order to allow sensitive measurements of the preScission™ reaction under conditions that fulfill Michaelis-Menten criteria.

A discontinuous enzyme assay coupled with in-gel western blotting of the samples provided estimates of the kinetic parameters of the preScission™ proteolytic reaction. However, it needs to be noted that the resulting values are not statistically significant, since they could not be repeated due to time restrictions. Computerized least-square fitting of the data was used to calculate the kinetic parameters. Linear methods such as a Lineweaver-Burk plot were considered unfeasible due to their inherent high margin of error, especially when working with few data points *(Dowd and Riggs, 1965; Tseng et al, 1990)*.

We chose C3S6 over C3S5 as the more promising candidate for the preScission™ assay due to its higher K_m. Kinetic parameters of the preScission™/C3S6 reaction determined in this study differ substantially from previous findings. While Long and colleagues determined a K_m of 3.1 mM (*Long et al, 1989*), the findings presented in this study suggest a K_m of 7.13 µM. Several factors might account for this divergence, most notably a difference in the techniques used to determine kinetic parameters. In their approach, Long and colleagues determined kinetic parameters of the short peptide substrate synthesized by the Merrifield solid phase technique and monitored cleavage via reverse phase chromatography. In our approach, we used the in-gel western approach in combination with a much longer His-ECFP-substrate-

EYFP fusion protein. Cordingley et al suggest that the recognition and cleavage of the substrate by the protease *in vivo* are not only dependent on the primary structure signals, but also upon secondary and tertiary structure of the protein (*Cordingley et al, 1990*). Furthermore, the presence of amino acids shortly upstream or downstream of the tested substrates has been shown to alter the k_{cat}/K_m values of the proteolytic reaction by several orders of magnitude (*Long et al, 1989; Cordingley et al, 1990*). It is therefore likely that the K_m and k_{cat} values of the reaction differ depending on whether His-ECFP-substrate-EYFP proteins or the substrate peptide alone is analyzed. The prey fusion proteins used in the preScission™ assay, EGFP-HA-substrate-GL-PP2A-Cα, might therefore also display different kinetic parameters. However, our results suggest that C3S5 was cleaved more efficiently than C3S6 *in vitro* and presumably also in mammalian cells. For determining the kinetic parameter values, the initial velocity of the reaction process has to be measured. However, substrate accumulation was analyzed after the reaction had proceeded for 180 minutes. This was necessary to allow sensitive and quantifiable analysis of the accumulated product. It is unclear whether quantitative analysis at an earlier time point would have provided different results. Our results also suggest a very low turnover number for both substrates C3S5 and C3S6. While enzymes usually cleave between 10^3 and 10^7 molecules per second (*Hagen, 2006*), the preScission™ only cleaved 11.3 or 14.7 molecules per hour. This could be explained by a general low activity of the protease under the tested conditions or by the low affinity of protease to the substrates. Moreover, the maximum substrate concentration tested in this study was 16 µM. As mentioned before, substrate concentrations that far exceed the estimated Km should be measured to gain exact values of kinetic parameters. All in all, repetitions of the experiment should aim at confirming the values that were obtained in the in-gel analysis and should extend the upper limit of the tested substrate concentration range.

4.2. Using the preScission™ assay to detect protein-protein interactions

The results suggested that the preScission™ assay is unsuited for detecting mammalian protein-protein interactions such as the ones between PP2A-B55α and PP2A-Cα when using C3S6 as a substrate. The tested bait fusion protein cleaved the prey fusion protein to an equal or to a lesser extent compared to the tested negative controls. Subsequent co-immunoprecipitation experiments were performed to assess the validity of the negative controls. Co-IPs were hampered by the low expression of bait-preScission™ fusion proteins, therefore detailed analysis of bait and prey interaction was not possible. However, the results suggested that endogenous Cα subunits bind to exogenous prey-B55 but not to exogenous Cα. Similarly, endogenous B55α subunits bind to exogenous Cα but not to exogenous B55α. This suggested that B55α subunits did not form oligomers and therefore clone 2C4 constituted a valid negative control in the preScission™ assay.

The "myc-preScission™-GL" fusion protein that constituted the negative control was significantly smaller than the bait fusion protein, as it lacked a PP2A-B55α subunit. While we have little information about the steric properties of our fusion proteins, it seems plausible that these properties might influence the kinetic parameters of the enzymatic reaction. It is conceivable that due to steric hindrance, the B55α subunit bait hindered the protease from cutting its substrate on the prey C subunit fusion protein. In this scenario, the catalytic efficiency could have been biased towards the negative control. This would be a possible explanation for the result of the preScission™ assay, where the "myc-preScission™-GL" protein cleaved the substrate more extensively than "myc- preScission™-GL-PP2A-B55α" was able to do.

Assuming inhibition of PP2A activity and methylation by adding okadaic acid during the preScission™ assay, the results suggested that proteolytic cleavage of the substrate is largely independent of an interaction between the B and C subunits located on the bait and prey fusion proteins respectively. One possible explanation for this is that the affinity of the protease to the C3S6 substrate was too high. However, we also showed that the expression levels of endogenous PP2A subunits far exceeded the levels of the ectopically expressed bait and were similar to expression of the prey. It is conceivable that during the assay, most of the ectopically expressed PP2A-B and C subunits were bound by their corresponding endogenous interaction partners. This might have depleted the pool of free recombinant bait and prey fusion proteins, and therefore the proteolysis detected in the assay is the residual background signal resulting from the inherent affinity of the protease to C3S6. This issue could potentially be resolved by knocking down the expression of endogenous PP2A-B55α and PP2A-Cα subunits via shRNAs. This could result in increased sensitivity of the assay, potentially allowing the detection of protein-protein interactions. Further experiments with other substrates or a mutated enzyme should also be performed in order to optimize the kinetic parameters of the preScission™ reaction for detecting transient protein-protein interactions.

5. References

Adair, W.S., D. Jurivich and U.W. Goodenough. (1978). "Localization of cellular antigens in sodium dodecyl sulfate-polyacrylamide gels." J Cell Biol 79:281-285.

Alessi, DR., Gomez, N., Moorhead, G., Lewis, T., Keyse, SM., Cohen, P. (1995): "Inactivation of p42 MAP kinase by protein phosphatase 2A and a protein tyrosine phosphatase, but not CL100, in various cell lines" Curr Biol, 5, pp. 283–29.

Barford D (1996). “Molecular mechanisms of the protein serine/threonine phosphatases”, Trends Biochemical Science 21 (11), pp.407 – 412

Barford, D., A. K. Das and M.P. Egloff (1998). "The Structure and mechanism of protein phosphatases: Insights into Catalysis and Regulation." Ann. Rev. of Biophysics and Biomolecular Structure 27: 133-16

Briggs, G.E.; Haldane, J.B.S. (1925). "A note on the kinematics of enzyme action". Biochem J 19 (2): pp. 338–339.

Baharians, Z and Schönthal, A. (1998) " Autoregulation of Protein Phosphatase Type 2A Expression". Journal of Biological Chemistry, 273 (30), pp. 19019-19024

Barnard, E.; Timson, D. J. (2010). "Split-EGFP Screens for the Detection and Localisation of Protein–Protein Interactions in Living Yeast Cells". "Molecular and Cell Biology Methods for Fungi". Methods in molecular biology (Clifton, N.J.). Methods in Molecular Biology 638: 303–317

Beckett, D., E. Kovaleva, and P.J. Schatz. (1999). „A minimal peptide substrate in biotin holoenzyme synthetase-catalyzed biotinylation“. Protein Sci. 8 pp. 921–929

Bergmeyer, H.U. (1974). Methods of Enzymatic Analysis. 4. New York: Academic Press. pp. 2066–72.

Boudart, M. (1995). "Turnover Rates in Heterogeneous Catalysis", Chem. Rev., 95, pp. 661 - 666

Bryant, J.C., Westphal, R.S., Wadzinski, B.E. (1999) "Methylated C-terminal leucine residue of PP2A catalytic subunit is important for binding of regulatory Balpha subunit." Biochem. J., 339(Pt 2), pp. 241-246

Burridge, K. (1976). "Changes in cellular glycoproteins after transformation: identification of specific glycoproteins and antigens in sodium dodecyl sulfate gels." Proc Natl Acad Sci U S A 73:4457-4461.

Chapman-Smith, A., and J.E. Cronan Jr. (1999). „Molecular biology of biotin attachment to proteins“. J. Nutr. 129(2S, Suppl): pp. 477S–484S.

Chen, I.; Howarth, M.; Lin, W.; Ting, A. Y. (2005). "Site-specific labeling of cell surface proteins with biophysical probes using biotin ligase" Nat. Methods, 2, pp. 99–104.

Cho, U.S., Xu, W. (2007): "Crystal structure of a protein phosphatase 2A heterotrimeric holoenzyme" Nature 445(7123), pp. 53-57.

Churchwella, M; Twaddlea, N; Meekerb, L; Doergea, D. (October 2005). "Improving Sensitivity in Liquid Chromatography-Mass Spectrometry". Journal of Chromatography B 825 (2): 134–143.

Clegg, R.M. (1996). "Fluorescence resonance energy transfer. Fluorescence Imaging Spectroscopy and Microscopy" ed. by X.F. Wang and B.Herman)", pp. 179–251. Chemical Analysis Series, Vol. 137.

Clegg, Robert (2009). "Förster resonance energy transfer—FRET: what is it, why do it, and how it's done". In Gadella, Theodorus W. J.. FRET and FLIM Techniques. Laboratory Techniques in Biochemistry and Molecular Biology, Volume 33. Elsevier. pp. 1–57.

Cohen, P. T. W., Brewis, N. D., Hughes, V. and Mann, D. J. (1990) Protein serine/threonine phosphatases; an expanding family. FEBS Lett. 268, 355–359

Cornish-Bowden, A. (1995), "Fundamentals of Enzyme Kinetics", Portland Press Limited, Third Edition

de Boer, E.; Rodriguez, P.; Bonte, E.; Krijgsveld, J.; Katsantoni, E.; Heck, A.; Grosveld, F.; Strouboulis, J. (2003), " Efficient biotinylation and single-step purification of tagged transcription factors in mammalian cells and transgenic mice" Proc. Natl. Acad. Sci. U.S.A. 2003, 100, pp. 7480–7485.

Denu J.M., Dixon J.E. (1995): “A catalytic mechanism for the dual-specific phosphatases”, Proc.Natl. Acad. Sci. USA, 270 (45), pp. 5910 - 5914

Dowd, John E., and Douglas S. Riggs. (1965) "A comparison of estimates of Michaelis-Menten kinetic constants from various linear transformations." J. biol. Chem 240.2 863-869.

Dünkler, A.; Müller, J.; Johnsson, N. (2012). "Detecting Protein–Protein Interactions with the Split-Ubiquitin Sensor". "Gene Regulatory Networks". Methods in molecular biology (Clifton, N.J.). Methods in Molecular Biology 786: 115–130

Felber L.M., Cloutier S.M., Kündig C., Kishi T., Brossard V, Jichlinski P, Leisinger HJ, and Deperthes D. (2004) "Evaluation of the CFP-substrate-YFP system for protease studies: advantages and limitations." Biotechniques. 36(5):878–85.

Fernández-Suárez M., Chen T.S., Ting A.Y. (2008). "Protein-Protein Interaction Detection in Vitro and in Cells by Proximity Biotinylation". J.Am.Chem.Soc. Vol 130, No. 29, pp. 9251-9253.

Fields S, Song O (1989). "A novel genetic system to detect protein-protein interactions" (abstract). Nature 340 (6230), pp. 245–6.

Floer, M. and Stock, J. (1994) "Carboxyl methylation of protein phosphatase 2A from Xenopus eggs is stimulated by cAMP and inhibited by okadaic acid." Biochem. Biophys. Res. Commun. 198, 372–379

Förster T. (1948). "Zwischenmolekulare Energiewanderung und Fluoreszenz." Ann. Physik. 437, 1948, S. 55

Fradelizi J., Friederich E., Beckerle M.C., and Golsteyn R.M. (1999). "Quantitative measure- ment of proteins by Western blotting with Cy5- coupled secondary antibodies." BioTechniques 26:484-494.

Gales, C. et al. (2005) Real-time monitoring of receptor and G-protein interactions in living cells. Nat. Methods 2, 177–184

Gingrich J.C., Davis D.R., and Nguyen Q. (2000). "Multiplex detection and quantitation of proteins on Western blots using fluorescent probes." Bio- Techniques 29:636-642.

Gossen M., Bujard H. (1992). "Tight Control of Gene Expression in Mammalian Cells by Tetracycline-Responsive Promoters.". Proc. Natl. Acad. Sci. U.S.A. 89 (12): 5547–51.

Gotz J, Probst A, Ehler E, Hemmings B, Kues W. (1998) "Delayed embryonic lethality in mice lacking protein phosphatase 2A catalytic subunit Calpha." Proc Natl Acad Sci USA 95(21):12370-12375.

Greco, W.R.; Hakala, M.T. (1979). "Evaluation of methods for estimating the dissociation constant of tight binding enzyme inhibitors,". J Biol Chem 254 (23): 12104–12109.

Green, N.M. (1963). "Avidin. 1. The Use of (14-C) Biotin for Kinetic Studies and for Assay". Biochem. J. 89, pp. 585–591

Gunawardena, J. (2012): "Some lessons about models from Michaelis and Menten", MBoC vol 23, pp. 517 - 519

Hagen J (2006). Industrial Catalysis: A Practical Approach. Weinheim, Germany: Wiley-VCH.

Harris, Daniel C. (2010). "Applications of Spectrophotometry". Quantitative Chemical Analysis (8th ed.). New York: W. H. Freeman and Co.. pp. 419–44

Haeseleer F., Sokal I., Gregory FD., Lee A. (2013): "Protein Phosphatase 2A Dephosphorylates CaBP4 and Regulates CaBP4 Function." Invest Ophthalmol Vis Sci. Jan 22. pii: iovs.12-11319v1. doi: 10.1167/iovs.12-11319. [Epub ahead of print]

Heim R, Cubitt A, Tsien R (1995). "Improved green fluorescence" (PDF). Nature 373 (6516): 663–4.

Heim R, Tsien R. (1996) "Engineering green fluorescent protein for improved brightness, longer wavelengths and fluorescence resonance energy transfer", Current Biology 1996, 6:178–182

Hein, P. et al. (2005) Dynamics of receptor/G protein coupling in living cells. EMBO J. 24, 4106–4114

Helms, Volkhard (2008). "Fluorescence Resonance Energy Transfer". Principles of Computational Cell Biology. Weinheim: Wiley-VCH. p. 202

Hemmings, B.A. et al (1990) "Alpha- and beta-forms of the 65-kDa subunit of protein phosphatase 2A have a similar 39 amino acid repeating structure." Biochemistry, 29(13), pp. 3166-3173.

Henderson, C.J. and. Wolf C.R. (1992). "Immunode- tection of Proteins by Western Blotting", pp. 221- 233. In M. Manson (Ed.), Methods in Molecular Biology. The Humana Press, Totowa, NJ.

Hendrix P, Turowski P, Mayer-Jaekel RE, Goris J, Hofsteenge J, Merlevede W, Hemmings BA. (1993). "Analysis of subunit isoforms in protein phosphatase 2A holoenzymes from rabbit and Xenopus" J Biol Chem 1993;268: pp. 7330 - 7.

Herold, J. & Andino, R. (2001). "Poliovirus RNA replication requires genome circularization through a protein–protein bridge." Mol. Cell 7, 581–591.

Hombauer, H. et al (2007) "Generation of active protein phosphatase 2A is coupled to holoenzyme assembly" PLoS Biol 5(6): e155. doi:10.1371/journal.pbio.0050155

Howarth, M.; Takao, K.; Hayashi, Y.; Ting, A. Y. (2005), " Targeting quantum dots to surface proteins in living cells with biotin ligase" Proc. Natl. Acad. Sci.U.S.A. 2005, 102, 7583–7588.

"In-Gel Western Detection Using Near-Infrared Fluorescence", LI-COR Biosciences, 2006, http://biosupport.licor.com

Janke et al, (2004): "A versatile toolbox for PCR-based tagging of yeast genes: new fluorescent proteins, more markers and promoter substitution cassettes." Yeast (2004) 21, 974 - 962

Janssens V. et al. (2008). "PP2A holoenzyme assembly: in cauda venenum (the sting is in the tail)". Trends in Biochemical Sciences, Vol, 33, No. 3, pp. 113 - 121.

Kaelin, W.G. et al. (1992). „Expression cloning of a cDNA encoding a retinoblastoma-binding protein with E2F-like properties“. Cell, Vol.70, pp. 351-364

Kamibayashi, C. and Mumby, M.C. (1995) "Control of protein phosphatase 2A by multiple families of regulatory subunits." Adv. Protein Phosphatases 9, 195–210

Kay, J. and Dunn, B.M. (1990) "Viral proteinases: weakness in strength." Biochem. Biophys. Acta 1048, 1-18

Keener, J.; Sneyd, J. (2008). Mathematical Physiology: I: Cellular Physiology (2 ed.). Springer.

Khew-Goodall, Y., Hemmings B.A. (1988) "Tissue-specific expression of mRNAs encoding alpha- and beta- catalytic subunits of protein phosphatase 2A." FEBS Lett. 238(2):265-8.
Kinoshita K, Nemoto T, Nabeshima K, Kondoh H, Niwa H, Yanagida M. (1996) "The regulatory subunits of fission yeast protein phosphatase 2A (PP2A) affect cell morphogenesis, cell wall synthesis and cytokinesis." Genes Cells 1(1):29-45

Kräusslich, H.-G., and Wimmer, E. (1988). "Viral proteinases" Annu. Rev. Biochem. 57, 701-754.

Kumar A, Pandurangan AK, Lu F, Fyrst H, Zhang M, Byun HS, Bittman R, Saba JD. (2012): "Chemopreventive sphingadienes downregulate Wnt signaling via a PP2A/Akt/GSK3β pathway in colon cancer." Carcinogenesis, Sep;33(9):1726-35.

Lawson, M.A., Semler, B.L. (1990). "Picornavirus protein processing: enzymes, substrates and genetic regulation." Curr. Topics Micro. Immun. 161, 49 - 87

Lehninger, A.L.; Nelson, D.L.; Cox, M.M. (2005). Lehninger principles of biochemistry. New York: W.H. Freeman.

Li, M. and Damuni, Z. (1994) "Okadaic acid and microcystin-LR directly inhibit the methylation of protein phosphatase 2A by its specific methyltransferase." Biochem.Biophys. Res. Commun. 202, 1023–1030

Lievens, S., Lemmens, I. and Tavernier, J. (2009) "Mammalian two-hybrids come of age", Trends in Biochemical Sciences, Vol. 38, No.11 pp.579 - 588

Lineweaver, H and Burk, D. (1934). "The Determination of Enzyme Dissociation Constants". Journal of the American Chemical Society 56 (3): 658–666

Long A. et al. (1989). "A consenus sequence for substrate hydrolysis by rhinovirus 3C protease". FEBS Letters, Vol. 258, Issue 1, pp. 75-78.

Longin S. et al. (2007) "Selection of protein phosphatase 2A regulatory subunits is mediated by the C terminus of the catalytic subunit. " J. Biol. Chem., 282(37), pp. 26971-26980

Manning, G., Whyte, D.B., Martinez, R., Hunter, T., and Sudarsanam, S. (2002). "The protein kinase complement of the human genome". Science 298, pp. 1912–1934.

Martin, M., Kettmann, R., Dequiedt, F. (2010) "Recent insights into Protein Phosphatase 2A regulation: the reasons why PP2A is no longer considered a lazy passive housekeeping enzyme." Biotechnol. Agron. Soc. Environ. 14 (1), pp. 243-252

Mathews, C.K.; van Holde, K.E.; Ahern, K.G. (1999). Biochemistry (3 ed.). Prentice Hall.

Matthews DA, Smith WW, Ferre RA, Condon B, Budahazi G, Sisson W, Villafranca JE, Janson CA, McElroy HE, Gribskov CL, Worland S. (1994). "Structure of human rhinovirus 3C protease reveals a trypsin-like polypeptide fold, RNA-binding site, and means for cleaving precursor polyprotein." Cell, 77(5):761-71

Mayer RE, Hendrix P, Cron P, Matthies R, Stone SR, Goris J, Merlevede W, Hofsteenge J, Hemmings BA. (1991). "Structure of the 55-kDa regulatory subunit of protein phosphatase 2A: evidence for a neuronal-specific isoform" Biochemistry 1991;30: 3589 - 97.

McCright B, Rivers AM, Audlin S, Virshup DM. (1996). " The B56 family of protein phosphatase 2A (PP2A) regulatory subunits encodes differentiation-induced phosphoproteins that target PP2A to both nucleus and cytoplasm" J Biol Chem 1996;271:22081 - 9.

Menten, L.; Michaelis, M.I. (1913), "Die Kinetik der Invertinwirkung", Biochem Z 49: 333–369

Mitra, R.D., C.M. Silva, and D.C. Youvan (1996). "Fluorescence resonance energy transfer between blue-emitting and red-shifted excitation derivatives of the green fluorescent protein." Gene 173, pp. 13-17

Morise H, Shimomura O, Johnson F, Winant J (1974). "Intermolecular energy transfer in the bioluminescent system of Aequorea". Biochemistry 13 (12): 2656–62.

Morseman J.P., Moss M.W., Zoha S.J., and Allnutt F.C.T. (1999). "PBXL-1: a new fluorochrome applied to detection of proteins on membranes." BioTechniques 26:559-563.

Murray, J.D. (2002). Mathematical Biology: I. An Introduction (3 ed.). Springer.

Nomenclature Committee of the International Union of Biochemistry (NC-IUB) (1979). "Units of Enzyme Activity". Eur. J. Biochem. 97 (2): 319–20.

Nooren I., Thornton J.M. (2003). "Structural Characterisation and Functional Significance of Transient Protein–Protein Interactions". Journal of Molecular Biology, Vol. 325, Issue 5: pp. 991-1018.

Nunbhakdi-Craig V, Machleidt T, Ogris E, Bellotto D, White CLIII, Sontag E., (2002) "Protein phosphatase 2A associates with and regulates atypical PKC and the epithelial tight junction complex." J Cell Biol;158:967–78

Nunbhakdi-Craig, V. et al (2007) "Expression of protein phosphatase 2A mutants and silencing of the regulatory B alpha subunit induce a selective loss of acetylated and detyrosinated microtubules." J. Neurochem. 101(4), pp. 959-971

Ogris, E., Du, X. et al (1999) " A Protein Phosphatase Methylesterase (PME-1) Is One of Several Novel Proteins Stably Associating with Two Inactive Mutants of Protein Phosphatase 2A" J. Biol. Chem, 274(20). 14382-14391.

Ogris, E., Mudrak, I. et al (1999) "Catalytically Inactive Protein Phosphatase 2A Can Bind to Polyomavirus Middle Tumor Antigen and Support Complex Formation with pp60 $^{c\text{-}src}$" J Virol. 73(9): 7390–7398

Oxford Dictionaries (2013) "rate", http://oxforddictionaries.com (03.June 2013)

Pallas D.C et al (2001). "Carboxymethylation of PP2A Catalytic Subunit in Saccharomyces cerevisiae is required for Efficient interaction with the B-type subunits cdc55p and Rts1p" Journal of Biological Chemistry 276 (2), pp. 1570 - 1577

Periasamy, A. (2001). "Fluorescene resonance energy transfer microscopy: a mini review" Journal of Biomedical Optics 6 (3), 287 - 291

Passonneau, J.V., Lowry, O.H. (1993). "Enzymatic Analysis. A Practical Guide. Totowa" NJ: Humana Press. pp. 85–110

Patonay G. and Antoine M.D. (1991). "Near-in- frared fluorogenic labels: new approach to an old problem." Anal. Chem. 63:321A-327A.

Patterson, G. et al (2001) "Fluorescent protein spectra" J Cell Sci 114, 837-838.

Reid, M.A., Wang, W.I., Rosales, K.R., Welliver, M.X., Pan, M., Kong, M. (2013). " The B55α subunit of PP2A drives a p53-dependent metabolic adaptation to glutamine deprivation." Mo. Cell. Mar 13. pii: S1097-2765(13)00136-6. doi: 10.1016/j.molcel.2013.02.008. [Epub ahead of print]

Roblek, M. et al (2010). "Monoclonal antibodies specific for disease-associated point-mutants: lamin A/C R453W and R482W." Plos One, 13;5(5):e10604

Roux KJ, Kim DI, Raida M, Burke B. (2012). " A promiscuous biotin ligase fusion protein identifies proximal and interacting proteins in mammalian cells.", J Cell Biol 2012 Mar 19;196(6) pp. 801-810

Schutz-Geschwender A., Zhang Y., Holt T., McDermitt D., and Michael Olive D. (2004). " Quantitative, Two-Color Western Blot Detection With Infrared Fluorescence." LI-COR™ Biosciences

Segel, L.A.; Slemrod, M. (1989). "The quasi-steady-state assumption: A case study in perturbation". Thermochim Acta 31 (3): 446–477.

Sharma, R., Raychaudhuri, S. & Dasgupta, A. (2004) "Nuclear entry of poliovirus protease-polymerase precursor 3CD: implications for host cell transcription shut-off." Virology 320, 195–205.

Sontag, E. et al (1993). "The interaction of SV40 small tumor antigen with protein phosphatase 2A stimulates the map kinase pathway and induces cell proliferation." Cell, Dec 3;75(5):887-97.

Sontag E. (2001). " Protein phosphatase 2A: the Trojan Horse of cellular signaling". Cellular Signalling 13, pp. 7-16.

Sowell J., Strekowski L., and Patonay G. (2002). "DNA and protein applications of near-infrared dyes." J. Biomed. Optics 7:571-575.

Spotts, J.M. et al. (2002): "Time-lapse imaging of a dynamic phosphorylation-dependent protein-protein interaction in mammalian cells". Proc. Natl. Acad. Sci. U. S. A. 99, 15142–15147

Stanevich, V. et al (2011): "The structural basis for tight control of PP2A methylation and function by LCMT-1." Mol. Cell, Feb 4;41(3):331-42. doi: 10.1016/j.molcel.2010.12.030.

Stanway, G. Hughes, P. J., Mountford, R.C., Minor, P. D. and Almond, J. W. (1984) "The complete nucleotide sequence of a common cold virus: human rhinovirus 14." Nucl. Acids Rs. 12, 7859 - 7875

Strack, S., J. A. Zaucha, et al. (1998). "Brain protein phosphatase 2A: Developmental regulation and distinct cellular and subcellular localization by B subunits." Journal Of Comparative Neurology 392(4): 515-527.

Strack, S., Cribbs J.T., Gomez L. (2004) "Critical role for protein phosphatase 2A heterotrimers in mammalian cell survival." J Biol Chem. 279(46):47732-9.

Stroppolo, M.E.; Falconi, M.; Caccuri, A.M.; Desideri, A. (2001). "Superefficient enzymes". Cell Mol Life Sci 58 (10): 1451–60.

Tanabe O, Nagase T, Murakami T, Nozaki H, Usui H, Nishito Y,Hayashi H, Kagamiyama H, Takeda M. (1996). "Molecular cloning of a 74-kDa regulatory subunit (B" or delta) of human protein phosphatase 2A" FEBS Lett 1996; 379:107 - 11.

Tay, KH. et al. (2012): "Suppression of PP2A is critical for protection of melanoma cells upon endoplasmic reticulum stress". Cell Death and Disease 3, e337; doi:10.1038/cddis.2012.79

Thastrup O, Tullin S, Kongsbak Poulsen L, Bjørn S (2001). "Fluorescent Proteins"

Tseng SJ, Hsu JP (August 1990). "A comparison of the parameter estimating procedures for the Michaelis-Menten model". J. Theor. Biol. 145 (4): 457–64.

Tsien, R. (1998) "The green fluorescent protein". Annu. Rev. Biochem. 1998. 67:509–44

Shimomura O, Johnson FH, Saiga Y. (1962)." Extraction, purification and properties of aequorin, a bioluminescent protein from the luminous hydromedusan, Aequorea" J. Cell. Comp. Physiol. 59:223– 39

Topper, J.N. et al. (1998) CREB binding protein is a required coactivator for Smad-dependent, transforming growth factor beta transcriptional responses in endothelial cells. Proc. Natl. Acad. Sci. U. S. A. 95, 9506–9511

Venkatesan, K. et al. (2009) An empirical framework for binary interactome mapping. Nat. Methods 6, 83–90

Virshup D.M., Shenolikar S. (2009). "From Promiscuity to Precision: Protein Phosphatases Get a Makeover", Molecular Cell 33, pp. 537-545.

Walker P.A. et al. (1994). "Efficient and rapid affinity purification of proteins using recombinant fusion proteases.", Biotechnology 12, pp. 601–605.

Wehr, M. C.; Laage, R.; Bolz, U.; Fischer, T. M.; Grünewald, S.; Scheek, S.; Bach, A.; Nave, K. A. et al. (2006). "Monitoring regulated protein-protein interactions using split TEV". Nature Methods 3 (12): 985–993.

Wehr, Michael C; Reinecke, Lisa; Botvinnik, Anna; Rossner, Moritz J (2008). "Analysis of transient phosphorylation-dependent protein-protein interactions in living mammalian cells using split-TEV". BMC Biotechnology 8: 55.

Wei, H. et al (2001) "Carboxymethylation of the PP2A catalytic subunit in Saccharomyces cerevisiae is required for efficient interaction with the B-type subunits Cdc55p and Rts1p." J. Biol. Chem, Jan 12;276(2):1570-7.

Wera, S, Hemmings, BA. (1995) Serine/threonine protein phosphatases." Biochem J. 311 (Pt 1):17-29.

Xing Y, Xu Y, Chen Y, Jeffrey PD, Chao Y, Lin Z, Li Z, Strack S, Stock JB, Shi Y. Structure of protein phosphatase 2A core enzyme bound to tumor-inducing toxins. Cell. 2006;127(2):341–353

Xu, Y. et al. (2006). "Structure of the protein phosphatase 2A holoenzyme." Cell, 127 (6), pp. 1239-1251

Xu, Y et al. (2008). "Structure of the protein phosphatase 2A holoenzyme: insights into B55-mediated tau dephosphorylation". Mol. Cell., 31 (6), pp. 873-885

Yang, Y., Rijnbrand, R., Watowich, S., Lemon, S.M. (2004) "Genetic evidence for an interaction between a picornaviral cis-acting RNA replication element and 3CD protein." J. Biol. Chem. (2004), 279(13):12659-67

Zhou, J., Pham, H.T., Ruediger, R., Walter, G. (2003) "Characterization of the Aalpha and Abeta subunit isoforms of protein phosphatase 2A: differences in expression, subunit interaction, and evolution." J.Biol. Chem. 369(2), pp. 387-398

Zuzuarregui A. et al (2012). "M-Track: detecting short-lived protein-protein interactions in vivo", Nature Methods 9, pp. 594-596

Notiz: Ich habe mich bemüht, sämtliche Inhaber der Bildrechte ausfindig zu machen und ihre Zustimmung zur Verwendung der Bilder in dieser Arbeit eingeholt. Sollte dennoch eine Urheberrechtsverletzung bekannt werden, ersuche ich um Meldung bei mir.

6. Appendix

The following figures comprise the vectors that were used in this study. The text below the vector maps summarizes the cloning steps and includes acknowledgements to the respective authors.

Vector name: pYM30
cloned by Janke C et al, 2004, from EUROSCARF

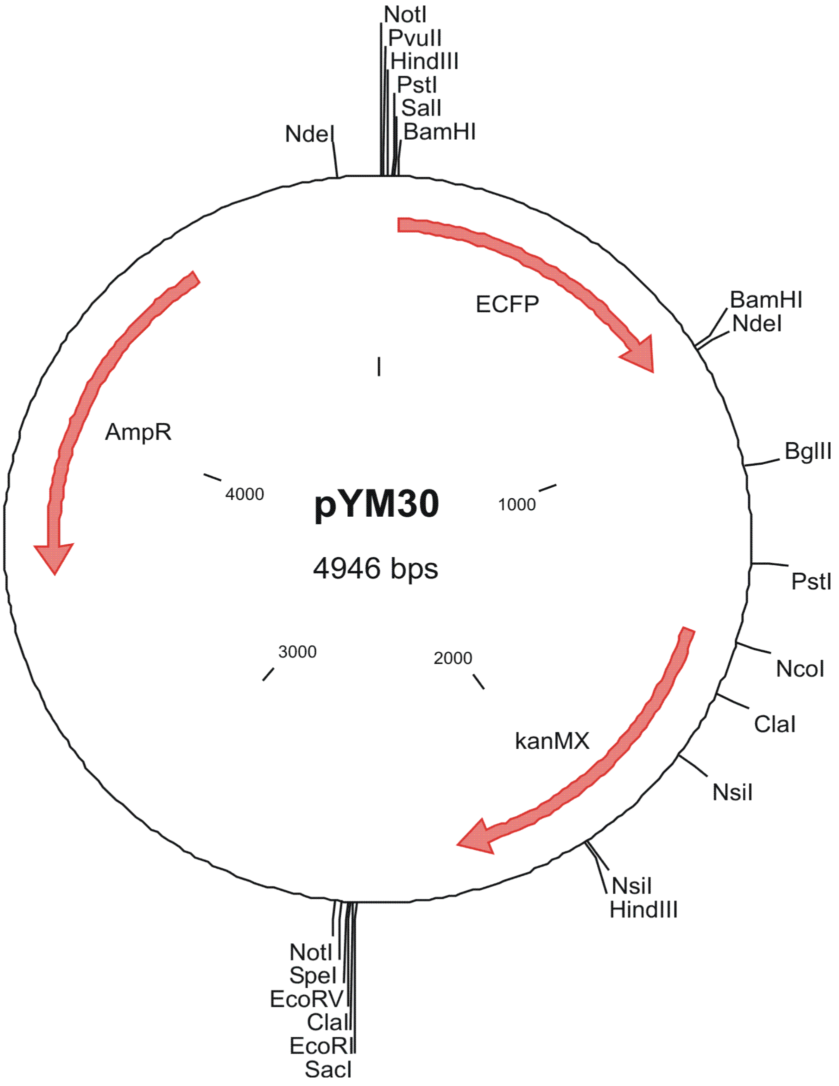
NotI
PvuII
HindIII
PstI
SalI
BamHI
NdeI
ECFP
BamHI
NdeI
BglII
AmpR
4000
pYM30
4946 bps
1000
PstI
3000
2000
NcoI
ClaI
kanMX
NsiI
NsiI
HindIII
NotI
SpeI
EcoRV
ClaI
EcoRI
SacI

Description: Vector of origin for PCR amplification of ECFP

Vector name: pYM39
cloned by Janke C et al, 2004, from EUROSCARF

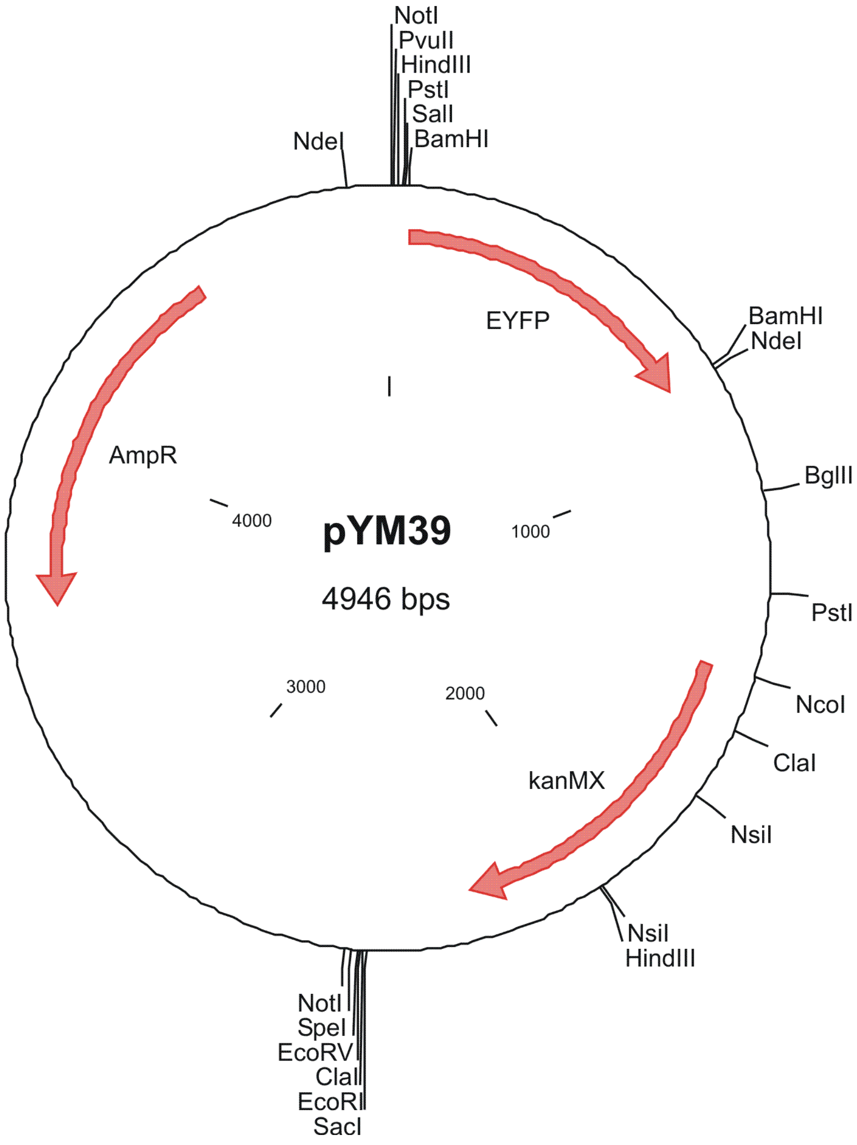
NotI
PvuII
HindIII
PstI
SalI
BamHI
NdeI
BamHI
NdeI
EYFP
BglII
AmpR
4000
pYM39
1000
4946 bps
PstI
NcoI
3000
2000
ClaI
kanMX
NsiI
NsiI
HindIII
NotI
SpeI
EcoRV
ClaI
EcoRI
SacI

Description: Vector of origin for PCR amplification of EYFP

Vector name: pB'his NP stop
cloned by Ingrid Mudrak

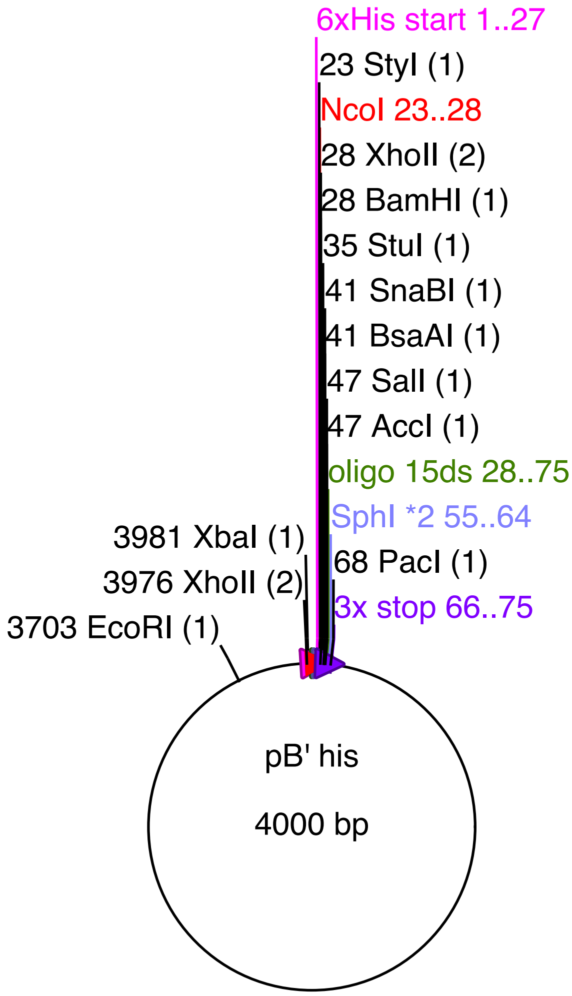
6xHis start 1..27
23 StyI (1)
NcoI 23..28
28 XhoII (2)
28 BamHI (1)
35 StuI (1)
41 SnaBI (1)
41 BsaAI (1)
47 SalI (1)
47 AccI (1)
oligo 15ds 28..75
SphI *2 55..64
68 PacI (1)
3x stop 66..75
3981 XbaI (1)
3976 XhoII (2)
3703 EcoRI (1)
pB' his
4000 bp

Important notes: Full sequence of vector backbone is unknown, approximately 2770 bp have not been sequenced, therefore the full vector length indicated in the center is an approximate value.

oligo 15 ds:

AA sequence:	G	S	E	A	L	R	S	R	H	A	C	M	L	I	N	*
5'- 3'	GGA	TCC	GAG	GCC	TTA	CGT	AGT	CGA	CAT	GCA	TGC	ATG	CTA	ATT	AAT	**TAA**

Stop codon marked in red.

Description: Used as a vector of origin for cloning "pB'His-CFP", "pB'His-YFP" and "pB'His-CFP mixed"

Vector name: pB'his-CFP mixed
cloned by Wolfgang Hintringer

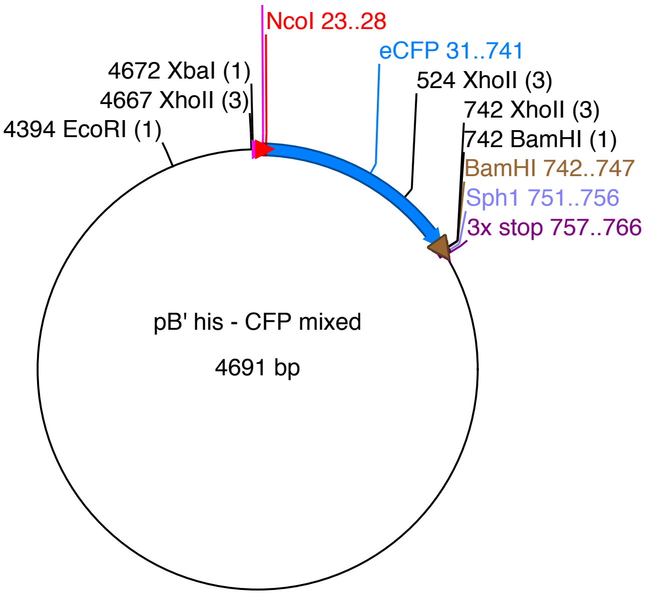
6xHis start 1..27
NcoI 23..28
eCFP 31..741
524 XhoII (3)
742 XhoII (3)
742 BamHI (1)
BamHI 742..747
Sph1 751..756
3x stop 757..766
4672 XbaI (1)
4667 XhoII (3)
4394 EcoRI (1)
pB' his - CFP mixed
4691 bp

Important notes: Full sequence of vector backbone is unknown, approximately 2770 bp have not been sequenced, therefore the full vector length indicated in the center is an approximate value.

Vector of origin: pB' His-NP digested with *NcoI* and *SphI.*

Insert: The insert was created by amplifying ECFP from pYM30 via PCR using the primers listed below. Fragments were analysed by agarose gel-electrophoresis, eluted from the gel, digested with restriction enzymes and subsequently purified to produce *NcoI*-**ECFP**-*BamHI*-*SphI* fragments compatible for ligaton to the linearised plasmid (see Materials and Methods for details).

Primer:

NcoI CFP2_fw	5'	agt ccc **atg** ggt **AGC AAG GGC GAG GAG C**	1491
SphI BamHI CFP_r	5'	a gtc gca tgc cgt gga tcc **CTT GTA CAG CTC GTC**	1462

A start codon is depicted in bold red, however, translation commencing from a start codon further upstream resulted in the His-tagged protein of interest. The stop codon is positioned downstream of the reverse primer.

Analytical digest using *BamHI* + *EcoRI* resulting in fragment sizes of approx. 4394 and 742 bp. The open reading frame translates to 253 amino acids, ECFP consists of 227 amino acids.

Sequence confirmed after subsequent cloning steps.

Description: This vector was used as a vector of origin for cloning "pB'His-CFP-YFP" and all "pB'His-CFP-substrate-YFP" vectors.

Vector name: pB'His-CFP
cloned by Wolfgang Hintringer

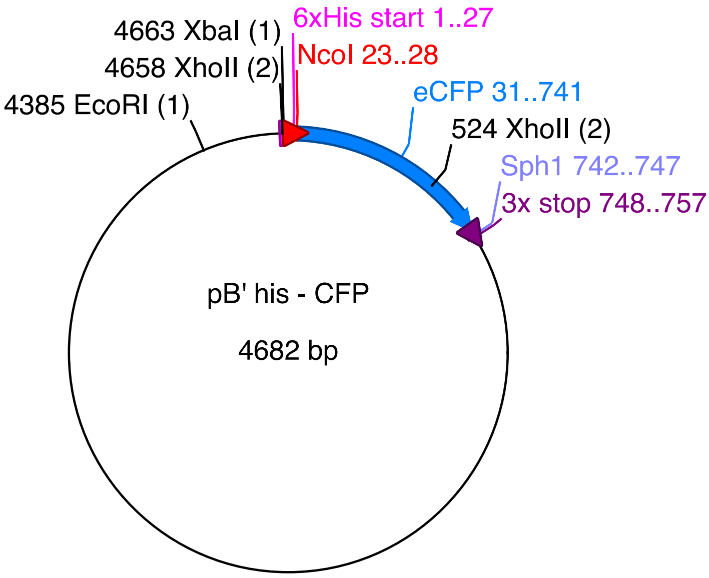

Important notes: Full sequence of vector backbone is unknown, approximately 2770 bp have not been sequenced and therefore the full vector length indicated in the center is an approximate value.

Vector of origin: pB' His-NP-stop digested with *NcoI* and *SphI*

Insert: *NcoI*-**ECFP**-*SphI* was ligated to the linearised plasmid. The insert was created by amplifying ECFP from pYM30 via PCR using the following primers:

Primer:

NcoI CFP2_fw	5'	agt ccc **atg** ggt **AGC AAG GGC GAG GAG C**	1491
SphI CFP_r	5'	a gtc gca tgc **CTT GTA CAG CTC GTC C**	1465

Analytical digest using *EcoRI* and *SphI,* resulting in fragment sizes of approx. 3643 and 1039 bp. The open reading frame translates to 250 amino acids, ECFP consists of 227 amino acids.

Sequencing primer:
pB-His forward new, binds 21 bp upstream of start ATG
pB-His reverse, binds 76 bp downstream of stop codon

Description: Used as a control in FRET studies. This vector was used instead of "pB'His-CFP mixed" since the resulting ECFP protein consisted of fewer additional amino acids that could potentially interfere with folding and thus fluorescence of the protein. Furthermore, the size of the protein was thus more similar to the EYFP protein used in the study

Vector name: pB'His-YFP
cloned by Wolfgang Hintringer

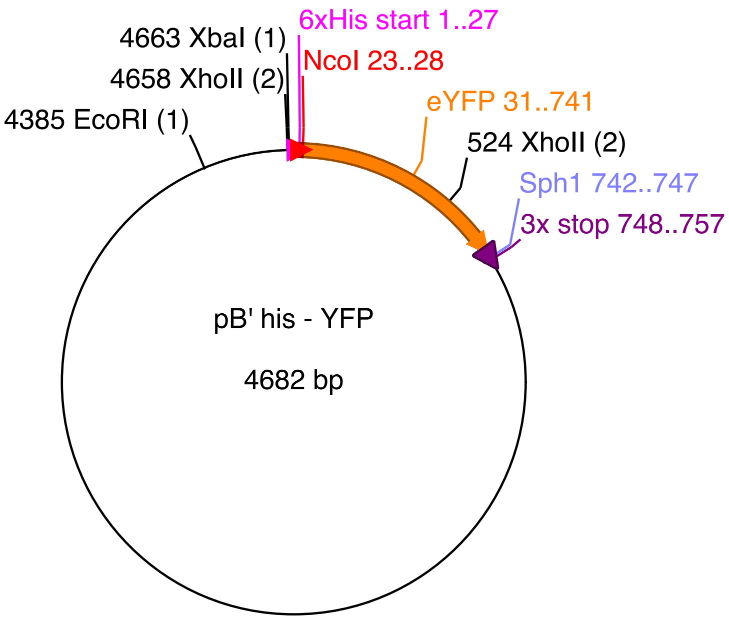
6xHis start 1..27
NcoI 23..28
4663 XbaI (1)
4658 XhoII (2)
4385 EcoRI (1)
eYFP 31..741
524 XhoII (2)
Sph1 742..747
3x stop 748..757
pB' his - YFP
4682 bp

Important notes: Full sequence of vector backbone is unknown, approximately 2770 bp have not been sequenced therefore the full vector length indicated in the center is an approximate value.

Vector of origin: pB' His-NP-stop digested with *NcoI* and *SphI*

Insert: *NcoI*-**YFP**-*SphI* was ligated to the linearised plasmid. The insert was created by amplifying EYFP from pYM39 via PCR using the following primers:

Primer:

NcoI YFP2_fw	5'	agt ccc **atg** ggt **AGC AAG GGC GAG GAG C**	1492
SphI YFP_r	5'	a gtc gca tgc **CTT GTA CAG CTC GTC C**	1467

Analytical digest using *EcoRI* and *SphI,* resulting in fragment sizes of approx. 3643 and 1039 bp. The open reading frame translates to 250 amino acids, EYFP consists of 237 amino acids.

Sequencing primer:
pB-His forward new, binds 21 bp upstream of start ATG
pB-His reverse, binds 76 bp downstream of stop codon

Description: Used as a control in FRET studies.

Vector name: pB'His-CFP-YFP
cloned by Wolfgang Hintringer

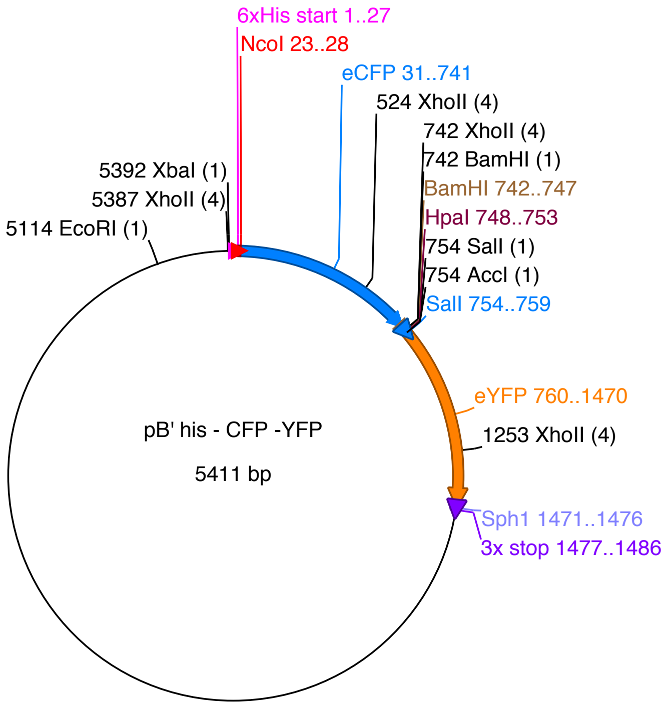
6xHis start 1..27
NcoI 23..28
eCFP 31..741
524 XhoII (4)
742 XhoII (4)
742 BamHI (1)
BamHI 742..747
HpaI 748..753
754 SalI (1)
754 AccI (1)
SalI 754..759
5392 XbaI (1)
5387 XhoII (4)
5114 EcoRI (1)
pB' his - CFP -YFP
5411 bp
eYFP 760..1470
1253 XhoII (4)
Sph1 1471..1476
3x stop 1477..1486

Important notes: Full sequence of vector backbone is unknown, approximately 2770 bp have not been sequenced, therefore the full vector length indicated in the center is an approximate value.

Vector of origin: pB' His-CFPmixed was digested with *BamHI* and *SphI*

Insert: *BamHI*-*HpaI*-*SalI*-**EYFP**-*SphI* was ligated to the linearised plasmid. The insert was created by amplifying EYFP from pYM39 via PCR using the following primers:

Primer:

BamHI HpaI SalI YFP_fw	5'	a gtc gga tcc gtt aac gtc gac **AGC AAG GGC GAG GAG C**	1463
SphI YFP_r	5'	a gtc gca tgc **CTT GTA CAG CTC GTC C**	1467

Analytical digest using *NcoI* and *SphI*, resulting in fragment sizes of approx. 3643 and 1768 bp. The open reading frame translates to 493 amino acids, ECFP and EYFP consist of 237 amino acids each.

Sequencing primer:
fw: CFP_fw, binds 209 bp downstream of start ATG
rev: YFP_r, binds 523 bp upstream of stop codon

sequenced nr. 9: correct

Vector name: pB'His-CFP-C3S5-YFP
cloned by Wolfgang Hintringer

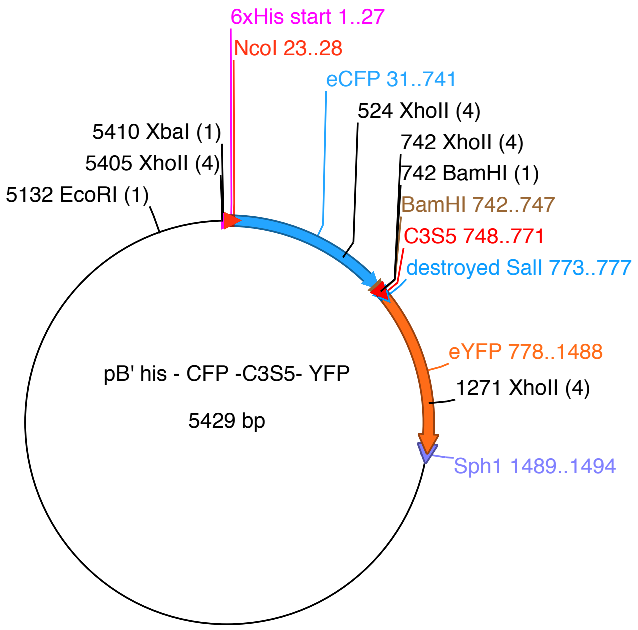
6xHis start 1..27
NcoI 23..28
eCFP 31..741
524 XhoII (4)
742 XhoII (4)
742 BamHI (1)
BamHI 742..747
C3S5 748..771
destroyed SalI 773..777
5410 XbaI (1)
5405 XhoII (4)
5132 EcoRI (1)
pB' his - CFP -C3S5- YFP
5429 bp
eYFP 778..1488
1271 XhoII (4)
Sph1 1489..1494

Important notes: Full sequence of vector backbone is unknown, approximately 2770 bp have not been sequenced, therefore the full vector length indicated in the center is an approximate value.

Vector of origin: pB' His-CFP-YFP Nr.9 was digested with *BamHI* and *SalI*

Insert: *BamHI*-**C3S5**-*destrSalI* was ligated to the linearised plasmid. The *SalI* site was destroyed in the cloning process. The insert was created by annealing the following oligonucleotides:

Oligonucleotides

AA sequence		L E V L F Q * G P	
C3S5_s	5´	ga tcc ctg gaa gtg ctg ttt cag ggc ccg c	1476
C3S5_as_new	3´	-----g gac ctt cac gac aaa gtc ccg ggc gag ct	1542

Analytical digest using *ApaI* and *EcoRI,* resulting in fragment sizes of approx. 4367 and 1062 bp. The open reading frame translates to 499 amino acids, ECFP and EYFP consist of 237 amino acids each, C3S5 consists of 9 amino acids.
* = preScission cleavage site.

Sequencing primer:
fw: CFP_fw, binds 209 bp downstream of start ATG

Description: Was used for FRET and in-gel studies.
AA sequence of C3S5: LEVLFQ*GP

Vector name: pB'His-CFP-C3S5gly-YFP
cloned by Wolfgang Hintringer

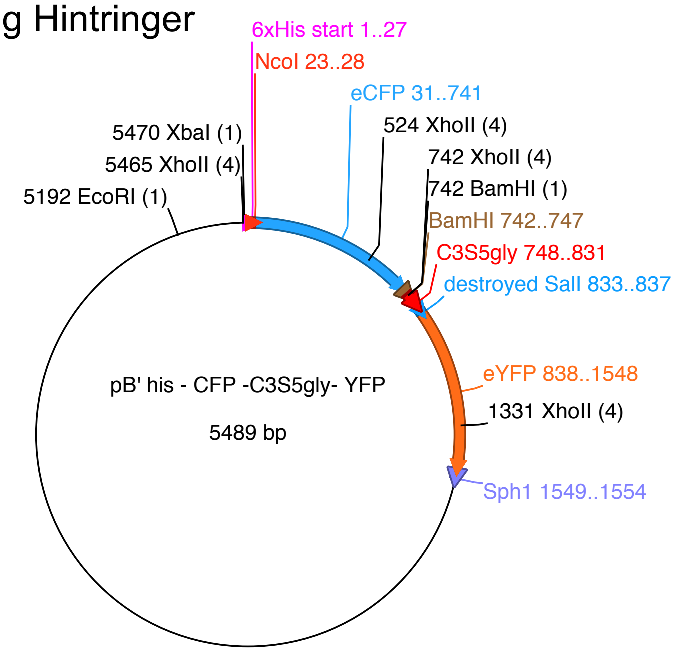
6xHis start 1..27
NcoI 23..28
eCFP 31..741
524 XhoII (4)
742 XhoII (4)
742 BamHI (1)
BamHI 742..747
C3S5gly 748..831
destroyed SalI 833..837
eYFP 838..1548
1331 XhoII (4)
Sph1 1549..1554
5470 XbaI (1)
5465 XhoII (4)
5192 EcoRI (1)
pB' his - CFP -C3S5gly- YFP
5489 bp

Important notes: Full sequence of vector backbone is unknown, approximately 2770 bp have not been sequenced, therefore the full vector length indicated in the center is an approximate value.

Vector of origin: pB' His-CFP-YFP was digested with *BamHI* and *SalI*

Insert: *BamHI*-GL-**C3S5**-GL-destr*SalI* was ligated to the linearised plasmid (GL= glycine linker). To avoid cross-annealing of the flanking GL sequences, the insert was created by annealing of the following four olgonucleotides in two subsequent steps. The *SalI* site was destroyed in the cloning process.

Oligonucleotides:

```
AA sequence                       G   G   G   G   S   G   G   G   G   S   L   E   V   L   F   Q
C3S5_gly_left_s       5'  ga tcc ggt ggc ggt ggc TCT gga ggt ggt ggg TCC ctg gaa gtg ctg t        1506
C3S5_gly_left_as      3'  ---- g cca ccg cca ccg AGA cct cca cca ccc AGG gac ctt cac gac aaa gt   1507

                                * G   P   G   G   G   G   S   G   G   G   G   S
C3S5_gly_right_s      5'  tt cag ggc ccg ggt ggc ggt ggc TCT gga ggt ggt ggg TCC c                1508
C3S5_gly_right_as_new 3'  ---- c ccg ggc cca ccg cca ccg AGA cct cca cca ccc AGG gag ct           1543
```

Analytical digest using *ApaI* and *EcoRI*, resulting in fragment sizes of approx. 4397 and 1092 bp. The open reading frame translates to 519 amino acids, ECFP and EYFP consist of 237 amino acids each, GL-C3S5-GL consists of 28 amino acids. * = preScission cleavage site.

Sequencing primer:
fw: CFP_fw, binds 209 bp downstream of start ATG

Description: Used for FRET and silver staining experiments.
AA sequence of C3S5gly: GGGGSGGGGSLEVLFQ*GPGGGGSGGGGS

Vector name: pB'His-CFP-C3S6-YFP
cloned by Wolfgang Hintringer

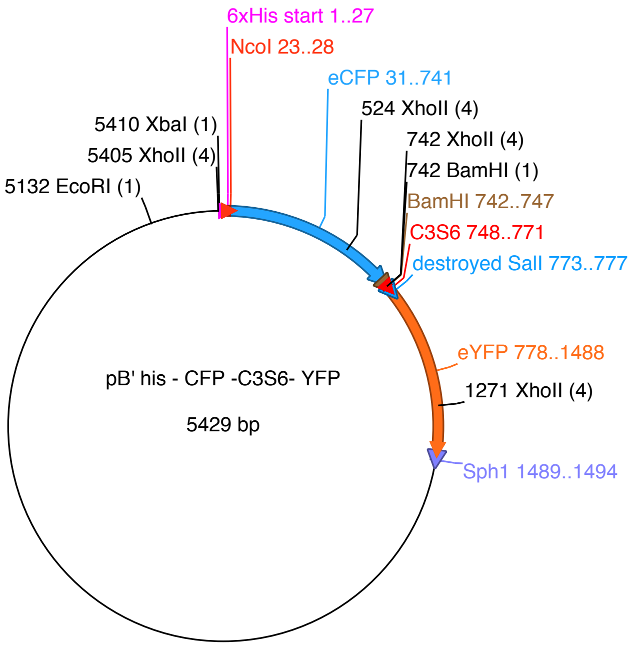
6xHis start 1..27
NcoI 23..28
eCFP 31..741
524 XhoII (4)
742 XhoII (4)
742 BamHI (1)
BamHI 742..747
C3S6 748..771
destroyed SalI 773..777
5410 XbaI (1)
5405 XhoII (4)
5132 EcoRI (1)
pB' his - CFP -C3S6- YFP
5429 bp
eYFP 778..1488
1271 XhoII (4)
Sph1 1489..1494

Important notes: Full sequence of vector backbone is unknown, approximately 2770 bp have not been sequenced, therefore the full vector length indicated in the center is an approximate value.

Vector of origin: pB' His-CFP-YFP Nr.9 was digested with *BamHI* and *SalI*

Insert: *BamHI*-**C3S6**-*destrSalI* was ligated to the linearised plasmid. The *SalI* site was destroyed in the cloning process. The insert was created by annealing the following oligonucleotides:

Oligonucleotides:

```
Amino acid sequence             R   P   V   V   V   Q * G   P
C3S6_s              5'  gatcc cgc ccg gtg gtg gtg cag ggc ccg c          1500
C3S6_as_new         3'  ----g gcg ggc cac cac cac gtc ccg ggc gagct      1544
```

Analytical digest using *ApaI* and *EcoRI,* resulting in fragment sizes of approx. 4367 and 1062 bp. The open reading frame translates to 499 amino acids, ECFP and EYFP consist of 237 amino acids each, C3S6 consists of 9 amino acids.
* = preScission cleavage site.

Sequencing primer:
fw: CFP_fw, binds 209 bp downstream of start ATG

Description: Used for FRET and in-gel experiments.
AA sequence of C3S6: RPVVVQ*GP

Vector name: pB'His-CFP-C3S6gly-YFP
cloned by Wolfgang Hintringer

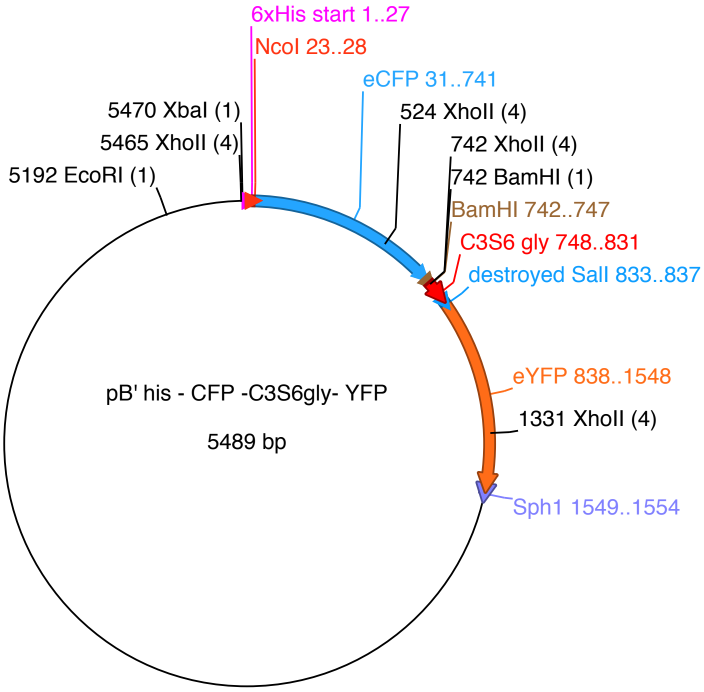
6xHis start 1..27
NcoI 23..28
eCFP 31..741
5470 XbaI (1)
5465 XhoII (4)
5192 EcoRI (1)
524 XhoII (4)
742 XhoII (4)
742 BamHI (1)
BamHI 742..747
C3S6 gly 748..831
destroyed SalI 833..837
eYFP 838..1548
1331 XhoII (4)
Sph1 1549..1554
pB' his - CFP -C3S6gly- YFP
5489 bp

Important notes: Full sequence of vector backbone is unknown, approximately 2770 bp have not been sequenced, therefore the full vector length indicated in the center is an approximate value.

Vector of origin: pB' His-CFP-YFP Nr.9 was digested with *BamHI* and *SalI*

Insert: *BamHI*-GL-**C3S6**-GL-destr*SalI* was ligated to the linearised plasmid. To avoid cross-annealing of the flanking GL sequences, the insert was created by annealing of the following four olgonucleotides in two subsequent steps. The *SalI* site was destroyed in the cloning process.

Oligonucleotides:

Amino acid sequence		G G G G S G G G G S **R P V V V Q**	
C3S6_gly_left_s	5′	ga tcc ggt ggc ggt ggc TCT gga ggt ggt ggg TCC **cgc ccg gtg gtg**	1502
C3S6_gly_left_as	3′	---- g cca ccg cca ccg AGA cct cca cca ccc AGG **gcg ggc cac cac cac g**	1503
		*** G P** G G G G S G G G G S	
C3S6_gly_right_s	5′	**gtg cag ggc ccg** ggt ggc ggt ggc TCT gga ggt ggt ggg TCC c	1504
C3S6_gly_right_as_new	3′	**---- tc ccg ggc** cca ccg cca ccg AGA cct cca cca ccc AGG gag ct	1545

Analytical digest using *ApaI* and *EcoRI*, resulting in fragment sizes of approx. 4397 and 1092 bp.
The open reading frame translates to 519 amino acids, ECFP and EYFP consist of 237 amino acids each, GL-C3S6-GL consists of 28 amino acids.
* = preScission cleavage site.

Sequencing primer:
fw: CFP_fw, binds 209 bp downstream of start ATG

Description: Used for FRET and silver staining experiments.
AA sequence of C3S6gly: GGGGSGGGGSRPVVVQ*GPGGGGSGGGGS

Vector name: pcDNA3puro EGFP-C3S6
cloned by Wolfgang Hintringer

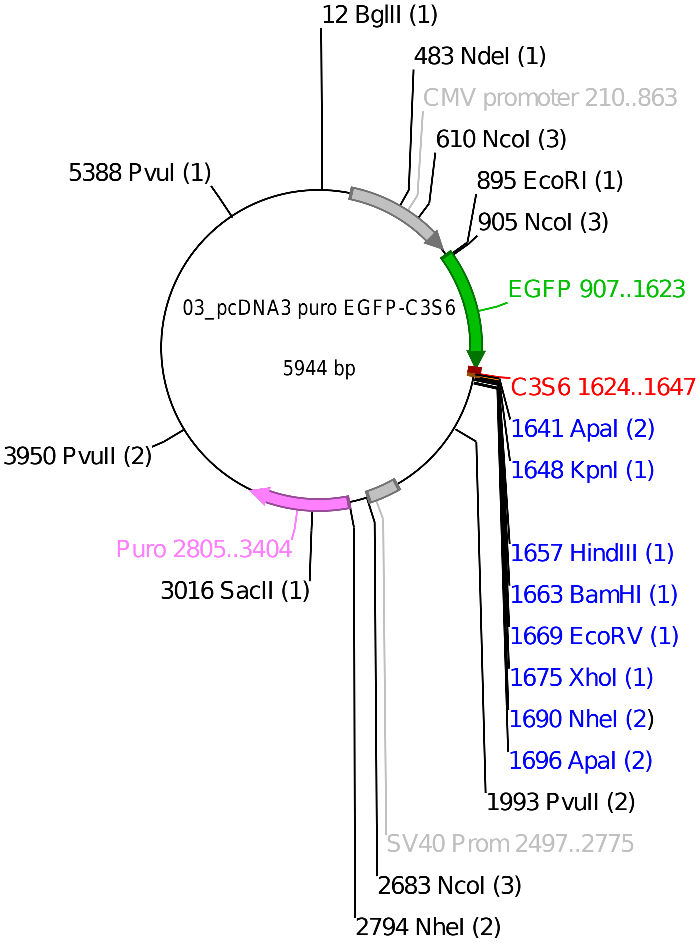
12 BglII (1)
483 NdeI (1)
CMV promoter 210..863
610 NcoI (3)
895 EcoRI (1)
905 NcoI (3)
5388 PvuI (1)
EGFP 907..1623
03_pcDNA3 puro EGFP-C3S6
5944 bp
C3S6 1624..1647
1641 ApaI (2)
1648 KpnI (1)
3950 PvuII (2)
1657 HindIII (1)
1663 BamHI (1)
1669 EcoRV (1)
1675 XhoI (1)
1690 NheI (2)
1696 ApaI (2)
Puro 2805..3404
3016 SacII (1)
1993 PvuII (2)
SV40 Prom 2497..2775
2683 NcoI (3)
2794 NheI (2)

Vector of origin: pcDNA3-puro-NP was digested with *EcoRI* and *KpnI*

Insert: *EcoRI*-Kozak-EGFP-C3S6-*KpnI* was ligated to the linearised plasmid. The insert was created by amplifying EGFP from pcDNA-NP-GFP1 puro via PCR using the following primers:

Primers:

EcoRI-Kozak-EGFP_F	at ccg GAA TTC gcc acc **ATG** GTG AGC AAG	1181
Kpn1_C3S6_EGFP_R	at cgg GGT ACC cgg gcc ctg cac cac cac cgg gcg CTT GTA CAG CTC GTC CAT G	1541

Analytical digest using *KpnI*, resulting in a fragment of 5944 bp. The open reading frame ranges from 907 - 1728 and translates to 237 amino acids. Start codon is highlighted.

Sequencing primer:
CMV-F, binds basepairs at position 769 - 789

Description: Used as a vector of origin for cloning "pcDNA3puro EGFP-C3S6-HA-GL"

Vector name: pcDNA3puro EGFP-C3S6-HA-GL
cloned by Wolfgang Hintringer

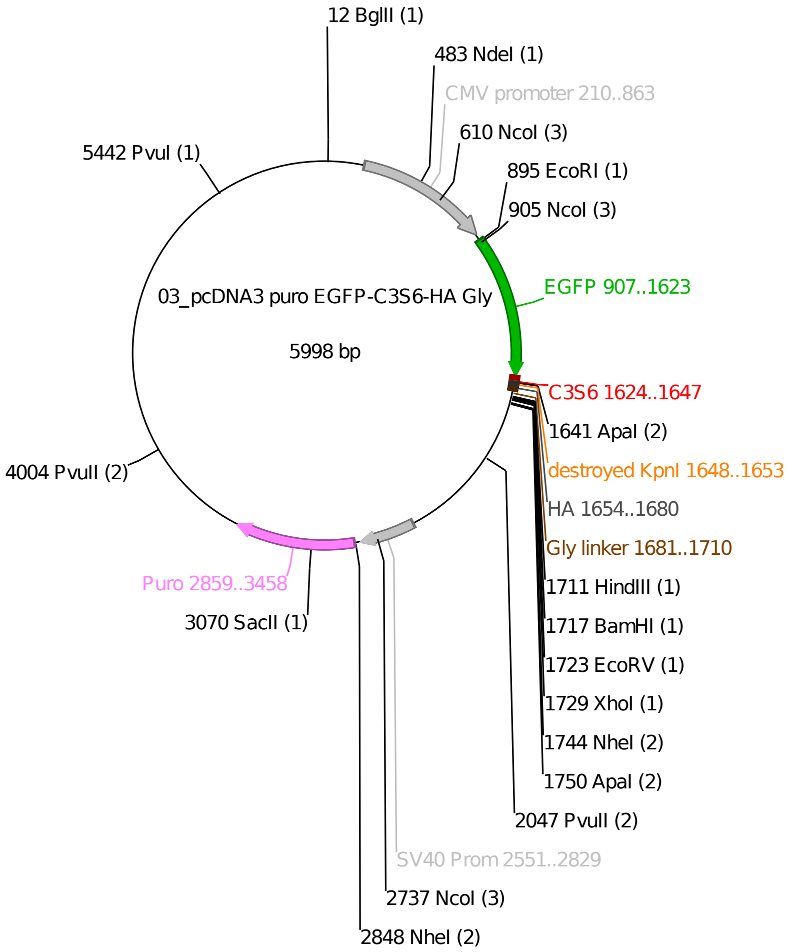
12 BglII (1)
483 NdeI (1)
CMV promoter 210..863
610 NcoI (3)
895 EcoRI (1)
905 NcoI (3)
5442 PvuI (1)
03_pcDNA3 puro EGFP-C3S6-HA Gly
5998 bp
EGFP 907..1623
C3S6 1624..1647
1641 ApaI (2)
destroyed KpnI 1648..1653
HA 1654..1680
Gly linker 1681..1710
1711 HindIII (1)
1717 BamHI (1)
1723 EcoRV (1)
1729 XhoI (1)
1744 NheI (2)
1750 ApaI (2)
2047 PvuII (2)
SV40 Prom 2551..2829
2737 NcoI (3)
2848 NheI (2)
4004 PvuII (2)
Puro 2859..3458
3070 SacII (1)

Vector of origin: pcDNA3-puro-EGFP-C3S6 was digested with *HindIII* and *KpnI*

Insert: *destrKpnI*-**HA**-Gly-*HindIII.* The *KpnI* site was destroyed in the cloning process.The insert was created by annealing the following oligonucleotides:

Oligonucleotides:

Kpn HA Gly HindIII_s	5'	`---- A TAT CCC TAT GAC GTC CCG GAC TAT GCA GGTGGCGGTGGCTCTGGAGGTGGTGGGTCC A----`	1183
Kpn HA Gly HindIII_as	3'	`CA TGT ATA GGG ATA CTG CAG GGC CTG ATA CGT CCACCGCCACCGAGACCTCCACCACCCAGG TTC GA`	1184

Analytical digest using *NcoI* and *KpnI,* resulting in fragment sizes of 3871, 1832 and 295 bp (*KpnI* shouldn't cut since the site was destroyed in the cloning process). The open reading frame ranges from 907 - 1782 and translates to 291 amino acids.

Sequencing primer:
fw: CMV-F, binds basepairs at position 769-789
rev: pcDNA3.1-R, binds basepairs at position 1795-1814

Description: Used as a vector of origin for cloning "pcDNA3puro EGFP-C3S6-HA-GL-B55α"

Vector name: pcDNA3puro EGFP-C3S6-HA-GL-B55α
cloned by Wolfgang Hintringer

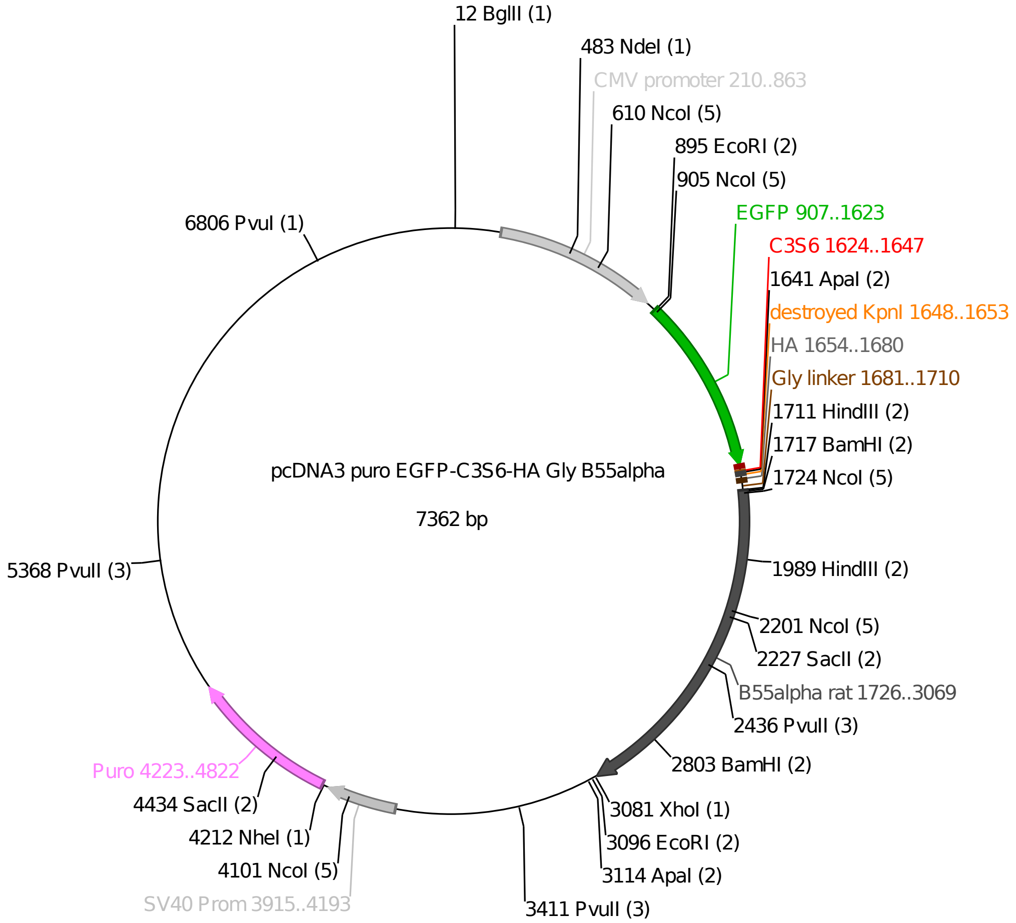
12 BglII (1)
483 NdeI (1)
CMV promoter 210..863
610 NcoI (5)
895 EcoRI (2)
905 NcoI (5)
EGFP 907..1623
C3S6 1624..1647
1641 ApaI (2)
destroyed KpnI 1648..1653
HA 1654..1680
Gly linker 1681..1710
1711 HindIII (2)
1717 BamHI (2)
1724 NcoI (5)
1989 HindIII (2)
2201 NcoI (5)
2227 SacII (2)
B55alpha rat 1726..3069
2436 PvuII (3)
2803 BamHI (2)
3081 XhoI (1)
3096 EcoRI (2)
3114 ApaI (2)
3411 PvuII (3)
SV40 Prom 3915..4193
4101 NcoI (5)
4212 NheI (1)
4434 SacII (2)
Puro 4223..4822
5368 PvuII (3)
6806 PvuI (1)
pcDNA3 puro EGFP-C3S6-HA Gly B55alpha
7362 bp

Vector of origin: pcDNA3-puro-EGFP-C3S6-HA-GL (Nr.2) was digested with *BamHI* and *XhoI*.

Insert: *BamHI*-B55α-*SalI*.
Insert was created by digesting pBABE-hygro-NP-4H3-2HA-g-L 55 (Nr.1) first with *SalI* o/n, followed by a partial digest using *BamHI*. *SalI* is compatible with *XhoI.*

Analytical digest using *HindIII* and *XhoI,* resulting in fragment sizes of 5992, 1092 and 278 bp. The open reading frame ranges from 907 - 3069 and translates to 720 amino acids.

Sequencing primer:
rev: pcDNA3.1-R, binds basepairs at position 3159 - 3178

Description: Used as a negative control in the preScission assay

Vector name: pcDNA3puro EGFP-C3S6-HA-GL-Cα
cloned by Wolfgang Hintringer

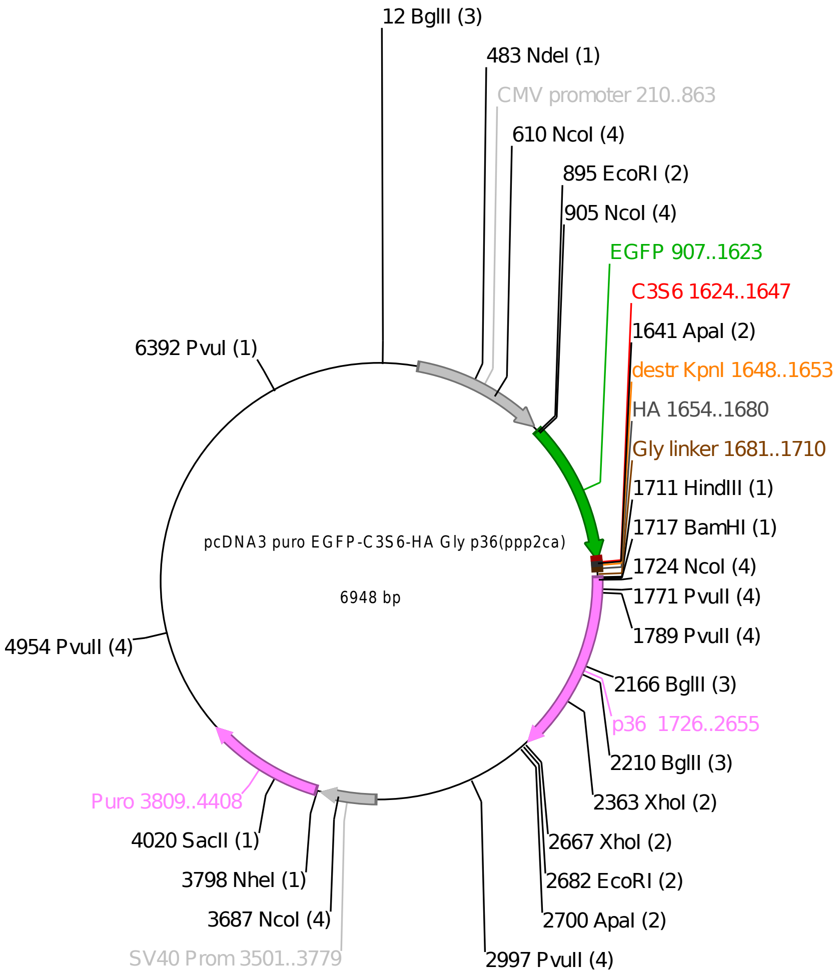
12 BglII (3)
483 NdeI (1)
CMV promoter 210..863
610 NcoI (4)
895 EcoRI (2)
905 NcoI (4)
EGFP 907..1623
C3S6 1624..1647
1641 ApaI (2)
destr KpnI 1648..1653
HA 1654..1680
Gly linker 1681..1710
1711 HindIII (1)
1717 BamHI (1)
1724 NcoI (4)
1771 PvuII (4)
1789 PvuII (4)
2166 BglII (3)
p36 1726..2655
2210 BglII (3)
2363 XhoI (2)
2667 XhoI (2)
2682 EcoRI (2)
2700 ApaI (2)
2997 PvuII (4)
SV40 Prom 3501..3779
3687 NcoI (4)
3798 NheI (1)
4020 SacII (1)
Puro 3809..4408
4954 PvuII (4)
6392 PvuI (1)
pcDNA3 puro EGFP-C3S6-HA Gly p36(ppp2ca)
6948 bp

Vector of origin: pcDNA3-puro-NP-EGFP-C3S6-HA-Gly (Nr.2) was digested with *HindIII* and *XhoI*

Insert: *HindIII*-p36-*SalI*
Insert was created by digesting pBABE-hygro-NP-4H3-2HA-g-L 36 wt (Nr.1) with *SalI* and *HindIII*. *SalI* is compatible with *XhoI*, the restriction site was destroyed in the process.

Analytical digest using *HindIII* and *XhoI* leading to fragment sizes of 5992, 652 and 304 bp. The open reading frame ranges from 907 - 2655 and translates to 582 amino acids.

Sequencing primer:
fw: CMV-F, binds basepairs at position 769 - 789
rev: pcDNA3.1-R, binds basepairs at position 2745 - 2764

Description: Used for expressing the prey fusion protein in the preScission assay

Vector name: pcDNA5to myc-preScission_new_stop-GL
cloned by Wolfgang Hintringer

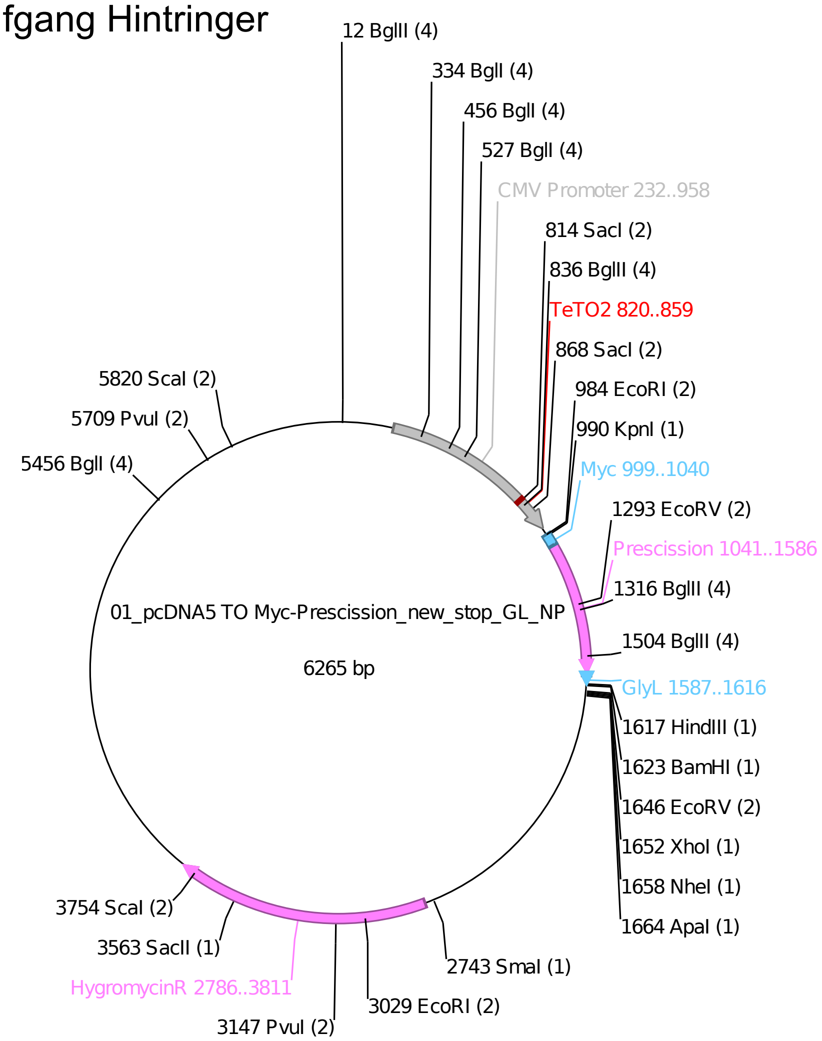
12 BglII (4)
334 BglI (4)
456 BglI (4)
527 BglI (4)
CMV Promoter 232..958
814 SacI (2)
836 BglII (4)
TeTO2 820..859
868 SacI (2)
984 EcoRI (2)
990 KpnI (1)
Myc 999..1040
1293 EcoRV (2)
Prescission 1041..1586
1316 BglII (4)
1504 BglII (4)
GlyL 1587..1616
1617 HindIII (1)
1623 BamHI (1)
1646 EcoRV (2)
1652 XhoI (1)
1658 NheI (1)
1664 ApaI (1)
2743 SmaI (1)
3029 EcoRI (2)
3147 PvuI (2)
HygromycinR 2786..3811
3563 SacII (1)
3754 ScaI (2)
5456 BglI (4)
5709 PvuI (2)
5820 ScaI (2)
01_pcDNA5 TO Myc-Prescission_new_stop_GL_NP
6265 bp

Vector of origin: pcDNA5to-myc-preScission-GL-NP (cloned by Ingrid Frohner) was digested with *BamHI* and *NheI*

Insert: *BamHI*-**new_stop**-*NheI* was ligated to the plasmid.
The insert was created by annealing the following oligonucleotides:

Oligonucleotides:

pyx-new-stop_s	5'	GATCC**TAA**CTGACTAGGTCGACGATATCCTCGAGG	1045
pyx-new-stop_as	3'	----G**ATT**GACTGATCCAGCTGCTATAGGAGCTCCGATC	1046

Analytical digest using *SmaI* + *NotI*, as well as *NotI* only. *NotI* should not cut since the site was removed in the cloning process. The open reading frame ranges from 999 - 1631.

Sequencing primer:
rev: pcDNA3.1-R, binds basepairs at position 1687 - 1706

Description: Used as a negative control in the preScission assay.

Vector name: pcDNA5to myc-preScission™-GL-B55α
cloned by: Ingrid Frohner

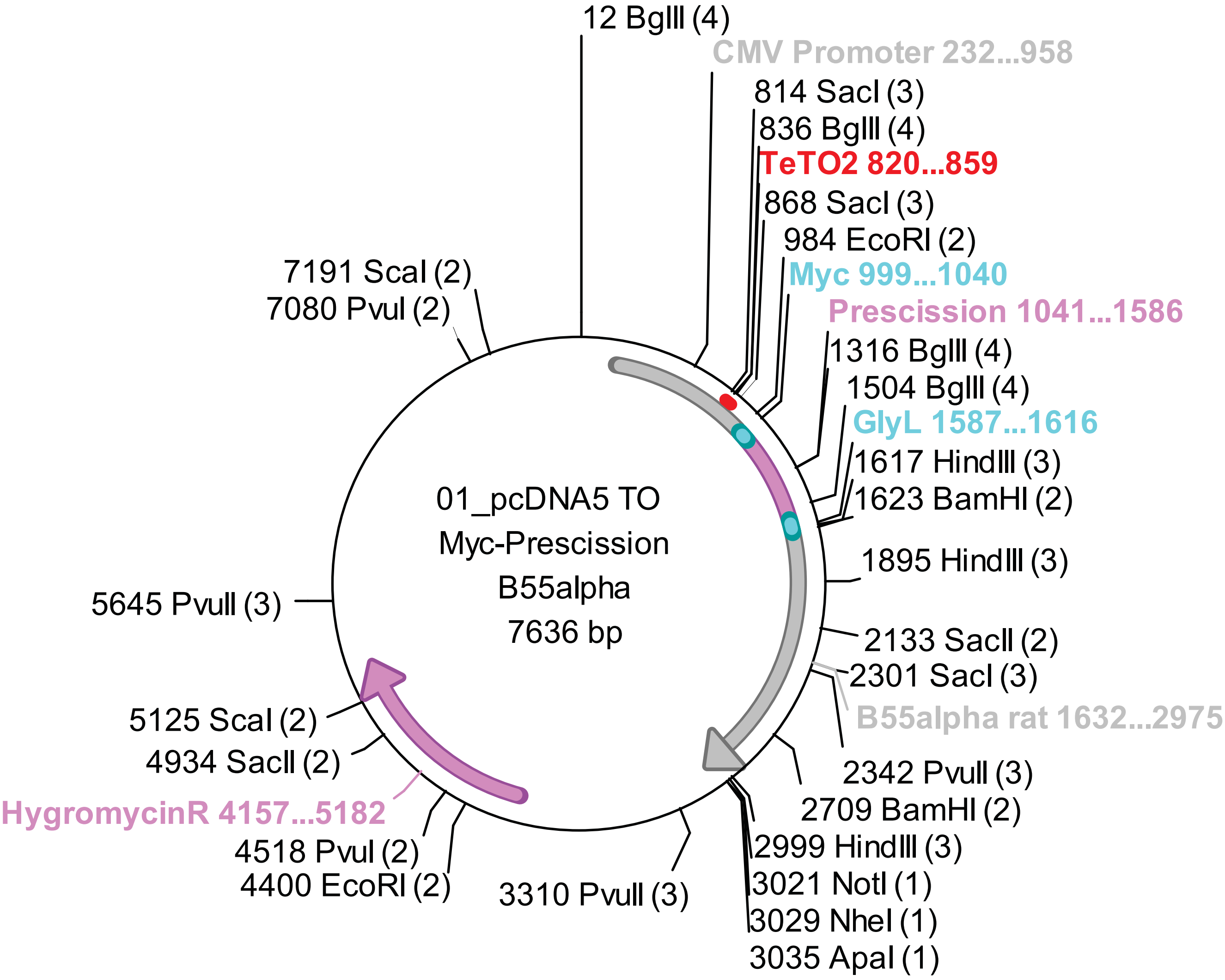
12 BglII (4)
CMV Promoter 232...958
814 SacI (3)
836 BglII (4)
TeTO2 820...859
868 SacI (3)
984 EcoRI (2)
Myc 999...1040
Prescission 1041...1586
1316 BglII (4)
1504 BglII (4)
GlyL 1587...1616
1617 HindIII (3)
1623 BamHI (2)
1895 HindIII (3)
2133 SacII (2)
2301 SacI (3)
B55alpha rat 1632...2975
2342 PvuII (3)
2709 BamHI (2)
2999 HindIII (3)
3021 NotI (1)
3029 NheI (1)
3035 ApaI (1)
3310 PvuII (3)
4400 EcoRI (2)
4518 PvuI (2)
HygromycinR 4157...5182
4934 SacII (2)
5125 ScaI (2)
5645 PvuII (3)
7080 PvuI (2)
7191 ScaI (2)
01_pcDNA5 TO
Myc-Prescission
B55alpha
7636 bp

Vector: pcDNA5TO-Myc Pres Gly (Nr1) 5.1.11 cut with BamHI and Xho1 (on)

Insert: B55alpha subunit cut from pBabe hygroNP- 4H3 2HA G-Linker B55alpha (IM 4.12.09)
cut with SalI total and BamHI partial

SalI and XhoI are destroyed upon ligation

Minis- 1-2 on 31.01.11
digest with NcoI Nr 1 and 2

Sequenced Nr1 OK

Midiprep 11.2.11 : Nr1

7. Curriculum Vitae

Personal Details:

Name: Hintringer
First name: Wolfgang
Sex: Male
Date of Birth: 24.07.1988, Linz, Austria
Address: Seitenberggasse 71, Top 30+31,
1160 Vienna, Austria, Europe
Phone: 0043-664 73800109
E-mail: a0702288@unet.univie.ac.at

Research Experience:

- October 2011 - August 2012: Master Thesis

Title: Developing a novel method for detecting transient protein-protein interactions in mammalian cells.

Location: Laboratory of Dr. Egon Ogris, Dept. Medical Biochemistry, Max F. Perutz Laboratories, Vienna, Austria

- June 2010: Bachelor Thesis

Title: Experiments on the cleavage site specificity and cleavage mechanism of the FMDV leader protease.

Location: Laboratory of Dr. Timothy Skern, Dept. Medical Biochemistry,
Max F. Perutz Laboratories, Vienna, Austria

Education:

2010 - Present: Master of Science, Molecular Biology, University of Vienna
Main subject: Molecular Medicine

2007 - 2010: Bachelor of Science, Biology, University of Vienna
Main subject: Molecular Biology
GPA: 2,0

1998 - 2006: Secondary education (Gymnasium) Linz International School Auhof, Linz, Austria
GPA: 1,3

Accomplishments:

2010: Scholarship for excellent academic achievements from the University of Vienna.
2009: Scholarship for excellent academic achievements from the University of Vienna.
2006: Graduated with distinction from the Linz International School Auhof,
2006: Received the International Baccalaureate Diploma scoring a total of 38 points.

Additional Skills and Interests:

Language proficiency:	Excellent command of both English and German Conversational proficiency in French
Personal interests:	Reading, sports and music